NSAID ENTEROPATHY: NOVEL ASPECTS OF PATHOPHYSIOLOGY, DIAGNOSIS, AND TREATMENT

A Dissertation

by

CANAAN M. WHITFIELD-CARGILE

Submitted to the Office of Graduate and Professional Studies of
Texas A&M University
in partial fulfillment of the requirements for the degree of

DOCTOR OF PHILOSOPHY

Chair of Committee,	Noah Cohen
Committee Members,	Robert Alaniz
	Joanne Hardy
	Sara Lawhon
	Jan Suchodolski
Head of Department,	Allen Roussel

December 2016

Major Subject: Biomedical Sciences

ABSTRACT

Although non-steroidal anti-inflammatory drugs (NSAIDs) are among the most frequently used classes of medications in the world, they are well-known to induce an enteropathy that is associated with high morbidity and mortality in upwards of 70% of users. The diagnosis of NSAID enteropathy is difficult. Furthermore, the underlying mechanisms by which NSAIDs induce enteropathy remain ill-defined although microbiota-host interactions appear to play an important role. Importantly, in addition to difficulty in diagnosing this disease, there are also no effective treatment strategies. Therefore, the purpose of this research was to determine if the microbiota-derived metabolite indole, could attenuate severity of NSAID enteropathy. A second goal was to determine if the transcriptome of exfoliated intestinal epithelial cells (IECs) found in the stool could be reflective of NSAID enteropathy, thereby allowing a non-invasive approach to studying how the mucosal transcriptome is altered by NSAIDs and potentially discriminating between healthy and diseased animals.

We utilized a mouse model of NSAID enteropathy, whereby mice were assigned to 1 of 4 groups: 1) NSAID; 2) indole; 3) NSAID + indole; and, 4) untreated controls. Disease severity was determined by a number of assays including: fecal calprotectin, microscopic pathology, neutrophil infiltration, and RNA-seq of the ileal mucosa. Diversity and composition of the fecal microbiota was determined by 16S rRNA sequencing. Non-invasive examination of the mucosal transcriptome was determined by isolation and sequencing of polyA+ RNA from the stool followed by novel

computational approaches to assess the inter-relatedness of exfoliated and tissue-level transcriptomes.

Results from these assays revealed that indole did in fact attenuate disease severity and this improvement appeared to be related to composition of the microbiota. In addition, approximately 96% of all genes that were mapped from the exfoliated cell RNA were also present in the tissue-level RNA and the pathways represented by these genes and their directional changes were similar in both the small intestinal mucosa and exfoliated IEC transcriptome. These findings demonstrate that the exfoliated cell transcriptome correlates to the tissue-level transcriptome and can be used to gain longitudinal information related to NSAID-induced alterations of the mucosal transcriptome and to discriminate between diseased and healthy animals.

ACKNOWLEDGEMENTS

I would like to thank my committee chair, Dr. Noah Cohen, and my committee members, Dr. Robert Alaniz, Dr. Joanne Hardy, Dr. Sara Lawhon, and Dr. Jan Suchodolski, for their guidance and support throughout the course of my graduate studies.

Thanks also go to my friends and colleagues and the department faculty and staff of the department of Large Animal Clinical Sciences for making my graduate studies at Texas A&M University a great experience.

Finally, thanks to my mother and father for their encouragement and to my wife and children for their patience, love, and constant entertainment.

CONTRIBUTORS AND FUNDING SOURCES

Contributors

This work was supported by a dissertation committee consisting of Dr. Noah Cohen (advisor) and Dr. Joanne Hardy from the Department of Veterinary Large Animal Clinical Sciences, Dr. Robert Alaniz from the Department of Microbial Pathogenesis and Immunology, Dr. Sara Lawhon from the Department of Veterinary Pathobiology, and Dr. Jan Suchodolski from the Department of Veterinary Small Animal Clinical Sciences.

Dr. Brad Weeks from the Department of Veterinary Pathobiology performed the microscopic pathology described in Chapter II. Dr. Joe Petrosino's lab at Baylor College of Medicine performed the 16S rRNA sequencing described in Chapter II. RNA-Seq described in both Chapter II and Chapter III was performed by the Texas AgriLife Genomics and Bioinformatics Services Core Facility. Linear discriminant analysis described in Chapter III was performed by Dr. Ivan Ivanov from the Department of Veterinary Physiology and Pharmacology. Sparse canonical correlation analysis, also in Chapter III, was performed by Mr. Kejun He from the Department of Statistics. Ms. Jennifer Goldsby from the Department of Nutrition and Food Science performed RNA isolations described in Chapter III. Finally, the idea of using the transcriptome of exfoliated cells found in feces came from Dr. Robert Chapkin from the Department of Nutrition and Food Science. All other work conducted for the dissertation was completed by the student independently.

Funding Sources

This work was funded in part by a research and graduate studies grant from the Department of Veterinary Large Animal Clinical Sciences, a post-doctoral trainee grant from the College of Veterinary Medicine, and Link Equine Research Endowment, College of Veterinary Medicine & Biomedical Sciences, Texas A&M University. This work was also supported by grants from the National Institutes of Health R35CA197707 and P30ES023512.

NOMENCLATURE

ANOSIM	Analysis of Similarity
CCA	Canonical Correlation Analysis
CYP	Cytochrome P450
COX	Cyclooxygenase
CRC	Colorectal Cancer
ER	Endoplasmic Reticulum
FDR	False Discovery Rate
GI	Gastrointestinal
IBD	Inflammatory Bowel Disease
IEC	Intestinal Epithelial Cell
IL	Interleukin
LDA	Linear Discriminant Analysis
LPS	Lipopolysaccharide
NSAID	Non-Steroidal Anti-Inflammatory Drug
NF-κB	Nuclear Factor Kappa-Light-Chain-Enhancer of activated B cells
PTGS	Prostaglandin Endoperoxide Synthase
OUT	Operational Taxonomic Unit
PCA	Principal Component Analysis
PAMP	Pathogen Associated Molecular Pattern
PPI	Proton Pump Inhibitor

PRR	Pattern Recognition Receptor
ROS	Reactive Oxygen Species
SBA	Secondary Bile Acids
SCFA	Short Chain Fatty Acid
SIMPER	Similarity Percentage
TLR	Toll-Like Receptor
TNF	Tumor Necrosis Factor
UC	Ulcerative Colitis
ZO	Zonula Occludens

TABLE OF CONTENTS

Page

LIST OF FIGURES

Page

LIST OF TABLES

Page

CHAPTER I

INTRODUCTION TO NON-STEROIDAL ANTI-INFLAMMATORY DRUG (NSAID) ENTEROPATHY WITH A FOCUS ON HOW THE GUT MICROBIOTA CONTRIBUTES TO THE DEVELOPMENT OF DISEASE

Introduction

Nonsteroidal anti-inflammatory drugs (NSAIDs) are among the most widely used class of medications in the world. These drugs are used daily by many millions of people to treat a host of inflammatory and painful conditions as well as for their anti-neoplastic affects. This class of medications, however, has several adverse effects of which ulceration and bleeding of the gastrointestinal (GI) tract are most common. Damage by NSAIDs occurs in 2 locations of the GI tract: 1) the upper GI tract involving the stomach and duodenum (termed NSAID gastropathy); and, 2) the lower GI tract, most commonly the distal small intestine in people (termed NSAID enteropathy). While NSAID-induced gastropathy remains a clinical concern, accurate diagnostic tests and effective management strategies exist. In contrast, NSAID enteropathy is difficult to diagnose and there are no effective management strategies, despite the fact that it occurs as or more frequently than NSAID-induced gastropathy. In fact, NSAID enteropathy affects up to 70% of people that use NSAIDs including short-term users.[1, 2]

The pathophysiology of NSAID enteropathy remains complex and ill-defined. The current paradigm for the pathophysiology of NSAID enteropathy involves a multi-step process whereby NSAIDs initially induce topical injury to the intestinal epithelial

cells (IECs) comprising the intestinal mucosa. This results in impaired intestinal barrier function resulting in invasion of intestinal bacteria and other luminal contents (e.g., lipopolysaccharide [LPS], bile acids). The deeper layers of the bowel wall (i.e., the lamina propria) are laden with immune cells that respond to defects in barrier function resulting in profound inflammation. Finally, healing is impaired due to decreased protective mucosal prostaglandins resulting from cyclooxygenase (COX) inhibition.

Although the steps described in this multi-hit theory are clearly important, there are aspects of NSAID enteropathy that are not adequately explained by this process. Increasing evidence indicates that interaction of NSAIDs with the gut microbiota contribute to the development of NSAID enteropathy. The purpose of this report is to review the pathophysiology of NSAID enteropathy with emphasis on interactions between NSAIDs, the host GI tract, and the gut microbiota and potential mechanisms by which the microbiota alters the severity of NSAID-induced intestinal injury. As described here, the gut microbiota plays a pivotal role in multiple aspects of the pathogenesis of NSAID enteropathy.

Canonical Pathogenesis of NSAID Enteropathy

Topical Effects of NSAIDs on IECs

It is well established that topical effects of NSAIDs on IECs are among the earliest events of NSAID-induced intestinal injury.[3, 4] The exact concentrations of orally administered NSAIDs in the lumen of the GI tract are unknown; however, biliary concentrations of NSAIDs have been shown to be much higher (i.e., low millimolar range) than plasma concentrations (i.e., low micromolar range), suggesting that

intestinal luminal concentrations are higher than those in bile.[5, 6] Thus, the membranes of IECs (enterocytes) are bathed in relatively high concentrations of NSAIDs when these drugs are administered. The NSAIDs and their metabolites have profound effects on IEC membranes including altering their hydrophobicity, fluidity, and biomechanical properties, which increase the permeability of IECs to luminal contents, including NSAID metabolites.[7] Additionally, NSAIDs are almost all weak organic acids that are lipophilic and thus may easily enter the cell membrane (especially at low pH), even in the absence of IEC membrane damage.

Once NSAIDs enter the enterocyte, the first intracellular organelles to become affected are the mitochondria and the endoplasmic reticulum (ER).[8, 9] These effects of NSAIDs on these organelles occur rapidly, perhaps within 1 hour.[4] NSAIDs induce ER stress due to an accumulation of misfolded proteins which leads to accumulation of intracellular calcium and apoptosis.[9] In the mitochondria, NSAIDs uncouple oxidative phosphorylation which also leads eventually to cell death via apoptosis.[10, 11] Specifically, NSAIDs result in opening of the mitochondrial permeability transition pore with secondary decrease in transmembrane potential, loss of oxidative phosphorylation, release of cytochrome C and calcium into the cytosol, and finally apoptosis.[8] The role of mitochondrial dysfunction in NSAID enteropathy is further supported by the finding that inhibition of c-jun-N-terminal kinase, a regulator of mitochondria-induced apoptosis, reduces the severity of NSAID enteropathy.[12] The exact mechanism by which NSAIDs induce mitochondrial damage is unclear, although mitochondrial production of reactive oxygen species (ROS) has been implicated.[10] Moreover, ROS

produced by the mitochondria have been shown to alter the expression of zonula occludens-1 (ZO-1), a protein important for intracellular tight cell junctions, resulting in increased mucosal permeability.[13] Mucosal permeability is further affected by decrease in ATP levels following mitochondrial damage.[14]

The topical effects of NSAIDs are related to the parent drug but can also be exacerbated by the presence of oxidative metabolites that arise from cytochrome P450 (CYP)-mediated metabolism of the parent drug. IECs within the small intestine have multiple CYP forms that generate oxidative metabolites of the parent drug that may further exacerbate the topical effects of NSAIDs.[15] Clearly the topical effects of NSAIDs on intestinal mucosa are an important component of NSAID enteropathy.

Inhibition of Cyclooxygenase

The well-described mechanism by which NSAID exert their anti-inflammatory effects is COX inhibition, encoded by prostaglandin endoperoxide synthase (PTGS).[16] COX is responsible for the breakdown of arachidonic acid into various prostanoids. Two isoforms of COX have been described: COX-1 and COX-2. It is generally accepted that COX-1 is the constitutively expressed form and is responsible for production of the beneficial prostaglandins that serve to maintain mucosal blood flow and mucus production, whereas COX-2 is the inducible isoform responsible for production of inflammatory prostaglandins.[17] This paradigm is the rationale for tremendous research and development efforts for developing COX-2-selective NSAIDs that would maintain the beneficial prostaglandins by preserving COX-1 but reduce inflammatory prostaglandins by inhibition of COX-2. Interestingly, COX-1 knock-out mice (PTGS-1-

/-) do not develop enteropathy and COX-2 knockout mice (PTGS-2-/-) do not develop the same enteropathy as seen with NSAID administration.[18, 19] Others have demonstrated repeatedly that some degree of concomitant inhibition of COX-1 and COX-2 is necessary to induce enteropathy and inhibition of one isoform results in upregulation of the other.[20] It has been suggested that COX-2 inhibition is more important than COX-1 inhibition in inducing NSAID enteropathy.[21] The importance of COX-2 in mucosal protection also has been shown by epidemiological studies demonstrating reduced NSAID gastropathy but no reduction, and perhaps even an increase, in the incidence of NSAID enteropathy in people despite the introduction of COX-2-selective NSAIDs to the market.[22] Taken together, these findings suggest that COX-2 does, in fact, provide mucosal protection and that while COX-inhibition can delay healing or increase the severity of NSAID enteropathy, COX-inhibition alone is not responsible for NSAID enteropathy.

Innate Inflammatory Response

Subsequent to the topical effects of NSAIDs on IECs, release of ROS, ROS-modified ZO-1 proteins, and loss of barrier function, there is an invasion of luminal contents into the bowel wall. This, in turn, activates the innate inflammatory response. The finding that Rag2-/- mice and athymic mice develop similar degrees of indomethacin-induced injury as do mice with competent adaptive immune responses indicates that NSAID enteropathy is primarily driven by ***innate*** rather than adaptive immune responses.[23, 24] In particular, Toll-like receptor 4 (TLR4) signaling activated by bacterial LPS plays a critical role in the pathogenesis of NSAID enteropathy. Mice

that lack TLR4 develop less severe lesions than isogeneic TLR4-competent strains.[25] Additionally, TLR4 deficiency also inhibited NSAID-induced upregulation of pro-inflammatory cytokines with concomitant decrease in disease severity.[26] TLR4 appears to be an important player in mucosal barrier function and inflammation.[27] Stimulation of TLR4 by ligands activates MyD-88 which, in turn, incites production of pro-inflammatory cytokines such as interleukin (IL)-1β and tumor necrosis factor alpha (TNF-α) which contribute to severity of disease.[28-30] These, in turn, recruit more inflammatory cells to the area, primarily neutrophils.

Neutrophilic inflammation is the hallmark of NSAID enteropathy and neutrophils are the key effector cells of this disease.[31-33] Neutrophils are recruited to the area following loss of barrier function and incite further inflammation by release of pro-inflammatory mediators including IL-1β and TNF-α. Highlighting the importance of this pathway is the fact that TNF-α knockout mice develop less severe enteropathy than wild-type mice, and treatment with anti-TNF-α pharmaceuticals lessens the severity of disease.[29, 30, 34] An additional mechanism by which neutrophils contribute to the inflammation in NSAID enteropathy is by further oxidation of parent NSAIDs (or their metabolites) to a more active form through the activity of myeloperoxidase.[35] It appears that the neutrophil response is not responsible for the initial break in barrier function but rather plays a critical role in progression of the injury.

Although the steps described in this multi-hit theory of NSAID enteropathy are clearly important and valid, some aspects of the pathogenesis of NSAID enteropathy are not adequately explained by this process. For example, it remains unclear why some

individuals are more sensitive to the effects of NSAIDs than others, why the most severely affected region of the GI tract is the distal small intestine, and how probiotics or diet influence the severity of disease. Some of these questions can be explained by interactions between the gut microbiota and NSAIDs. The remainder of this review will address the complex interactions between NSAIDs and the microbiota, and how the microbiota influences diseases severity.

Effects of NSAIDs on the Microbiota

We first consider the effects of NSAIDs on the intestinal microbiota. It is well-established that NSAID administration causes a dysbiosis that contributes to development of disease.[36-38] This dysbiosis is characterized by an increase in gram negative bacteria and this shift in composition of the microbiota is consistently observed both in animal models and in people using NSAIDs clinically.[32, 39-42] In concert with an increase in gram negative bacteria, there appears to be a loss of specific gram positive bacteria including Bifidobacteriaceae, Lachnospiracea, and Lactobacillacea.[39, 43, 44] Administration of probiotics containing these families of microbes ameliorates NSAID enteropathy, further suggesting this particular shift in the microbiota composition is important to the development of NSAID enteropathy.[44-47] Moreover, co-administration of proton pump inhibitors (PPI), which induce an enteropathy characterized by loss of similar types of microbes as NSAIDs, worsens NSAID-enteropathy.[48, 49]

The mechanism by which NSAIDs cause dysbiosis is unknown. One possibility is that ROS released from IECs following NSAID-induced mitochondrial damage

contributes to this dysbiosis, because ROS molecules released during intestinal inflammation can induce a dysbiosis.[50] When ROS molecules react with luminal substrates such as thiosulphates, they subsequently act as electron receptors for pathogens that use respiration which allows the respiring bacteria to outcompete commensal bacteria that use fermentation for generating energy.[51] Although this mechanism of dysbiosis has not been demonstrated for NSAID enteropathy as it has for other models of mucosal inflammation that generate ROS, ROS are released by IECs secondary to topical effects of NSAIDs.[10, 11, 52] It is unclear for NSAID enteropathy to what degree these ROS molecules from IECs enter the lumen of the GI tract and interact with the microbiota. Another mechanism by which NSAIDs might induce a dysbiosis is the antimicrobial properties of some NSAIDs.[53-55] Irrespective of the mechanism, the dysbiosis associated with NSAIDs appears to greatly influence all other aspects of the pathophysiology of NSAID enteropathy.

Effects of the Microbiota on NSAIDs and NSAID Enteropathy

The microbiota is critically important to host health. This is certainly true for GI diseases where alterations of the intestinal microbiota, and host response to the microbiota, have been linked to numerous diseases including peptic ulcers, inflammatory bowel disease (IBD), ulcerative colitis (UC), colorectal cancer (CRC), and many others. This interaction appears to play a crucial role in NSAID enteropathy. Pretreatment with antibiotics that primarily target gram-negative bacteria greatly ameliorates NSAID enteropathy.[39, 56] Moreover, germ-free animals do not develop enteropathy in response to NSAIDs.[39, 57] While these findings demonstrate an association between

the microbiota and NSAID-induced enteropathy, they do not address the mechanistic basis of this relationship. Thus, we next consider mechanisms by which the microbiota can impact the development of NSAID enteropathy.

The Microbiota Influences the Topical Effects of NSAIDs

The microbiota has been shown to enhance the topical effects of NSAIDs by bacterial β-glucuronidation. Many bacteria, including some found in the gastrointestinal tract, possess β-glucuronidase enzymatic activity. When NSAIDs are administered (orally or parenterally) they undergo enterohepatic circulation. In the liver, NSAIDs are conjugated via glucuronidation and released into the biliary tree.[58-60] Bacterial β-glucuronidases remove the glucuronide group, releasing either the parent drug or the oxidized metabolite such that NSAIDs are able to damage IEC membranes and then re-enter these cells. Pharmacologic inhibition of bacterial β-glucuronidases attenuates the severity of NSAID enteropathy indicating that bacterial β-glucuronidation contributes to development of NSAID enteropathy.[6, 61] Interestingly, the distal small intestine contains higher β-glucuronidase activity than the remainder of the GI tract.[62] This might explain in part the finding that the most severe NSAID-induced intestinal injury occurs in the distal small intestine despite the fact that higher concentrations of NSAIDs are likely to be found more proximally in the small intestine following their release in the bile.

In a related manner, the dysbiosis caused by NSAIDs may contribute to the severity of NSAID enteropathy by the action of the microbiota on bile acids. Primary bile acids are made in the hepatocyte, and are secreted in the proximal small intestine

where they come into contact with the gut microbiota.[63] Some bacteria in the gut are capable of acting on hydroxyl groups of primary bile acids to form secondary bile acids (SBAs).[64] The SBAs can have adverse effects. For example, SBAs (e.g., deoxycholic acid and lithocholic acid) have been shown to result in increased paracellular permeability in the gut and to damage the cell membrane of IECs, thus enhancing the topical effects of NSAIDs which leads to further mucosal damage and loss of barrier function.[65, 66] The SBAs function in digestion of nutrients and are critical for enterohepatic circulation. Fecal and even circulating levels of SBAs have been associated with a number of different alimentary diseases including CRC, liver cancer, and IBD. Dysbiotic states can alter the capacity of the microbiota to modify bile acids by increasing or decreasing the types of bacteria that act on primary bile acids and this may be the case with NSAID-induced dysbiosis.[67, 68] It is important to note that the balance of bile acids is important: decreased bile acid concentrations in the GI tract lead to bacterial overgrowth of some types of bacteria whereas increased bile acid concentrations can result in inflammation and disease.[69]

Interestingly, bile acids, and specifically SBAs, have been linked to NSAID enteropathy. A number of studies have suggested bile acids increase NSAID-induced cytotoxicity, thereby enhancing the topical effects of NSAIDs on the mucosa.[70, 71] In addition, bile duct ligation in rodent models of NSAID-enteropathy prevents NSAID induced intestinal injury, thus highlighting the importance of bile and enterohepatic circulation in this phenotype.[72] Taken together these findings suggest that dysbiosis resulting in an altered bile acid profile in the GI tract that enhances the topical effects of

NSAIDs might be another mechanism by which the microbiota influences the topical effects of NSAIDs and thus overall disease severity in NSAID enteropathy.

The Microbiota Influences the Host Innate Immune Response

Microbes have highly conserved molecular signatures, referred to as pathogen associated molecular patterns (PAMPs), that are recognized by the host via germ-line-encoded receptors, referred to as pattern recognition receptors (PRRs) including the TLRs. The interaction of PAMPs and PRRs is central to the innate immune response of the host and has been well-reviewed.[73] In the GI tract, the interaction of PAMPs with TLR4 has been shown to be critically important for maintenance of GI mucosal homeostasis as well as for mediating inflammation that may lead to diseases such as IBD, CRC, and NSAID enteropathy.[32, 74-76] Bacterial recognition by TLR receptors have been shown to modulate intestinal function; therefore, perturbations of the microbiota (i.e., NSAID-induced dysbiosis) can alter these pathways and result in increased intestinal dysfunction and damage.[77] For example, NSAIDs are known to increase gram negative bacteria. Because LPS is a component of the cell wall of gram negative bacteria, it is logical that increased gram negative bacteria will result in increased LPS, the canonical ligand of TLR4 resulting in increased TLR4 signaling.[32, 39-41] Increased amounts of LPS invading the deeper layers of the intestinal wall following NSAID-induced loss of barrier function could bind to TLR4 and result in downstream signal transduction. Indeed, LPS, TLR4, and its downstream pathways including MyD-88 have been shown to be critical players in the pathophysiology of

NSAID enteropathy and expression of TLR4 appears to be upregulated during NSAID-induced inflammation (similar to what is found in people with IBD).[25, 32, 78]

Another mechanism by which NSAID-induced dysbiosis might influence TLR signaling is by altering the expression and/or spatial location of TLRs on IECs. Enteropathy associated with NSAIDs (and other GI inflammatory diseases) results in increased expression by IECs of some TLRs, particularly TLR4.[32, 40, 79] The IECs are polarized and as such TLR molecules can be located on the apical side and the basolateral surface. Apical molecules are located on the luminal side of the IEC and therefore are likely to come into contact with PAMPs associated with the gut microbiome. In contrast, basolaterally-located molecules only come into contact with PAMPs that have traversed the mucosal barrier (i.e., following intestinal injury). Differences in spatial arrangement of TLRs have been shown to be important in some inflammatory disorders of the GI tract such as IBD. A hallmark of Crohn's disease is lack of tolerance to the microbiota.[80] Interestingly, people with active Crohn's disease express TLR4 on the apical portion of colonic IECs at a much higher concentration than unaffected people, implicating alteration in spatial location of TLR4 in development of inflammatory disorders of the GI tract.[79] The gut microbiota can influence the spatial orientation of TLRs on IECs by increasing apical expression.[81] It is thus plausible that the composition of the microbiota not only alters expression of TLRs but also the location/distribution of the TLRs on IECs. It remains to be determined whether the spatial orientation of TLRs and other PRRs are altered by NSAID administration or during NSAID enteropathy, and whether this spatial alteration is microbiota-dependent.

Dysbiosis Alters Microbiota-Derived Metabolite Profile with Multiple Implications for NSAID Enteropathy

Dysbiosis results in intestinal inflammation and loss of barrier function.[82] The mechanism by which dysbiosis induces inflammation, however, remains unclear. One possible explanation is the loss of commensal bacteria during dysbiosis. Some commensals produce metabolites that are beneficial for host IECs and maintenance of intestinal barrier function. For example, people with Crohn's disease have a dysbiosis that is characterized by a loss of the critically important commensal bacteria Fecalibacterium and Roseburi which produce large quantities of short-chain fatty acids (SCFAs).[83-85] The SCFAs generated by intestinal commensal bacteria exert several beneficial effects on the host including maintaining gut homeostasis and reducing inflammation; therefore, any dysbiosis that results in loss of SCFAs might contribute to inflammation.[48, 86, 87] Several reports document that NSAIDs reduce the number of intestinal bacteria of the phylum Firmicutes and, less frequently, Bacteroidetes, both of which produce SCFAs.[32, 36, 42, 78] Interestingly, some reports have indicated that culture supernatant alone (i.e., no platonic bacteria) can successfully prevent NSAID enteropathy.[48, 86] These findings further indicate that microbiota-derived metabolites are critically important in affording protection from NSAID-induced intestinal injury and that dysbiosis, resulting in loss of these metabolites, contributes to disease severity.

In addition to SCFAs, the microbiota produces many other metabolites thought to be largely responsible for microbiota-host interactions.[88] The metabolome of the microbiota has been shown to be altered in dysbiotic states. It is reasonable, therefore, to

assume that NSAID-induced dysbiosis alters the intestinal metabolome which in turn might contribute to intestinal injury by altering inter-kingdom signaling.[89, 90] For example, several microbiota-derived tryptophan metabolites are involved in inter-kingdom signaling between the host and the intestinal microbiota.[91] Moreover, many tryptophan metabolites exert anti-inflammatory activities on the host via a variety of mechanisms, many of which have yet to be identified.[92, 93] Recently, we reported that co-administration of indole, a tryptophan microbiota-derived metabolite, attenuated severity of NSAID enteropathy in a murine model.[32] Currently, it is unknown to what degree NSAID-induced dysbiosis alters the metabolome and to what extent this altered microbiota function contributes to disease severity. The fact, however, that co-administration of this microbiota-derived metabolite decreased disease severity gives further support to the idea that the mechanism by which the microbiota might alter disease severity is via the presence or absence of metabolites that regulate host immune response and that help maintain mucosal homeostasis.

Conclusion

The pathophysiology of NSAID enteropathy is complex and much work remains to determine the exact mechanisms by which it develops. All NSAIDs inhibit COX activity in a microbiota-independent manner. While this inhibition may be a factor in disease severity or recovery form NSAID-induced damage, COX inhibition alone does not fully explain the pathophysiology of NSAID enteropathy. It is increasingly evident that the microbiota influences many aspects of this prevalent condition. Use of NSAIDs can also induce a dysbiosis due to the antimicrobial effects of NSAIDs, a shift in

metabolites produced by the microbiota resulting from NSAID-induced inflammation, or both factors (possible acting synergistically). This NSAID-associated dysbiosis subsequently greatly impacts other determinants of the pathogenesis of NSAID enteropathy. Undoubtedly, NSAIDs have a topical effect whereby their presence at the mucosal surface induces epithelial cell damage and eventually cell death via alterations of cell membranes, mitochondrial injury, and ROS production. Although this aspect of the pathophysiology exists independent of the microbiota, it can be modulated by the microbiota due to β-glucuronidase activity of microbiota as well as production of SBAs that render IECs more permeable to NSAIDs and increase enterophepatic circulation of NSAIDs. Following topical injury, barrier function becomes compromised and bacteria and other luminal contents invade the mucosa and induce an innate immune response. The innate immune response can be greatly influenced by the microbiota, either worsened by factors such as the relative amounts of pro-inflammatory mediators like LPS, or ameliorated by the presence of anti-inflammatory microbiota-derived metabolites such as SCFAs or indole. Finally, host-microbiota interaction is mediated by PRRs and PAMPs, and dysbiosis can alter both the expression and location of host-derived PRRs as well as relative abundance of PAMPs further contributing to NSAID enteropathy. Taken together these findings suggest an important role for the microbiota in the pathophysiology of NSAID-induced intestinal injury. Further elucidation of the role of the microbiota and its metabolites in NSAID enteropathy will likely contribute novel approaches to control this highly prevalent if under-recognized health problem that is of global concern. The therapeutic value, relatively low cost, and widespread

availability of NSAIDs indicate that these drugs will continue to be used despite their adverse effects. Thus, there is great need for the identification of novel diagnostic methods for earlier identification of the condition and for therapeutic or prophylactic medications that can be co-administered with NSAIDs to reduce the impact of NSAID enteropathy. Further elucidation of the role of the microbiota and its metabolites in NSAID enteropathy will likely contribute novel approaches to control this highly prevalent if under-recognized problem that is a global health concern.

CHAPTER II

THE MICROBIOTA-DERIVED METABOLITE INDOLE DECREASES MUCOSAL INFLAMMATION AND INJURY IN A MURINE MODEL OF NSAID ENTEROPATHY*

Introduction

Non-steroidal anti-inflammatory drugs (NSAIDs) are among the most frequently used medications worldwide for routine relief of pain or fever, to manage various forms of arthritis and inflammatory intestinal disorders, and to prevent or treat alimentary cancers.[94, 95] Despite their effectiveness for managing these varied and highly prevalent conditions, NSAIDs cause damage to the gastrointestinal (GI) tract. Although methods for diagnosis and effective treatment of NSAID-induced lesions of the proximal GI tract (i.e., gastropathy) have been well documented, the pathogenesis, diagnosis, and treatment of NSAID-induced damage of the GI tract distal to the duodenum (known as NSAID enteropathy, primarily affecting the distal jejunum and ileum) remain unclear.[96, 97] The magnitude of the problem of NSAID enteropathy is alarmingly high. In the United States, NSAID enteropathy results in approximately 100,000 hospitalizations and 16,500 deaths each year.[98] Additionally, 2-thirds of both short- and long-term NSAID users develop distal small intestinal lesions.[2, 99] Although the

---

* The Microbiota-derived Metabolite Indole Decreases Mucosal Inflammation and Injury in a Murine Model of NSAID Enteropathy, Canaan M. Whitfield-Cargile, Noah D. Cohen, Robert S. Chapkin et al (2016), *Gut Microbes*, 7 (3): 246-261, reprinted by permission of Taylor & Francis LLC, (http://tandfonline.com).

use of either NSAIDs considered to be safer for the GI tract or other ancillary therapies have reduced the incidence and severity of NSAID-induced gastropathy, the incidence of NSAID enteropathy has remained constant or has increased.[22]

The pathophysiology of NSAID enteropathy is complex and incompletely understood.[100] It appears to involve deleterious effects of NSAIDs on the intestinal mucosa including enterocyte cell death, increased mucosal permeability, and interaction of the damaged mucosa with luminal contents including bacteria (GI microbiota) and bacterial products or components such as lipopolysaccharide (LPS).[10, 97] The GI microbiota has been implicated as an important contributor to NSAID enteropathy.[23, 39, 42, 49, 78] Administration of NSAIDs causes a dysbiosis characterized by a reduction of the predominately gram-positive phylum Firmicutes and a corresponding increase of gram-negative bacteria.[42, 78] Germ-free rats lacking intestinal microbiota do not develop NSAID enteropathy, whereas they develop NSAID-induced intestinal lesions when colonized with gram-negative bacteria.[39] Concurrent administration of NSAIDs and antimicrobials targeting gram-negative bacteria reduces the severity of NSAID-induced gastrointestinal lesions in rats.[23]

A mechanism by which the microbiota might influence NSAID-induced intestinal mucosal damage is by producing metabolites that protect intestinal epithelial cells.[92, 101] Previously, we identified tryptophan metabolites, including indole, as an important class of GI microbiota-derived compounds.[91] Indole is a quorum-sensing molecule produced by bacterial metabolism of L-tryptophan that mediates communication among bacterial population and inter-kingdom signaling between the

host and microbe.[92, 102, 103] Indole improves barrier function and decreases intestinal inflammation in vitro and in vivo.[92, 101] Moreover, several other tryptophan metabolites reportedly exert similar salutary effects on the intestinal epithelium.[93, 104] Therefore, we hypothesized that indole would mitigate the severity of NSAID enteropathy. To investigate this hypothesis, we co-administered indole with the NSAID indomethacin and demonstrated a reduction in severity of mucosal injury caused by indomethacin alone. To determine whether the protective effects of indole were associated with alterations in the GI microbiota, we characterized the effects of administration of NSAIDs, indole, and their co-administration on the composition and diversity of the fecal microbiota. We observed that the co-administration of indole with indomethacin resulted in maintenance of or even an increase of an important member of the Firmicutes phylum. Finally, to better understand the mechanisms of NSAID enteropathy and the effects of indole on these processes, we performed RNA-Seq of the distal small intestinal epithelium in mice that were untreated or treated with indomethacin, indole alone, or the combination of indomethacin and indole. Pro-inflammatory pathways associated with innate immune responses were up-regulated by indomethacin administration relative to control mice, and co-administration of indole significantly mitigated the up-regulation of these pathways concomitant with reduced GI pathology.

Materials and Methods

Animal protocols were approved by the Texas A&M Institutional Animal Care and Use Committee in accordance with appropriate institutional and regulatory bodies' guidelines.

Mice and Treatments

Eight- to 10-week-old specific-pathogen-free C57BL/6J mice were purchased and allowed to acclimate for 2 weeks. Mice were fed standardized laboratory rodent diet and sterile water ad libitum. Mice were randomly divided into the following 4 groups (n=5 mice/group): 1) NSAID (indomethacin); 2) indole; 3) NSAID + indole; and, 4) untreated controls. Mice were then rehoused on the basis of treatment group assignment, with 5 animals/group-cage. To induce NSAID enteropathy, mice in group 1 were gavaged once daily with indomethacin (5 mg/kg; for 7 days; Sigma Aldrich, St. Louis, MO) dissolved in DMSO (Sigma Aldrich, St. Louis, MO) and further diluted in phosphate buffered saline (PBS). Mice in group 2 received indole by gavage (20 mg/kg; once daily for 7 days; Sigma Aldrich, St. Louis, MO) dissolved in sterile water warmed to 55°C. Mice in group 3 received indole co-administered with indomethacin by gavage at the dosages described above. All mice were gavaged with equal volumes (200 μL) and equal concentrations of DMSO (0.001%).

Sample Collection

Feces were collected daily by placing individual animals in sterile plastic cups that were RNase- and DNase-free until they passed feces. The mice were immediately returned to their home cages and the feces immediately flash frozen at -80°C. All

animals were euthanized via CO2 asphyxiation on day 8 (i.e., after 7 days of treatment). The small intestine was harvested, opened longitudinally, rinsed with ice-cold PBS, and the distal 1/3 of the intestinal mucosa was scraped for tissue gene expression analysis. The remaining small intestine was fixed in 4% paraformaldehyde, Swiss-rolled, paraffin-embedded, and stained with hematoxylin and eosin. The spleen and mesenteric lymph nodes (MLN) were harvested, and immediately placed in ice cold RPMI-1640-c + 10% fetal calf serum (FCS: Life Technologies, Carlsbad, CA), homogenized, and prepared as a single cell suspension for flow cytometric analysis as previously described.[105]

Fecal Calprotectin ELISA

A murine calprotectin ELISA kit (HK214, Hycult Biotech, Plymouth Meeting, PA) was used according to the manufacturer's protocol with slight modifications. Briefly, 100 mg of feces was homogenized in extraction buffer (0.1 M Tris, 0.15 M NaCl, 1.0 M urea, 10 mM CaCl2, 0.1 M citric acid monohydrate, 5 g/l bovine serum albumin (BSA) and 0.25 mM thimerosal [pH 8.0]). The homogenate was centrifuged at 10,000 x g at 4°C for 20 minutes and the supernatant used as directed in manufacturer's protocol.

Tissue RNA Extraction, Sequencing, and Processing

RNA was extracted from the mucosal scrapings using an RNeasy mini kit (QIAGEN, Redwood City, CA) following the manufacturer's instructions and including on-column DNase treatment. RNA quantity was determined using a Nanodrop spectrophotometer (Fisher Thermoscientific) and the quality was assessed using the Nano6000 chip on a Bioanalyzer 2100(Agilent Technologies). Only RNA with an

integrity number (RIN) > 8 was used. The samples were randomized before beginning the RNA-Seq library preparation. Sequencing libraries were made using 250 ng of RNA and the TruSeq RNA Sample Preparation kit (Illumina) following the manufacturer's instructions. A volume of 2.5 µl of ERCC spike-in RNA control mix (Life Technologies) was added to the starting RNA at a dilution of 1:1000. The libraries were pooled and sequenced on an Illumina HiSeq 2500 at the Texas AgriLife Genomics and Bioinformatics Services Core Facility (College Station, TX). Sequencing data were provided in a de-multiplexed format and aligned using Spliced Transcripts Alignment to a Reference (STAR) software with default parameters and referenced against the genome of Mus musculus (Ensembl version GRCm38).[106] Differentially expressed genes were determined using EdgeR based on the matrix of gene counts.[107]53 Gene lists were analyzed through use of QIAGEN's Ingenuity ® Pathway Analysis (IPA, QIAGEN, Redwood City, CA http://www.qiagen.com/ingenuity). Sequence data were uploaded into NCBI small reads archive (Accession number PRJNA290483).

Microbiota DNA Extraction, Sequencing, and Processing

Microbiota 16S rRNA gene sequencing methods were adapted from the methods developed for the NIH-Human Microbiome Project.[108, 109] Briefly, bacterial genomic DNA was extracted using MO BIO PowerSoil DNA Isolation Kit (MO BIO Laboratories) according to the manufacturer's protocol. The 16S rDNA V4 region was amplified by PCR and sequenced in the MiSeq platform (Illumina) using the 2 x 250-bp paired-end protocol yielding paired-end reads that overlap almost completely.[110] The primers used for amplification contain adapters for MiSeq sequencing and dual-index

barcodes so that the PCR products can be pooled and sequenced directly. The software suite Quantitative Insights Into Microbial Ecology (QIIME v1.9 [http://qiime.sourceforge.net]) was used for data processing and analysis.[111] The raw sequence data were de-multiplexed, and low-quality reads were filtered using the database's default parameters. Chimeric sequences were detected using Uchime and removed prior to further analysis.[112] Sequences were then assigned to operational taxonomic units (OTUs) using an open-reference OTU picking protocol [http://qiime.org/scripts/pick_open_reference_otus.html] with UCLUST software in QIIME based on 97% identity with the Greengenes database (v13_5).[113-115] To adjust for uneven sequencing depth among the samples, each sample was rarefied to an even sequencing depth (10,512 reads/sample) prior to further analysis.

Alpha rarefaction, beta diversity measures, richness, taxonomic summaries, and tests for significance were calculated and plotted using QIIME. The weighted and unweighted Unifrac distances were calculated for comparison of beta diversity. Differences in microbial communities among the treatment groups were investigated by visual assessment of clustering on principal component analysis (PCA) and by analysis of similarity (ANOSIM) calculated on unweighted UniFrac distance metrics.[116-118] ANOSIM is a non-parametric test of difference between 2 or more groups based on a distance metric. This test gives an R value between -1 and 1 where large positive R values indicate a large magnitude of dissimilarity between the groups and small R values indicate small magnitudes of dissimilarity; the P value provides statistical significance. When ANOSIM identified significant differences among groups, then pairwise

ANOSIM was performed to determine which groups differed significantly and similarity percentage (SIMPER) was used to examine which features contributed to the differences among groups. ANOSIM, SIMPER, and PCA plots were performed with PAST v3.05.[119]

The software Phylogenetic Investigation of Communities by Reconstruction of Unobserved States (PICRUSt) was used to predict the metagenome.[120] Sequencing data were prepared as described above, but sequences were then clustered into OTUs using a closed-reference OTU picking protocol at the 97% sequencing identity level [http://qiime.org/scripts/pick_closed_reference_otus.html]. The resulting OTU table was normalized by the expected copy number(s) of the 16s rRNA gene in each OTU. PICRUSt was then used to predict the metagenome [https://picrust.github.io/picrust/tutorials/metagenome_prediction.html#metagenome-prediction-tutorial]. Each sample was rarefied to an even sequencing depth to adjust for uneven sequencing depth prior to further analysis. Differences in the metagenomes among the groups were investigated by visual assessment of clustering on PCA and by analysis of similarity (ANOSIM) calculated on Bray Curtis dissimilarity metric.

Metabolite Extraction from Fecal Samples

Metabolites from the fecal contents were extracted using a solvent-based method as previously described.[91] Briefly, fecal pellets were homogenized using a homogenizer (Omni International) with equal volume of cold methanol and half volume of chloroform. The samples were then centrifuged at 10,000 g at 4°C (Thermo Fisher Scientific) for 10 min. Supernatant was passed through a 70-μm sterile nylon cell

strainer (Falcon) and 0.6 ml of ice cold water was added. The samples were vortex and centrifuged again at 10,000 g for 5 minutes. The upper phase and lower phase were collected and 400 µl of upper phase was dried to a pellet using a vacufuge (Eppendorf, Hauppauge, NY), and then reconstituted in 50 µl of methanol/water (1:1, v/v). The samples were stored at −80°C until analysis. Tryptophan metabolites in the samples were detected and quantified on a triple quadrupole linear ion trap mass spectrometer (3200 QTRAP, AB SCIEX, Foster City, CA) coupled to a binary pump HPLC (Prominence LC-20, Shimazu, Concord, Ontario, Canada).

Flow Cytometry

Spleens and MLNs were processed individually to single-cell suspensions with frosted glass slides in RPMI-c + 10% FCS, and spleen cells underwent red blood cell lysis.[121] Cell suspensions were plated in individual wells, washed with 0.5% BSA in PBS, surface-stained for CD11b-AlexaFluor488 (eBioscience cat. #53-0112-82) and Gr-1-biotin (BD cat. #553125), followed by streptavidin-PE (eBioscience cat. #12-4317), fixed with 0.4% paraformaldehyde, and samples were acquired on a BD FACS Aria II in the College of Medicine Cell Analysis Facility (COM-CAF) at the Texas A&M Health Science Center.

Histology and Small Intestinal Morphometric Measurements

The stained sections of the small intestine were analyzed by a board-certified veterinary pathologist (BRW) blinded to treatment group. The slides were scored as previously described for intestinal inflammation.[122] Briefly, mucosal injury was determined by the following parameters scored from 0 (no evidence) to 3 (marked):

mucosal ulceration, mucosal erosion, and presence of squamified epithelium. Inflammatory changes were scored similarly based on the following parameters: lymphocytic infiltration, plasma cell infiltration, and neutrophilic infiltration. Finally, an overall evidence of injury score was used to document total injury graded from 0 (none) to 4 (marked). Morphological parameters were obtained from digitally scanned slides using SPOT vr 5.0 software. Three sets of measurements from 3 separate sections were recorded for each animal by an observer blinded to treatment group. Measurements consisted of villus height, crypt depth, and submucosal mural thickness. The ratio of the villus height to crypt depth was calculated (Figure A-1.1).

Data Analysis

Results were expressed as mean ± 95% confidence interval unless indicated otherwise. For all analyses, significance was set $P \leq 0.05$. Data were analyzed using S-PLUS statistical software (Version 8.2, TIBCO Inc., Seattle, WA) unless otherwise noted. Histology scores, the proportion of neutrophils in the spleen and MLNs, ratios of villus height to crypt depth, submucosal thicknesses, paired differences between Day 7 and Day 0 in phyla and families, and fecal tryptophan metabolites were compared among treatment groups using a generalized linear model with post hoc testing for pairwise differences among groups using the method of Sidak.[123] To meet statistical assumptions underlying the generalized linear model, the histology scores were converted to ranks and the neutrophil data were log10 transformed prior to analysis. Ratios of villus height to crypt depth and submucosal thicknesses were compared among groups using a generalized linear model with post hoc testing for pairwise differences

among groups using the method of Sidak. Fecal calprotectin concentrations were analyzed as a function of treatment group, time (Day 0 [baseline] and Day 7), and their interaction using linear mixed-effects modeling with treatment group and time modeled as fixed, categorical effects and individual mouse modeled as a random effect to account for repeated measures on individual mice. Paired differences between Day 0 and Day 7 in phyla and families were compared among groups using a generalized linear model and post hoc testing for pairwise differences among groups using the method of Sidak.

Results

Indole Reduced the Severity of NSAID Enteropathy

Calprotectin ELISA of fecal samples collected on days 0 and 6 revealed that co-administration of indole with indomethacin significantly decreased fecal calprotectin levels (Figure 1A). Moreover, attenuation of NSAID-induced small intestinal damage was confirmed by microscopic pathology scores (Figure 1B and C) of mice in which indole was co-administered with indomethacin. The reduction in mean microscopic pathology scores were corroborated by morphological parameters which revealed maintenance of villus height:crypt depth ratio (Figure 1D) and thickness of the submucosal layers (Figure A-1.1) in mice in which indole was co-administered. Indomethacin had a negligible effect on the large intestine (data not shown), consistent with evidence that indomethacin induces small intestinal ulcerations in mice in a location similar to where NSAIDs injure people.[29, 124-127]

Indole reduced indomethacin-induced neutrophilic infiltration of spleen and MLN

Neutrophilic inflammation is primarily responsible for NSAID enteropathy, therefore, we quantified the abundance of neutrophils in the spleen and MLNs as measures of systemic neutrophilic response and trafficking of neutrophils though the GI tract, respectively.[31, 33] Indomethacin treatment resulted in a significant increase in neutrophils (defined as both CD11b- and GR-1 double-positive; Figure A-1.2) in both the spleen (Figure 1E) and MLNs (Figure 1F), and co-administration of indole significantly decreased neutrophilic infiltration of these tissues.[128] Taken together, these data demonstrate that indomethacin induced small intestinal injury in mice that was accompanied by neutrophilic infiltration of the spleen and mesenteric lymph node and that co-administration of indole attenuated the small intestinal injury and limited neutrophilic infiltration of the spleen and MLN caused by indomethacin.

Pairwise ANOSIM R-values				
	Control	NSAID	Indole	NSAID+Indole
Control		**0.5487***	0.2	0.2813
NSAID	**0.5487***		0.2615	0.4444
Indole	0.2	0.2615		0.1938
NSAID+Indole	0.2813	0.4444	0.1938	

Table 1 Pairwise ANOSIM reveals differences between NSAID-treated and control mice**.**

Pairwise ANOSIM R-values based on the unweighted Unifrac distance metric at day 7. Only the difference between control and NSAIDs was significantly different than 0. * R values is significantly ($P < 0.05$) different than a value of 0.

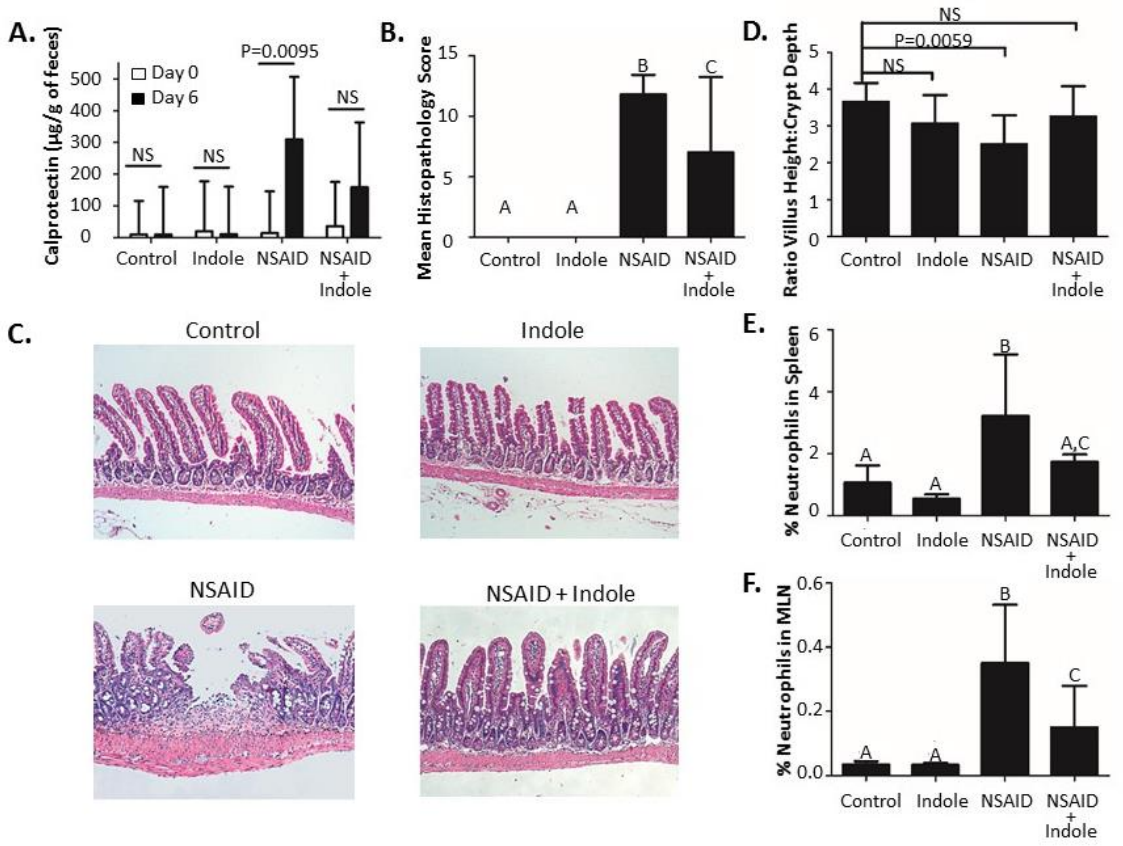

Figure 1 Indole attenuates severity of NSAID enteropathy.
A) Fecal calprotectin levels were determined by ELISA on fecal samples on Day 0 and then again after 6 days of therapy with indomethacin, indole, or the combination. B) Microscopic pathology scores from analysis of Swiss-rolled H&E stained small intestinal sections (n=5/group). Error bars represent 95% confidence intervals about the mean score. Groups with different letters differed significantly ($P < 0.05$). C) Representative H&E stained sections of small intestine. D) Ratio of villus height to crypt depth taken from small intestinal mucosa. E) % CD11b- and GR--positive cells (i.e., neutrophils) in the spleen after 7 days of treatment. F) % CD11b positive and GR-1-positive cells (i.e., neutrophils) in the mesenteric lymph nodes (MLN) after 7 days of treatment.

Indole Prevented Indomethacin-Induced Fecal Microbiota Shift and Alterations of the Inferred Metagenome

Because NSAIDs alter the intestinal microbiota, we evaluated the composition and diversity of the fecal microbiota in the 4 groups of mice. To adjust for uneven sequencing depth among the samples, each sample was rarefied to an even sequencing depth of 10,000 reads per sample prior to analysis. Alpha rarefaction curves and Good's coverage index estimates indicated that over 90% of the species were represented across all samples at this sequencing depth (Figure A-1.3). Using analysis of similarities (ANOSIM), no significant difference in the unweighted Unifrac distance metric among the groups was observed on day 0 (R=0.10; P=0.11); however, by day 7 there was a significant difference among the groups (R=0.3007; P=0.0031). Pairwise comparisons between groups revealed that a significant difference in the Unifrac distance metric existed only between NSAID and control animals (Table 1) and that co-administration of indole with indomethacin attenuated this change in the beta diversity of the fecal microbiota.

The primary gram-positive and gram-negative phyla found in murine feces are Firmicutes and Bacteroidetes, respectively.[129] At the phylum level, PCA revealed a separation of NSAID-treated mice from the other groups characterized by increase in members of the phyla Bacteroidetes in the NSAID-treated animals between day 0 and day 7 (Figure 2A and 2B). Interestingly, PCA revealed qualitatively that co-administration of indole counteracted the increase in Bacteroidetes and instead appeared to shift the group closer to the phylum Firmicutes. Based on the results of PCA, we

compared the abundance of members of the phyla Firmicutes and Bacteroidetes and found no significant difference after treatment with NSAIDs, indole, or their combination (Figure A-1.4). At lower taxonomic levels, however, significant differences were observed. For example, co-administration of indole with indomethacin prevented a decrease in Clostridiales and instead this group had a significant increase in several members of the Clostridales order (Figure 2C). Furthermore, similarity percentage (SIMPER) based on the Bray Curtis dissimilarity measure at phylum, order, and family levels further confirmed that indomethacin treatment resulted in the gain of members of the Bacteroidales S24-7 family, a major family of Bacteroidetes found in murine feces, indicating that gain in this family contributed to the dissimilarity between NSAID and the other groups.[130] Co-administration of indole prevented this increase in Bacteroidales and instead resulted in an increase in Clostridiales with marginal increases in several other members of the Firmicutes phyla (Figure 2D).

PCA of the inferred metagenome revealed clustering and separation of the NSAID-treated mice from the other groups (Figure 2E and 2F), although ANOSIM based on the Bray Curtis dissimilarity metric indicated this difference was not significant ($P>0.05$). Consistent with the microbiota data, the distance among groups was greatest between the NSAID group and the NSAID + indole group. The major up- and down-regulated inferred functional pathways between NSAID and NSAID + indole groups were tabulated (Table A-1.1).

Figure 2 Indole increases abundance of Clostridiales and prevents NSAID-induced shift of the microbiota and inferred metagenome.

A) Principal component analysis (PCA) plots of 16S rRNA sequencing of the fecal microbiota at the phylum level with biplot overlay and ANOSIM based on the unweighted Unifrac distance metric (located in the lower right quadrant) of the OTU table from day 0 revealed no significant differences among the groups at day 0. The area of the gray shaded shapes reflects the variation among individuals in a group. B) Principal component analysis (PCA) plots of 16S rRNA sequencing of the fecal microbiota at the phylum level with biplot overlay and ANOSIM based on the unweighted Unifrac distance metric (located in the lower right quadrant) of the OTU table from day 7 reveal that there is a significant difference among the groups at day 7. After 7 days, the NSAID group is significantly shifted from the other 3 groups, and this shift was associated with a qualitative increase in the phylum Bacteroidetes and loss of Firmicutes. C) Abundance of *Clostridales* from Day 0 (orange) and Day 7 (green) and *Bacteroidales* Day 0 (white) and Day 7 (black). *Clostridiales* were significantly increased on Day 7 relative to Day 0 by co-administration of indole with the NSAID indomethacin. D) Mean abundance of several families of *Clostridiales* at Day 0 and Day 7 for each of the treatment groups depicting reduction of these families following NSAID therapy but expansion indole is co-administered. E) PCA plots of inferred metagenome of the fecal microbiota from Day 0. ANOSIM based on the Bray Curtis distance measure revealed no significant difference among the groups at day 0. F) PCA plots of inferred metagenome of the fecal microbiota from Day 7. ANOSIM based on the Bray Curtis distance measure revealed that, consistent with the microbiota data, the NSAID group visually separated from the other groups; however, this apparent difference was not significant ($P > 0.05$ by ANOSIM based on Bray Curtis dissimilarity measure).

PCA Microbiota Phylum Level Day 0

A

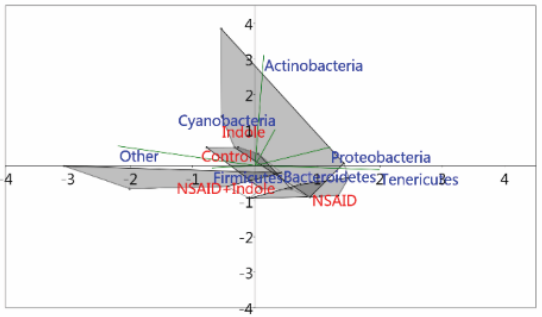

PCA Microbiota Phylum Level Day 7

B

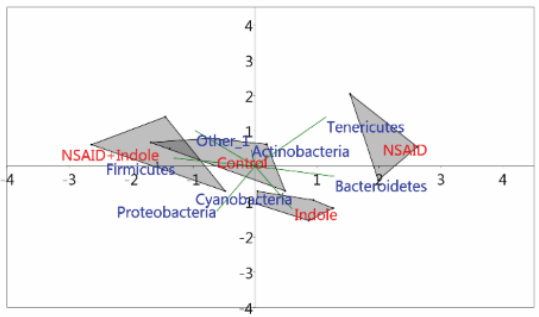

C

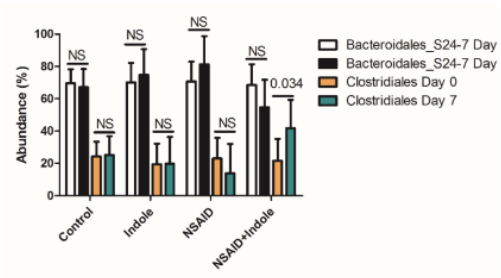

D

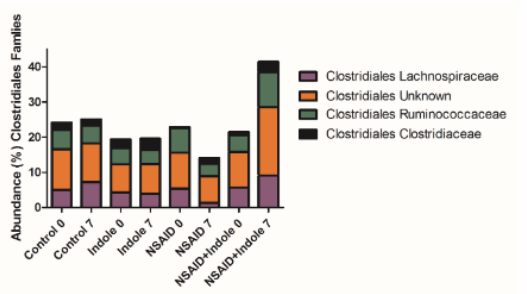

PCA Inferred Metagenome Day 0

E

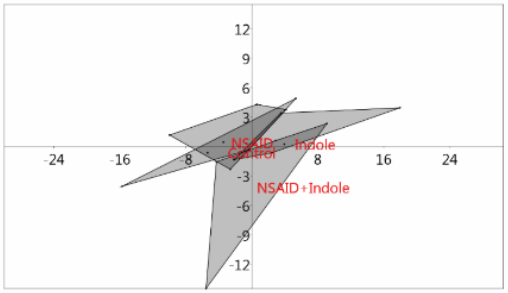

PCA Inferred Metagenome Day 7

F

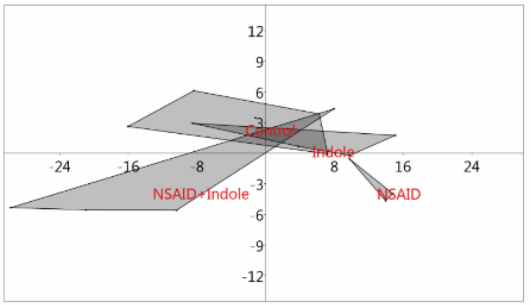

Co-administration of Indole Prevents the Indomethacin-induced Tryptophan-derived Metabolite Disruption in Feces

We have identified multiple tryptophan-derived metabolites produced by the microbiota predicted to be bioactive and exert effects on the host.[91] Given the importance of the microbiota in NSAID enteropathy, we chose to examine whether the effects of indole on the intestinal epithelium and microbiota (Figure 2) were correlated with tryptophan metabolites. No single tryptophan metabolite was significantly correlated with fecal calprotectin (data not shown). Only the metabolite tyramine was significantly ($P<0.01$) correlated with microscopic pathology scores (Table A-1.2). Examination of the fecal profile of all tryptophan metabolites using PCA revealed a visible separation of the NSAID-treated mice from the remaining groups on day 7, while co-administration of indole appeared to prevent this separation, however, ANOSIM of the Bray Curtis dissimilarity measure indicated this apparent difference was not significant ($P=0.55$) (data not shown). Examination of tryptophan metabolite concentrations by treatment group revealed a significant increase in tyramine in the NSAID group that was attenuated by co-administration of indole (Table 2); moreover, several other tryptophan metabolites tended to be increased only in the feces of mice treated exclusively with indomethacin, indicating that NSAID treatment caused differences that were attenuated by co-administration of indole (Table 2). Relative to controls, mice in the indole-only and indomethacin-only groups had significantly more indole; although fecal indole concentrations were generally higher in the NSAID + indole mice, this difference was not significant.

Metabolite	Group effect	Magnitude (95% CI)	P value
5-Hydroxytryptamine	↑ NSAID only	13.9 (-1.4 to 29.3)	0.1029
5-Hydroxyindole	↑ NSAID only	27.2 (-2.2 to 56.6)	0.0657
Arginine	↔		
Glutamine	↔		
Indole-3-acetamide	↔		
Indole-3-acetate	↔		
Indole-3-carboxaldehyde	↔		
Indole	↑ NSAID	6.7 (1.6 to 28.2)	0.0255
	↑Indole	5.3 (1.1 to 24.7)	0.0364
	↑NSAID + Indole	4.7 (0.9 to 24.7)	0.0641
Kyneurine	↔		
Ornithine	↔		
Phenylalanine	↔		
Serotonin	↑ NSAID only	1.6 (-0.3 to 3.5)	0.0895
Tryptamine	↔		
Tryptophan	↔		
Tyramine	↑ NSAID only	6.7 (1.3 to 33.6)	0.0024
Tyrosine	↔		

Table 2 NSAID treatment altered fecal concentrations of tryptophan-derived metabolites.
Group effects of tryptophan-derived metabolites identifying the direction and magnitude of change in fecal concentration between Days 0 and 7. Several tryptophan-derived metabolites tended to be increased in the NSAID treated mice (5-hydroxytryptamine, 5-hydroxyindole, indole, serotonin, tyramine). Fecal concentrations of indole increased in the groups in which indole was administered.

Co-administration of Indole Attenuates NSAID-induced Pro-inflammatory Mucosal Transcriptomic Changes

We performed RNA-Seq of the distal small intestinal mucosa to examine the in vivo transcriptomic changes associated with NSAID enteropathy and to gain insight into how the co-administration of indole altered gene expression. The Ingenuity Pathway Analysis software package was used to identify pathways represented by differentially expressed genes. Several canonical pathways were altered in NSAID-treated mice relative to controls (Figure 3A). Several of the pathways that were modulated by NSAID administration were either shifted to the opposite direction (i.e., inhibited or activated, respectively), or the degree of activation or inhibition was markedly attenuated by co-administration of indole (Figure 3B). Moreover, transcription of specific pro-inflammatory cytokines (interleukin [IL]-1α, IL-1β, TNF, IL-6) and chemokines (CXCL1, CXCL3, CXCL2, CXCL5, CCL2, CCL7) was significantly up-regulated in NSAID-treated mice; however, when indole was co-administered the degree of up-regulation was not significantly different than control mice (Figure A-1.5). Based on our results, a proposed schema of the interaction of NSAIDs, the host mucosal epithelium, the microbiota, and indole is presented (Figure 4).

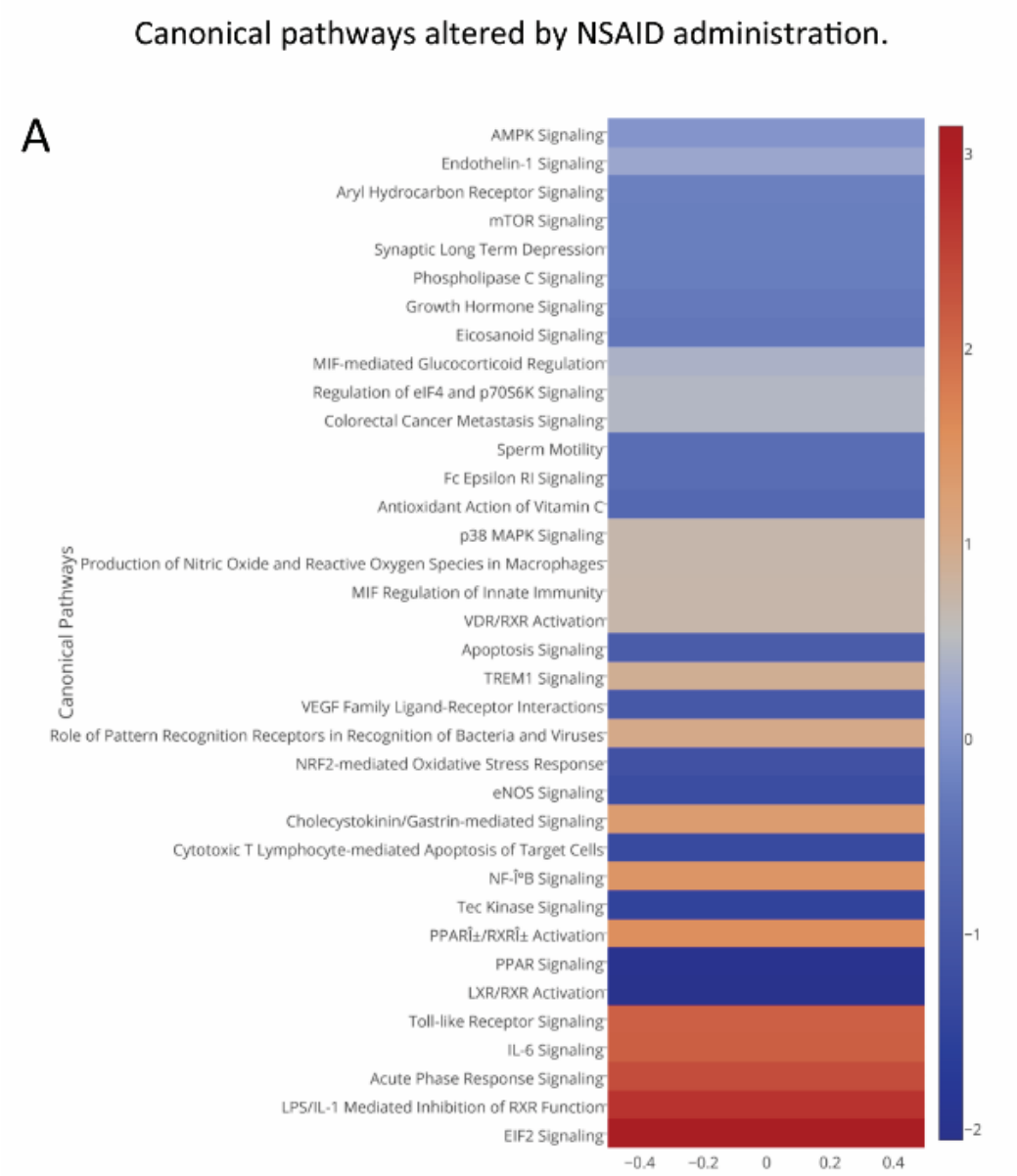

Figure 3 NSAID enteropathy results in upregulation of innate immune response pathways and the co-administration of indole regulates this response.
A) Heatmap showing upregulated (red) and down regulated (blue) pathways in the small intestinal mucosa from NSAID-treated mice compared with control animals. B) 2-column heatmap showing upregulated (red) and down-regulated (blue) pathways in the small intestinal mucosa from NSAID-treated mice compared with control mice (left column) and NSAID + indole versus control mice (right column).

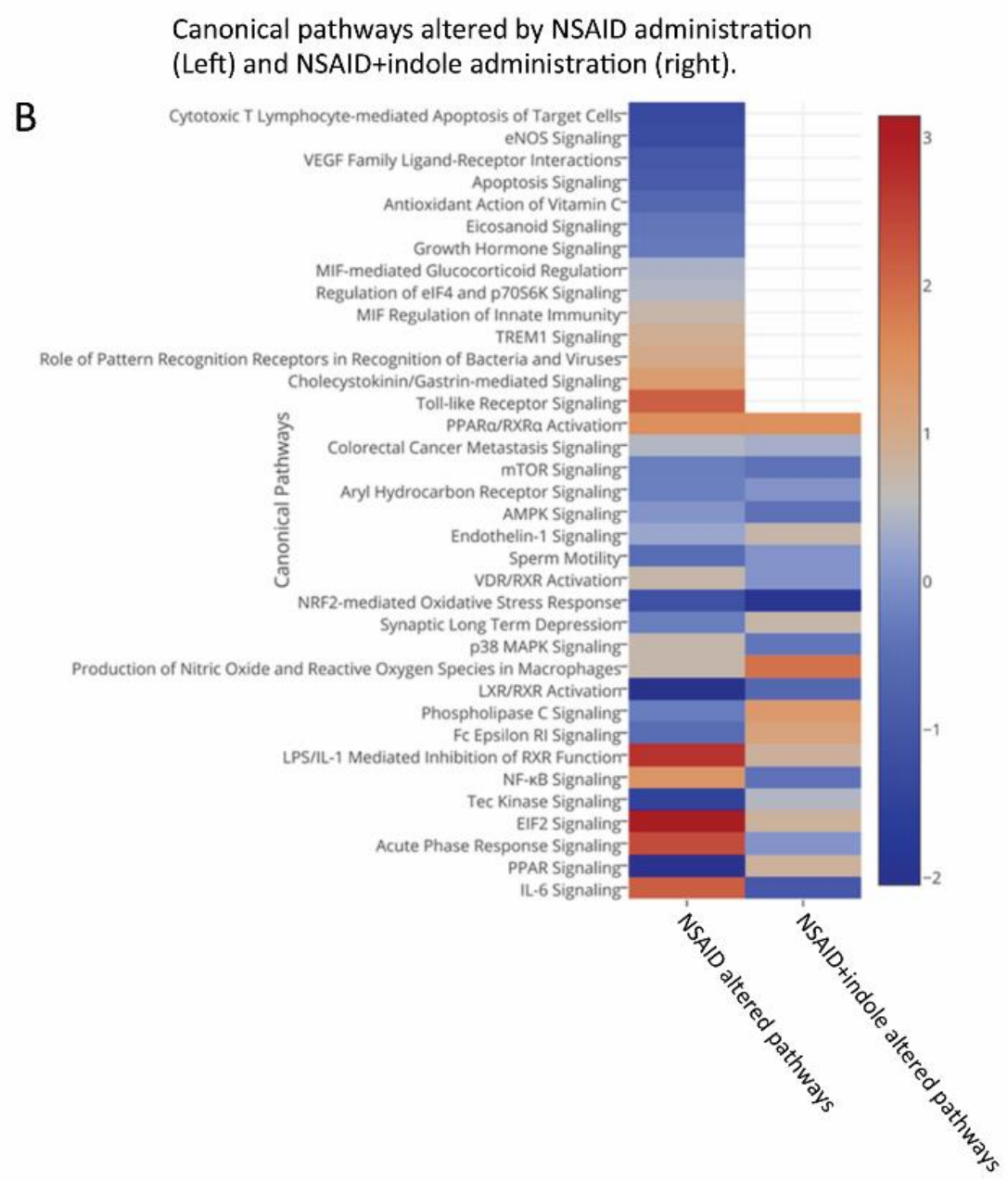

Figure 3 Continued

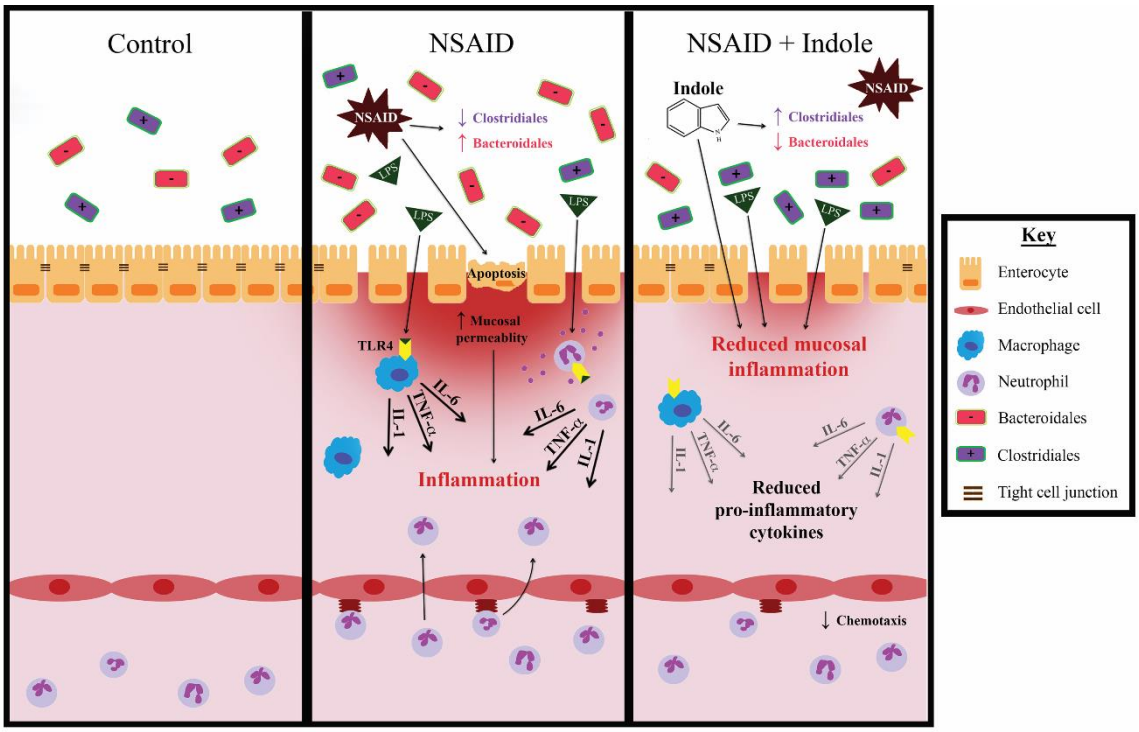

Figure 4 Co-administration of indole with indomethacin attenuates NSAID enteropathy and indole may exert these beneficial effects through several possible mechanisms. NSAID enteropathy is characterized by a loss of barrier function resulting in an influx of luminal contents and a massive innate immune response. Indole is known to have direct effects on intestinal epithelial cells including upregulation of tight-cell junctional proteins, effects on immune responses including inhibition of NF-κB, and regulating the overall innate immune response. Moreover, co-administration of indole with NSAID administration resulted in an increase in the abundance of F*irmicutes*, principally *Costridales*, known to be important in maintaining intestinal homeostasis, and appeared to prevent any increase in *Bacteroidales*.

Discussion

Co-administration of indole attenuated small intestinal mucosal damage induced by administration of indomethacin in mice as manifested by reduced microscopic pathology and fecal calprotectin concentration. Fecal calprotectin is a well-established, non-invasive indicator of intestinal mucosal injury induced by NSAIDs in human patients and animal models, and correlates well with 4-day fecal excretion of 111Indium-labelled leukocytes.[72, 131] The findings of decreased fecal calprotectin and decreased microscopic pathology have important clinical implications. A variety of NSAIDs are used widely for an array of clinical conditions ranging from pain-relief for minor injuries to management of rheumatoid arthritis or cancer. The relatively low cost, high effectiveness, and lack of alternatives to NSAIDs indicate that their use will continue to be highly prevalent. Consequently, agents that might be co-administered with NSAIDs to diminish NSAID enteropathy would be clinically important. Further evaluation of indole to ameliorate NSAID enteropathy in animal models and naturally-occurring disease is warranted by our findings.

Administration of NSAIDs increases the proportion of gram-negative organisms at the expense of gram-positive organisms in the intestinal microbiota, and this shift has been shown to contribute to NSAID-induced intestinal injury.[25, 43, 78] Specifically, NSAID administration decreases various members of the class Clostridia and increases members of the class Bacteroidia.[41] Mice treated with indole and indomethacin did not have a change in the abundance of Bacteroidia but did have an increase in several members of the gram-positive family Clostridiales in concert with diminution of the

severity of intestinal mucosal damage. Evidence exists that the microbiota plays an important role in the development of NSAID enteropathy. Germ-free rats treated with NSAIDs develop less severe enteropathy than specific-pathogen-free rats or germ-free rats that have been colonized with gram-negative bacteria.[57] Toll-like receptor (TLR) 4-deficient mice develop less severe lesions than isogeneic TLR4-competent strains.[25] Dramatic NSAID-induced alterations of the gut microbiota are well-documented and most often characterized by a loss of gram-positive bacteria with a concurrent increase in gram-negative bacteria.[38, 78] Moreover, this particular shift in the microbiota has been associated with increased severity of intestinal mucosal injury, and preventing this shift can reduce mucosal injury.[39] The classic indomethacin-induced increase in types of Bacteroidia we observed in our study were not significant, but this was likely attributable to limited power to detect a statistically significant difference resulting from our small sample size. It is not clear why increased abundance of gram-negative bacteria worsens the severity of NSAID enteropathy, but direct effects of LPS and the host innate immune response to LPS appear to be important.[23, 39] It is also possible that loss of beneficial gram-positive bacteria is important. Commensal Clostridia have been shown to be critically important in gut homeostasis, specifically members of Clostridium cluster XIVa and Clostridium cluster IV.[132] Interestingly, several members of these 2 clostridial clusters were increased in the NSAID-treated animals in which indole was co-administered.

The host response to the microbiota might be more important than the microbiota itself in the pathogenesis of NSAID enteropathy. Neutrophils are key effector cells of

innate immunity and are critically important in the pathogenesis of NSAID enteropathy.[31, 133] Neutrophils are recruited to the site of injury by the influx of luminal contents following increased mucosal permeability. The resident innate immune cells present in the epithelium and lamina propria release cytokines and chemokines that attract circulating neutrophils. These neutrophils, along with other innate immune cells, then release pro-inflammatory cytokines, typically characterized by an abundance of the IL-1 super family, TNF-α, IL-6, and others, that are responsible for the damage to the lower GI tract.[30, 134] This critical role for neutrophils in NSAID enteropathy is supported by our findings of neutrophilic infiltration of both the spleen and MLN following NSAID administration and reduced neutrophil concentrations in these tissues with co-administration of indole. Our data also affirm the importance of the innate immune response in the pathophysiology of NSAID enteropathy because many of the most up-regulated pathways identified by RNA-Seq reflected the innate immune response (viz., NF-κB pathway, TLR signaling pathways, and the LPS/IL-1 response). Moreover, at the individual gene level, several of the classic pro-inflammatory cytokines associated with neutrophil activation and known to be important in NSAID enteropathy (e.g., TNF-α, IL-1, and IL-6) were up-regulated among NSAID-treated mice.[30, 135, 136] Co-administration of indole, however, attenuated or reversed up-regulation of genes associated with innate immunity and inflammation that contribute to the pathogenesis of NSAID enteropathy. In addition, several chemokines that attract neutrophils were up-regulated in the NSAID-treated mice and this up-regulation was dramatically attenuated by the co-administration of indole. These data indicate that

indole can mitigate the host innate immune response to the influx of luminal contents across injured epithelia. Indole has been shown to inhibit NF-κB signaling in intestinal epithelial cells.[92] It is thus plausible that indole exerts similar effects on neutrophils and other innate immune cells, thereby reducing cytokines dependent upon NF-κB signaling. Although NF-κB signaling was activated by administration of both NSAID and NSAID + indole, activation of this pathway was greatly diminished by co-administration of indole with NSAIDs, suggesting indole might mitigate NSAID damage in part by inhibiting NF-κB. It is important to note that the mRNA for RNA-seq was isolated from mucosal scrapings. These scrapings likely contain epithelial cells as well as cells residing in the lamina propria (i.e., immune cells recruited to the inflamed gut due to loss of barrier function) and therefore we cannot be sure the exact source of gene expression profiles. NSAID enteropathy is characterized as a mucosal injury and we felt examining the transcriptome of this location would be more informative than examining the transcriptome of whole tissue.[137] The observed anti-inflammatory effects of indole may be due to indole's effects on epithelial cells, immune cells in the lamina propria, or both.

It is unclear how indole prevented the characteristic shifts in the composition of the microbiota associated with NSAID administration. Indole has long been recognized as a quorum-sensing molecule so it is possible that indole directly affected the microbial community by acting as an intra-kingdom signaling molecule.[102, 103] It is, however, also plausible that changes in the microbiota associated with NSAID use occur secondary to mucosal inflammation because mucosal inflammation has been shown to

alter the luminal environment.[51] Indole might have attenuated mucosal damage, which in-turn prevented the expected changes in the microbiota. Finally, it has been shown that GI microbiota can vary with environment including cage-dependent variation and cage-dependent clustering.[138] In order to mitigate this phenomenon, after acclimation and immediately prior to starting the study (Day 0), we randomly assigned mice into treatment groups and then moved them into cages based on the group to which they were randomly assigned. There were no significant differences in the fecal beta diversity among the groups at day 0. It is possible, however, that were some cage-dependent microbiota changes that occurred over the 7 days of treatment that might have influenced the composition of the microbiota after treatment.

Indole is present in the GI tract of humans and animals at relatively high concentrations (~250-1,100 μM).[139, 140] It has been speculated that, because intestinal epithelial cells are continually exposed to indole, indole may act as an interkingdom signaling molecule. Indeed we have shown, in vitro, that indole does behave in this manner and has anti-inflammatory effects on intestinal epithelial cells and upregulates expression of genes associated with tight cell junctions.[92] We therefore expected increasing the concentration of indole within the lumen of the GI tract might mitigate NSAID enteropathy because of the in vitro effects of indole on intestinal epithelial cells. As expected, we observed that mice gavaged with indole (alone or in combination with indomethacin) had increased fecal concentration of indole. Interestingly, the NSAID-only treated mice also had increased fecal concentrations of indole. Although both gram-negative and gram-positive bacteria produce indole, the list

of gram-negative bacteria known to produce indole is much larger than gram-positive bacteria.[103] Thus, the observed increase in gram-negative bacteria in the NSAID treated mice might explain their increased fecal concentrations of indole. The beneficial effects of indole in this study were observed at the distal small intestine, but the concentration of indole and the microbiota diversity were determined using fecal samples. Fecal metabolite and microbiota characterization do not always correlate well with those of more proximal mucosal locations in the GI tract.[141, 142] Therefore, it is possible that indole was present in higher concentrations in the distal small intestine of mice treated with NSAID combined with indole compared with mice treated with the NSAID alone, thus contributing to the attenuation of NSAID-induced injury by indole administration. Interestingly, several tryptophan metabolites that act as neurotransmitters including serotonin and 5-hydroxytryptamine were also increased in NSAID-treated mice. Hypermotility of the GI tract is induced by NSAIDs and contributes to the pathophysiology of NSAID enteropathy.[143, 144] The microbiota shift induced by NSAIDs might result in production of prokinetic metabolites that contribute to GI hypermotility.

In summary, indole supplementation of mice attenuates the deleterious effects of NSAIDs on the distal small intestine and modulates NSAID-induced alterations in the composition of the fecal microbiota. The major events in the onset of NSAID enteropathy are intestinal epithelial cell death, increased mucosal permeability, influx of luminal contents, and host innate immune response to the microbiota.[43, 145, 146] Indole likely reduces intestinal injury induced by NSAIDs at multiple levels, including

neutrophilic infiltration, NSAID-induced dysbiosis, and pro-inflammatory pathways in the distal small intestine. Future work will focus on interrogating the potential mechanisms by which indole exerts this beneficial effect in order to further elucidate means to control or prevent NSAID enteropathy.

CHAPTER III

NON-INVASIVE TRANSCRIPTOME IS REFLECTIVE OF TISSUE-LEVEL TRANSCRIPTOME IN A MOUSE MODEL OF NSAID ENTEROPATHY

Introduction

Non-steroidal anti-inflammatory drugs (NSAIDs) are among the most frequently consumed pharmaceuticals worldwide because of their anti-inflammatory, anti-neoplastic, and analgesic effects. Their use, however, can result in an enteropathy that has an alarmingly high rate of morbidity and mortality. In the United States alone, NSAID enteropathy results in approximately 100,000 hospitalizations and 16,500 deaths each year [98]. An additional 2/3 of both short- and long-term NSAID users develop subclinical or undiagnosed distal small intestinal lesions [99]. Although detection and management of NSAID-induced lesions of the proximal GI tract (i.e., gastropathy) have been well documented, diagnosis and treatment of NSAID-induced damage of the GI tract distal to the duodenum (also known as NSAID enteropathy, affecting primarily the distal jejunum and ileum) remains elusive [96, 97]. The incidence of NSAID enteropathy is expected to increase due to greater use of NSAIDs for the treatment of rising numbers of inflammatory conditions, by the aging population of North America, and for their anti-neoplastic effects [147]. The lower GI tract of multiple mammalian species is affected by NSAIDs in a similar manner in terms of location and type of injury, and magnitude of the clinical complications [148-150].

The pathophysiology of NSAID enteropathy is complex and poorly understood [100]. It has been proposed to involve deleterious effects of NSAIDs on the intestinal mucosa including enterocyte cell death, increased mucosal permeability, and interaction of the damaged mucosa with luminal contents including bacteria (GI microbiota) and bacterial products or components such as lipopolysaccharide (LPS) [97, 137]. The resulting inflammatory cascade is mediated by the innate immune response to LPS and several pro-inflammatory cytokines including tumor necrosis factor (TNF), interleukin (IL)-1, and IL-6 [25, 151, 152]. The GI microbiota has recently been implicated as an important contributor to NSAID enteropathy, with the host-microbiota interaction playing a critical role in the pathophysiology of NSAID enteropathy although the exact mechanisms remain to be elucidated [23, 39, 42, 49, 78].

An important limitation to understanding the pathogenesis of NSAID enteropathy (and other gastrointestinal disorders) is the difficulty in obtaining longitudinal (sequential) data from individuals regarding intestinal function and health. Great clinical and investigative need exists for the development of non-invasive methods to characterize the health and function of the GI tract distal to the stomach to more effectively identify, study, and manage NSAID enteropathy (and other intestinal mucosal disorders).

Up to 1/3 of human colonic epithelial cells (up to 10^{10} cells in an adult) are exfoliated and shed in feces each day [153]. Isolation and sequencing the mRNA (host transcriptome) from exfoliated intestinal epithelial cells (IECs) has been validated in the context of colon carcinogenesis in rats and humans, and in characterizing human

neonatal gastrointestinal development [154-158]. Exfoliated IECs, however, have not been utilized to evaluate the small intestine. The exact number of cells exfoliated from the small intestinal mucosa in human stool is unknown, and it is thus unknown whether evaluating the exfoliated cell transcriptome of feces can be informative and accurate for small intestinal lesions. Thus, the objective of this study was to determine whether exfoliated IECs could be a suitable non-invasive approach for identifying and studying NSAID enteropathy in a murine model. Specifically, we performed RNA-Seq on both small intestinal mucosa and exfoliated IECs in feces. We then applied novel computational approaches, e.g., linear discriminant analysis (LDA) and sparse canonical correlation analysis (CCA), to analyze the inter-relatedness of these data. The goals of these studies were: 1) to determine whether the transcriptome of exfoliated IECs is reflective of that of the small intestinal mucosa; 2) to demonstrate that the transcriptome of exfoliated IECs can be used to differentiate healthy and diseased phenotypes; and, 3) to generate hypotheses regarding key biological pathways and processes involved in the pathogenesis of NSAID enteropathy.

Materials and Methods

Animals and Sample Collection

Animal protocols were approved by the Texas A&M Institutional Animal Care and Use Committee in accordance with appropriate institutional and regulatory bodies' guidelines. Animals were handled and treated as previously described [32]. Briefly, eight- to 10-week-old specific-pathogen-free C57BL/6J mice were purchased and allowed to acclimate for 2 weeks. Mice were fed standardized laboratory rodent diet and

sterile water ad libitum. Mice were randomly divided into the following 4 groups (n=5 mice/group): 1) NSAID (indomethacin); 2) indole; 3) NSAID + indole; and, 4) untreated controls. Mice were then rehoused on the basis of treatment group assignment, with 5 animals/group-cage. To induce NSAID enteropathy, mice in group 1 were gavaged once daily with indomethacin (5 mg/kg; for 7 days; Sigma Aldrich, St. Louis, MO) dissolved in DMSO (Sigma Aldrich, St. Louis, MO) and further diluted in phosphate buffered saline (PBS). Mice in group 2 received indole by gavage (20 mg/kg; once daily for 7 days; Sigma Aldrich, St. Louis, MO) dissolved in sterile water warmed to 55°C. Mice in group 3 received indole co-administered with indomethacin by gavage at the dosages described above. All mice were gavaged with equal volumes (200 μL) and equal concentrations of DMSO (0.001%). Feces were collected daily by placing individual animals in sterile plastic cups that were RNase- and DNase-free until they passed feces. The mice were immediately returned to their home cages and the feces immediately flash frozen at -80°C.

Extraction of mRNA from Exfoliated Intestinal Epithelial Cells and Library Preparation

PolyA+ RNA was isolated from stool samples from mice similarly as previously described [158, 159]. Each mouse sample was processed with the NuGEN Ovation 3′-DGE kit (San Carlos, CA) to convert RNA into cDNA followed by NuGEN Encore Rapid Library kit to create Illumina libraries, as per manufacturer's instructions. Sequencing on Illumina HiSeq 2500 platforms (San Diego, CA) were carried out using standard Illumina protocols. Briefly, 30 ng of each sample were used to synthesize first and second strand cDNA, which was purified using Agencourt RNAClean XP beads

(Brea, CA) included in the kit. The cDNA was linearly amplified using the NuGEN SPIA primer, and cDNA quality and quantity were determined using an Agilent 2100 Bioanalyzer and Nanodrop spectrophotometer. Two micrograms of cDNA were fragmented using a Covaris S2 sonicator with the following settings: duty cycle 10%, intensity 5, cycles/burst 100, time 5 min. Fragmented samples were concentrated using the MinElute Reaction Cleanup kit (Qiagen, Venlo, Netherlands) as per manufacturer's instructions. Samples were quantified using the Nanodrop. Following cDNA fragment repair and purification, Illumina adaptors were ligated onto fragment ends followed by amplification to produce the final library. Libraries were quantified using the Kapa Library Quantification kit (Kapa Biosystems) and run on an Agilent DNA High Sensitivity Chip to confirm appropriate sizing and the exclusion of adapter dimers.

Tissue mRNA Extraction and Library Preparation

RNA was extracted from ileal mucosal scrapings using an RNeasy mini kit (QIAGEN, Redwood City, CA) following the manufacturer's instructions and including on-column DNase treatment. RNA quantity was determined using a Nanodrop spectrophotometer (Fisher Thermoscientific) and the quality was assessed using the Nano6000 chip on a Bioanalyzer 2100(Agilent Technologies). Only RNA with an integrity number (RIN) > 8 was used. The samples were randomized prior to RNA-Seq library preparation. Sequencing libraries were made using 250 ng of RNA and the TruSeq RNA Sample Preparation kit (Illumina) following the manufacturer's instructions. A volume of 2.5 µl of ERCC spike-in RNA control mix (Life Technologies) was added to the starting RNA at a dilution of 1:1000.

RNA Sequencing and Downstream Processing

Libraries were pooled and sequenced on an Illumina HiSeq 2500 at the Texas AgriLife Genomics and Bioinformatics Services Core Facility (College Station, TX). Sequence data were uploaded into NCBI small reads archive (Accession number PRJNA290483). Sequencing data were provided in a de-multiplexed format and aligned using Spliced Transcripts Alignment to a Reference (STAR) software with default parameters and referenced against the genome of Mus musculus (Ensembl version GRCm38) [106]. Differentially expressed genes were determined using EdgeR based on the matrix of gene counts [107]. Gene pathway involvement and intersections were analyzed using QIAGEN's Ingenuity ® Pathway Analysis (IPA, QIAGEN, Redwood City, CA http://www.qiagen.com/ingenuity) by uploading appropriate gene lists with fold change and false discovery rate (FDR) P-values.

Sparse Canonical Correlation Analysis (CCA)

In order to take into account the multivariate structure when assessing and ranking genes, we analytically quantified the multivariate relationships between the exfoliated cell and tissue transcriptomic data sets. Sparse CCA provides measures of the strength of multivariate association between variable sets as well as a means to interpret the role of variables in terms of the underlying multivariate relationship [157]. Briefly, for the two random vectors $\mathrm{x} = (x_1, x_2, \dots, x_p)^T$ and $\mathrm{y} = (y_1, y_2, \dots, y_q)^T$ CCA aims to find two projection directions $u_1 \in \mathbb{R}^p$ and $v_1 \in \mathbb{R}^q$ so that

$$(u_1, v_1) = \underset{u,v}{\operatorname{argmax}}\, \operatorname{Corr}(u^T x, v^T y) = \underset{u,v}{\operatorname{argmax}} \frac{u^T \Sigma_{xy} v}{\sqrt{(u^T \Sigma_{xx} v)\left(v^T \Sigma_{yy} v\right)}},$$

where, $\Sigma_{xy}, \Sigma_{xx}, \Sigma_{yy}$ are covariance and variance matrices. Let X and Y denote $n \times p$ and $n \times q$ data matrices as the observations from random vectors x and y, respectively. Then the empirical version of the above objective function can be written as

$$\begin{aligned} \max_{u,v} \quad & u^T X^T Y v \\ \text{subject to} \quad & u^T \frac{X^T X}{n} u = 1,\ v^T \frac{Y^T Y}{n} v = 1. \end{aligned}$$

This objective function, however, does not have closed-form solution when the sample size n is less than $\min(p, q)$. In addition, the result does not perform variable selection and hence usually lacks biological interpretability. To overcome these limitations the sparse CCA adds a regularization conditions to obtain the sparse solution with a reduced the computational cost as previously described [160-162]. The main idea of this approach is to utilize

$$\begin{aligned} \max_{u,v} \quad & u^T X^T Y v \\ \text{subject to} \quad & u^T X^T X u \leq 1,\ v^T Y^T Y v \leq 1 \\ & \| u \|_1 \leq c_1,\ \| v \|_1 \leq c_2, \end{aligned}$$

where the tuning parameters c_1, c_2, are positive. It has been shown that in high-dimensional problems, treating the covariance matrix as a diagonal one yields satisfactory results [160,161]. Thus,

$$\begin{aligned} \max_{u,v} \quad & u^T X^T Y v \\ \text{subject to} \quad & \| v \|_2 \leq 1,\ \| u \|_2 \leq 1, \\ & \| u \|_1 \leq c_1,\ \| v \|_1 \leq c_2, \end{aligned}$$

yields the first pair of sparse canonical correlation loadings. The algorithm to solve this

optimization problem uses soft-thresholding, binary search, and finds the second pair of sparse canonical correlation components via the deflation method [160,163]. In our implementation of the sparse CCA method, a pair of tuning parameters (c_1, c_2) with values between 0 and 1 were utilized. To select the tuning parameters, the leave-one-out cross validation was used. Specifically, a grid of dense values from $(0,1) \times (0,1)$ were used as potential values of (c_1, c_2) and the absolute value of correlation without penalty was calculated as the criterion function in a cross validation method.

Linear Discriminant Analysis (LDA)

We used the edgeR output of genes differentially expressed between NSAID and control animals with false discovery rate (FDR) P value of less than 0.05 for feature set identification. Subsequently, we used a previously described method to determine, within the differentially expressed genes, which genes (1-feature) or pairs of genes (2-feature) accurately discriminated NSAID treated animals from control animals as given by the classification error rates [155]. Estimation of the classification error is of critical importance when the number of potential feature sets is large. When sample size is limited, an error estimator may have a large variance and, therefore, may often be low, even if it is approximately unbiased. This can produce many feature sets and classifiers with low error estimates. In this case, the problem was mitigated by applying a bolstered error estimation technique that has been previously described.[155, 164] The result of this approach is a list of feature sets (1 and 2-feature) that are ranked with respect to their bolstered classification error estimates.

Results

Data Pre-processing and Normalization

RNA sequencing reads for mucosal scrapings and exfoliated IEC's mapped to 25,907 genes and 22,783 genes, respectively. Genes present in low abundance (i.e., ≤ 4 animals or ≤ 20 times) across all samples, were removed from both datasets and the remaining genes subjected to downstream analysis. This reduced the number of transcripts for downstream analysis in the exfoliated IEC data-set to 13,884 genes and mucosal scrapings to 19,255 genes. Although the total number of genes in the tissue were reduced by 16% and in the exfoliated IEC data by 39% due to filtering, the total number of reads was negligibly affected (tissue reduced from 520,911,030 reads across all samples to 520,870,404 – a 0.008% reduction; exfoliated IEC data reduced from 59,406,107 to 59,338,338 – a 0.001% reduction). Total gene counts and the number of reads/gene obtained for each sample of the raw, filtered data for both tissue and exfoliated IEC data-sets are shown (Figure 5a-d. Given the apparent between-sample variation in total mapped reads (Figure 5b), especially as compared with the tissue data, we investigated if this was due to differences in library size. Examination of the relative abundance of 500 murine house-keeping genes in each sample indicated that indeed, differences in between-sample total counts were represented by similar magnitudes of differences in abundance of these 500 house-keeping genes (Figure 5e).

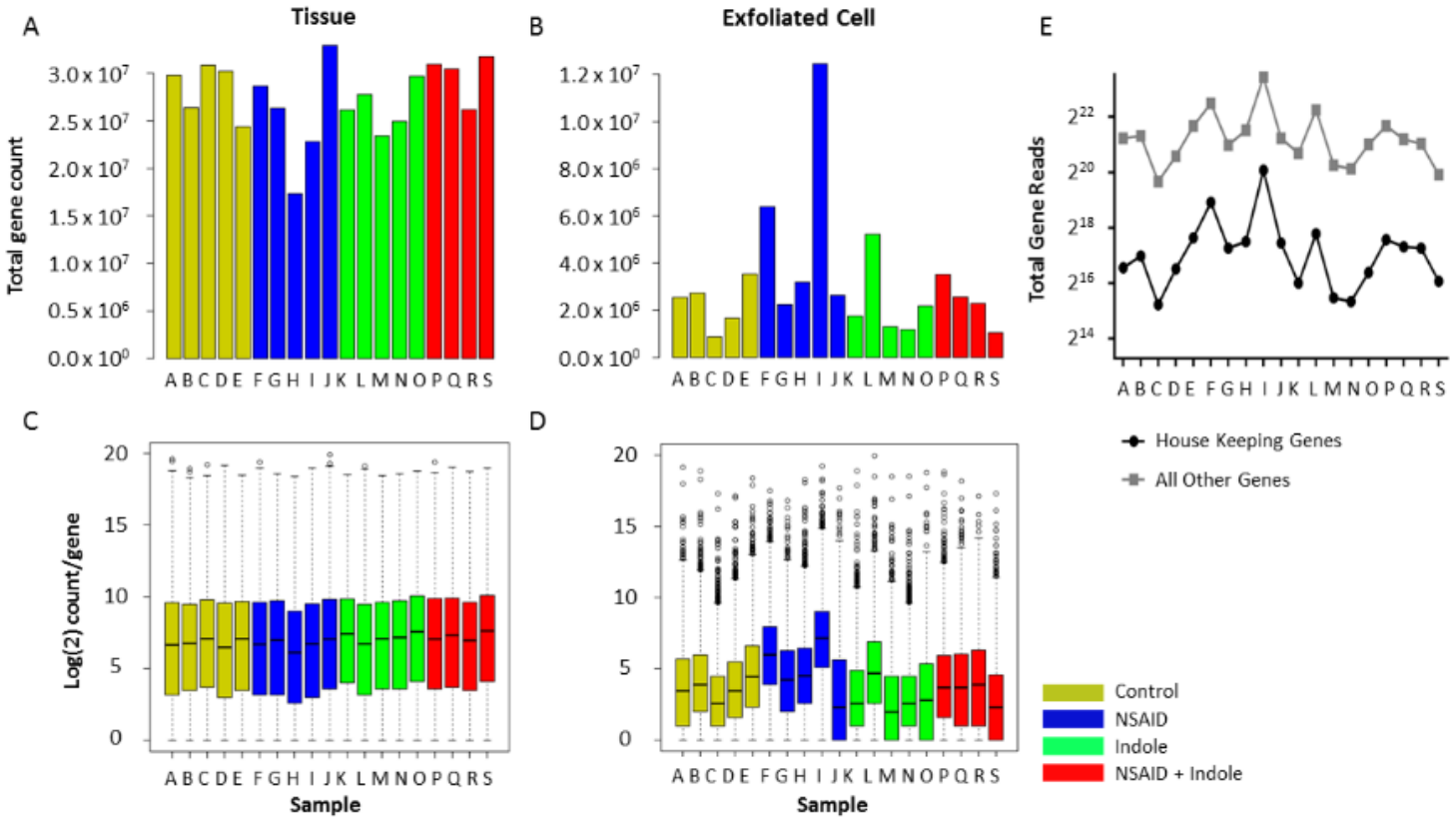

Figure 5 Exfoliated IEC reads exhibit more between sample variation than mucosal reads.
A) Total gene counts after filtering for each sample across all treatment groups from the sequenced RNA extracted from the tissue. B) Total gene counts after filtering for each sample across all treatment groups from the sequenced RNA extracted from the exfoliated IECs. C) log(2) counts per gene per sample across all treatment groups from the sequenced RNA extracted from the tissue after filtering. D) log(2) counts per gene per sample across all treatment groups from the sequenced RNA extracted from exfoliated IECs after filtering. E) log(2) total gene reads of 500 murine house-keeping genes (black) and all other genes (purple) from the exfoliated IEC data after filtering

To account for between-sample differences in read-counts (i.e., sequencing depth) RNA-seq data was normalized with edgeR accounting for group effects using the function calcNormFactors and the upper-quartile method. Total gene-counts and boxplots of the number of reads/gene for each sample of the normalized data for both tissue and exfoliated cell data sets are shown (Figure 6a-d). Variability in abundance of post-normalization total house-keeping genes was also improved (Figure 6e). Biological variability in the exfoliated IEC data was assessed by plotting the biological coefficient of variation (BCV) versus the mean log counts per million (CPM) and multi-dimensional scaling (MDS) plots were used to visually assess the similarity of the samples within each treatment group (Figure A-2.1). These results demonstrate a relatively high degree of variation among the exfoliated IEC data (common dispersion 0.6548 and BCV 0.8012) (Figure A-2.1a) with no visually apparent differences among the groups (Figure A-2.1b). The common dispersion and BCV were slightly improved by normalization (common dispersion = 0.59188 and BCV = 0.7693) and group effects were unchanged (Figure A-2.1c, d). The biological variance in these data was much higher than in the tissue samples with a post-normalization common dispersion of 0.14334 and BCV of 0.3786 (Figure A-2.1e, f).

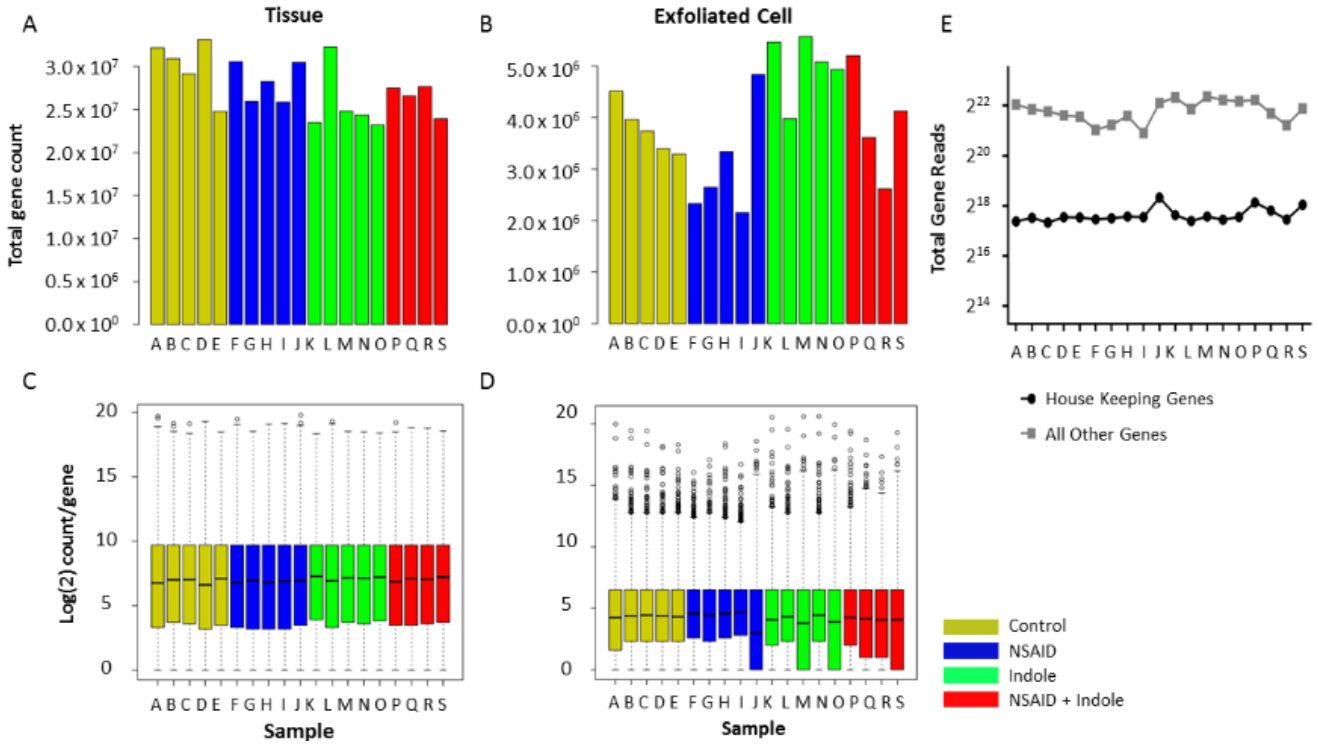

Figure 6 Raw data after filtering and normalization show that the between sample variation in exfoliated IEC reads are improved and similar to tissue reads.
A) Total gene counts after filtering and normalization for each sample across all treatment groups from the sequenced RNA extracted from tissue. B) Total gene counts after filtering and normalization for each sample across all treatment groups from sequenced RNA extracted from exfoliated IECs. C) log(2) counts per gene per sample across all treatment groups from sequenced RNA extracted from tissue samples after filtering and normalization. D) log(2) counts per gene per sample across all treatment groups from sequenced RNA extracted from exfoliated IECs after filtering and normalization. E) log(2) total gene reads of 500 murine house-keeping genes (black) and all other genes (purple) from the exfoliated IEC data after filtering and normalization.

Exfoliated IEC Transcriptome is Reflective of the Tissue-level Transcriptome

We next examined the similarities and differences in the gene expression profiles from exfoliated cells compared with those from the scraped intestinal mucosa. Gene lists were uploaded into IPA and the intersection of various gene lists were calculated. We initially examined the intersection of genes represented in the 2 most divergent treatment groups (NSAID-treated and control). The Venn diagram (Figure 7a) shows the intersection of all genes represented in these datasets. Approximately, 96% of all genes that were mapped from the exfoliated IEC RNA were also present in the tissue-level RNA. Similarly, 77% of genes that were mapped from the tissue-level RNA were present in the exfoliated IEC RNA. We then mapped these gene lists to pathways according to IPA's ingenuity knowledge base. Both datasets (i.e., tissue and exfoliated IEC) exhibited similar occupancy and predicted directionality (z-score) (Figure 7b, c). Figure 8b shows the canonical pathways to which the differentially expressed genes between control and NSAID-treated animals were mapped. In addition, Figure 3c shows the predicted upstream regulators represented by the same comparisons and again colored by predicted activation and inhibition. The visual similarity and high correlation of these pathways and the directions of their activation are shown in Figure 7. In addition to the apparent visual agreement a quantitative correlation was also observed. The Pearson correlation coefficient of the Z scores of the upstream regulators was 0.769 with a P value < 0.0001. For the canonical pathways, the Pearson correlation coefficient was (0.537) and significant (P = 0.0022).

Initial visual inspection of the global transcriptomic heat maps (Figure 7b, c) and quantitative data suggests a strong correlation between the exfoliated IECs and the tissue. To further examine the interdependent relationship between these 2 profiles, we utilized sparse CCA, a novel multivariate statistical analysis approach. Sparse CCA is a dimensionality reduction technique that identifies the fewest numbers of genes that show the greatest amount of correlation between data sets according to specific optimality criteria. Although the sparse CCA plots should not be assigned any particular biological interpretation, they could be considered a stringent method for determining correlation of large data sets.[161] Sparse CCA plots positioned by 1st and 2nd component scores from the exfoliated IECs and colored by the 1st component tissue scores (Figure 8a) closely mirrored sparse CCA plots positioned by 1st and 2nd component scores from the tissue and colored by 1st component scores from exfoliated cells (Figure 8b). These similarities are also revealed when specifically examining the boxplots of these scores across data sets where the same patterns of scores between the groups are present in both the exfoliated IEC and intestinal mucosa data (Figure 8c, d). Taken together, these data indicate that the global transcriptome profiles from exfoliated intestinal epithelial cells reflect and correlate well with the transcriptome profile of the distal ileum.

Figure 7 The exfoliated IEC transcriptome is similar to the tissue transcriptome as shown by similar gene lists and pathways. A) Venn diagram of the intersection of the list of genes found in exfoliated cells and gene list found in the tissue. B) Heat map of the Z-scores of the canonical pathways to which the differentially expressed genes between control and NSAID-treated animals were mapped from the tissue (left column) and the exfoliated cells (right column). C) Heat map of the Z-scores of the upstream regulators to which differentially expressed genes between control and NSAID-treated animals were mapped from the tissue (left column) and the exfoliated cells (right column).

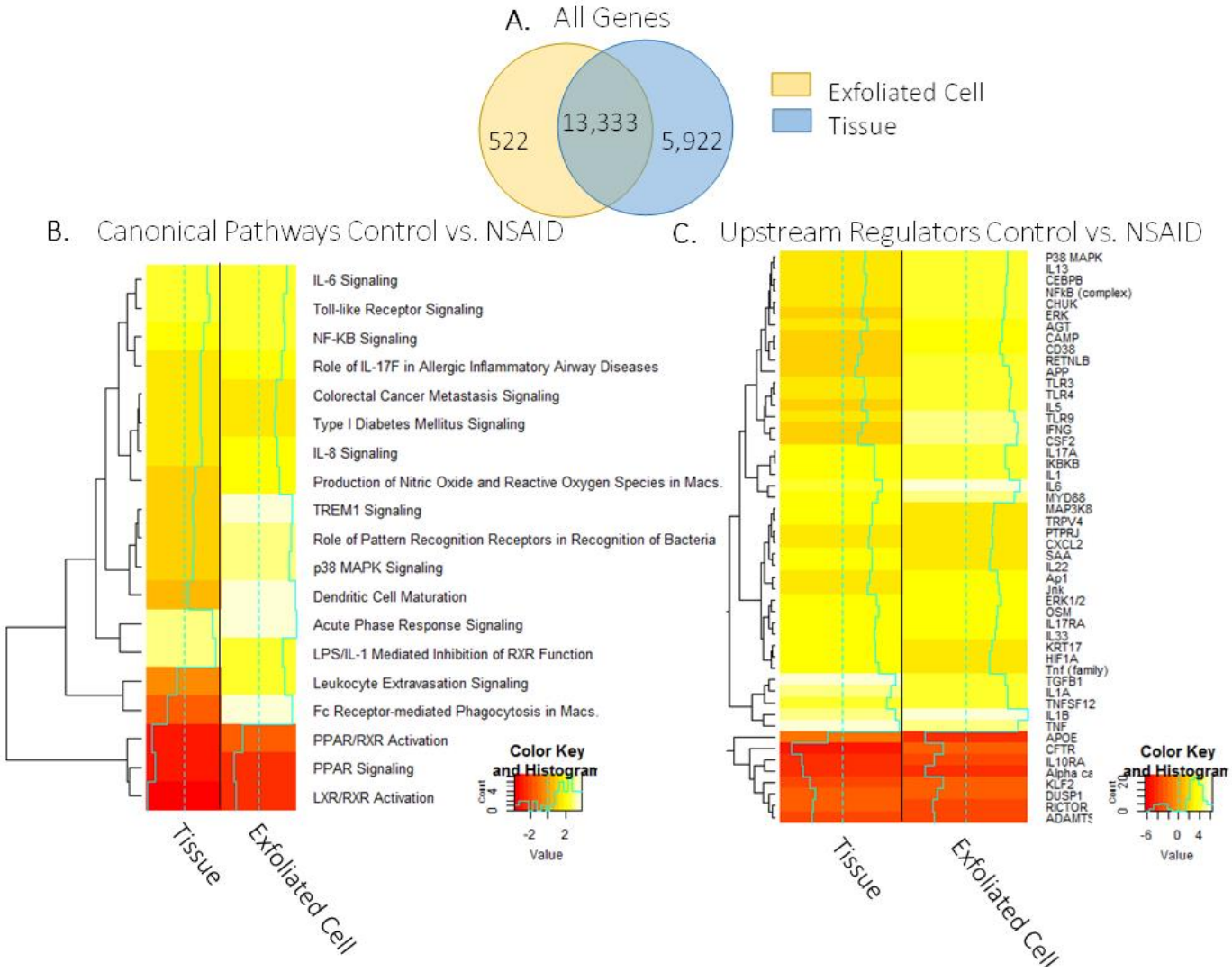
A. All Genes
522
13,333
5,922
Exfoliated Cell
Tissue
B. Canonical Pathways Control vs. NSAID
IL-6 Signaling
Toll-like Receptor Signaling
NF-KB Signaling
Role of IL-17F in Allergic Inflammatory Airway Diseases
Colorectal Cancer Metastasis Signaling
Type I Diabetes Mellitus Signaling
IL-8 Signaling
Production of Nitric Oxide and Reactive Oxygen Species in Macs.
TREM1 Signaling
Role of Pattern Recognition Receptors in Recognition of Bacteria
p38 MAPK Signaling
Dendritic Cell Maturation
Acute Phase Response Signaling
LPS/IL-1 Mediated Inhibition of RXR Function
Leukocyte Extravasation Signaling
Fc Receptor-mediated Phagocytosis in Macs.
PPAR/RXR Activation
PPAR Signaling
LXR/RXR Activation
Color Key and Histogram
Count
Value
Tissue
Exfoliated Cell
C. Upstream Regulators Control vs. NSAID
P38 MAPK
IL13
CEBPB
NFkB (complex)
CHUK
ERK
AGT
CAMP
CD38
RETNLB
APP
TLR3
TLR4
IL5
TLR9
IFNG
CSF2
IL17A
IKBKB
IL1
IL6
MYD88
MAP3K8
TRPV4
PTPRJ
CXCL2
SAA
IL22
Ap1
Jnk
ERK1/2
OSM
IL17RA
IL33
KRT17
HIF1A
Tnf (family)
TGFB1
IL1A
TNFSF12
IL1B
TNF
APOE
CFTR
IL10RA
Alpha ca
KLF2
DUSP1
RICTOR
ADAMTS
Color Key and Histogram
Count
Value
Tissue
Exfoliated Cell

Figure 8 Sparse canonical correlation analysis (CCA) reveals the global transcriptome profiles from exfoliated intestinal epithelial cells correlates well with the transcriptome profile of the distal ileum.
A) Sparse CCA plots positioned by 1st and 2nd component scores from the exfoliated IECs and colored by the 1st component tissue scores. B) sparse CCA plots positioned by 1st and 2nd component scores from the tissue and colored by 1st component scores from exfoliated cells. C) Boxplots of the sparse CCA scores (first and second component) from exfoliated cells for each treatment group. D) Boxplots of the sparse CCA scores (first and second component) from tissue for each treatment group.

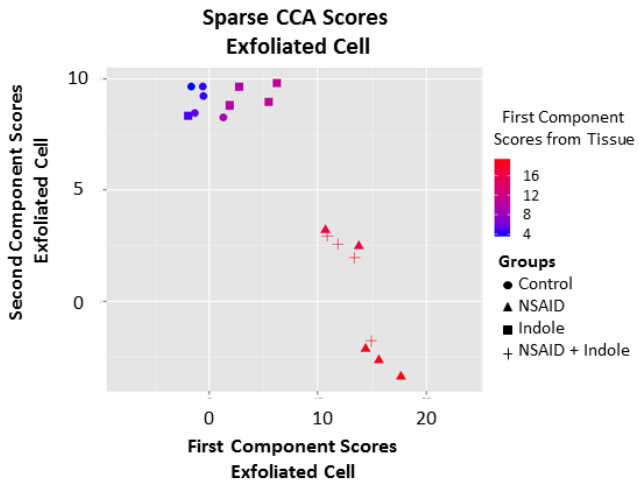
Sparse CCA Scores
Exfoliated Cell
Second Component Scores
Exfoliated Cell
10
5
0
0
10
20
First Component Scores
Exfoliated Cell
First Component
Scores from Tissue
16
12
8
4
Groups
Control
NSAID
Indole
NSAID + Indole

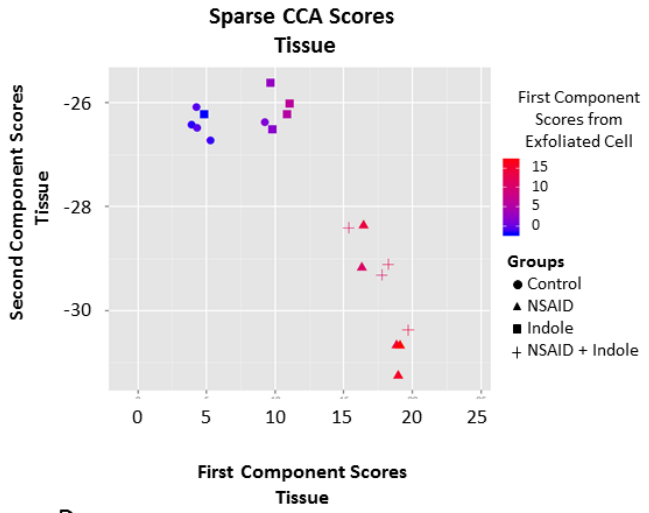
Sparse CCA Scores
Tissue
Second Component Scores
Tissue
-26
-28
-30
0
5
10
15
20
25
First Component Scores
Tissue
First Component
Scores from
Exfoliated Cell
15
10
5
0
Groups
Control
NSAID
Indole
NSAID + Indole

C

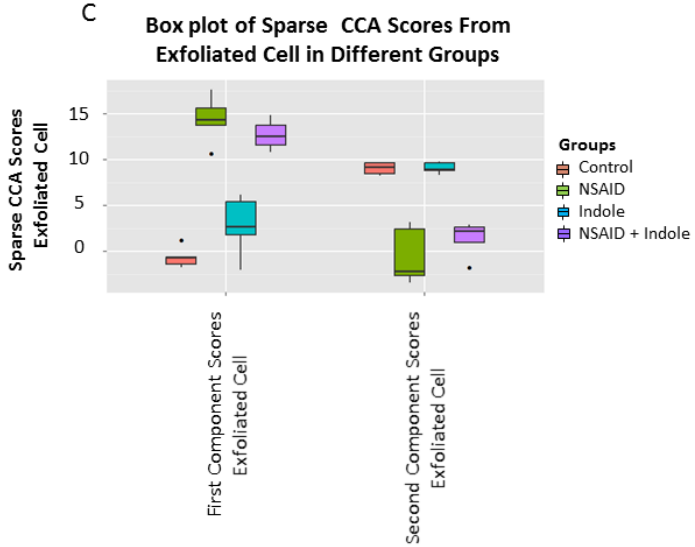
Box plot of Sparse CCA Scores From
Exfoliated Cell in Different Groups
Sparse CCA Scores
Exfoliated Cell
15
10
5
0
First Component Scores
Exfoliated Cell
Second Component Scores
Exfoliated Cell
Groups
Control
NSAID
Indole
NSAID + Indole

D

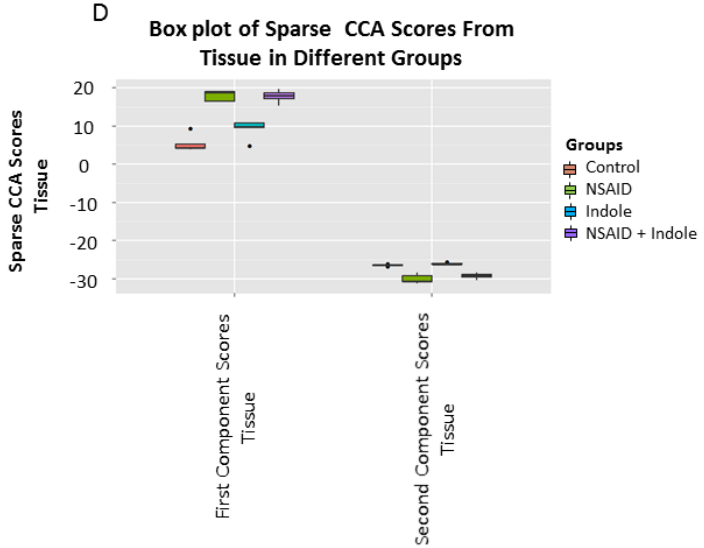
Box plot of Sparse CCA Scores From
Tissue in Different Groups
Sparse CCA Scores
Tissue
20
10
0
-10
-20
-30
First Component Scores
Tissue
Second Component Scores
Tissue
Groups
Control
NSAID
Indole
NSAID + Indole

Transcriptome of Exfoliated IECs Classifies Healthy and Diseased Phenotypes

In order to derive biological meaning from the tissue and exfoliated cell data-sets, we performed a series of data reduction techniques. Linear discriminate analysis was performed on the counts of genes, from exfoliated IECs, identified as being differentially expressed between indomethacin-treated and control animals. There were 691 genes identified as being differentially expressed between these treatment groups, and 1-feature (i.e., single gene) LDA identified 50 of these genes as being able to classify NSAID and non-NSAID treated animals with less than 5% resubstituted error rate, the top 20 are shown (Table A-2.1). [164] These genes were subsequently uploaded into IPA along with their respective P-values and fold-changes in order to determine which pathways and upstream regulators identified by LDA are best suited to classify NSAID versus control animals with respect to all differentially expressed genes. The top (lowest P-value) upstream regulators and the networks to which these genes belong are shown (Table A-2.2 and Figure A-2.2 a, respectively). As previously shown, a substantial decrease in classification error was observed when pairs of genes (i.e., 2-feature-based LDA) were used to discriminate NSAID from control animals (Table A-2.3) [155]. We specifically queried the data with respect to pairs of genes that performed better than either of the genes individually in order to identify sets of genes that perform in a multivariate manner to provide strong classification (Table A-2.4). These genes were subsequently uploaded into IPA along with their respective P-values and fold-changes in order to determine which pathways and upstream regulators provide strong classification in a multivariate manner (Figure A-2.2 b and Table A-2.5).

Analysis of Exfoliated IEC Transcriptome Generates Hypotheses Regarding the Pathophysiology of NSAID Enteropathy and its Clinical Management

From our study that first reported indole regulation of host cell function, we extended these findings to a model of intestinal damage and inflammation to demonstrate that the co-administration of indole attenuated the severity of GI injury associated with NSAID use [32, 92]. The mechanism by which indole exerted this effect, however, was unclear. The major effects of indole based on the tissue-transcriptome appeared to be mediated by a reduction of the innate immune response via alterations in the gut microbiota [32]. Because the exfoliated IEC and tissue-level gene expression profiles were similar (Figure 7 and Figure 8), we sought to examine the differences in the exfoliated IEC transcriptome between control versus indomethacin-treated animals and control versus indole+indomethacin-treated animals. For this purpose, the top 40 canonical pathways altered in exfoliated IECs were sorted based on differences in Z-scores between the 2 treatments (Figure 9a). Similarly, the top 50 upstream regulators altered in exfoliated IECs are shown in Figure 9b. While these data reveal pathways consistent with reduced inflammation, as has been shown previously, it is unclear how this anti-inflammatory effect occurred and which of these upstream regulators mediate indomethacin induced GI injury and the protective effects observed by the co-administration of indole. To address this question, we mapped the network of the top 15 upstream regulators identified by our novel data reduction approach and analysis of 2-feature LDA in the context of NSAID vs control animals (Figure 10a). We then overlaid the fold change and false discovery rate (FDR) P-values of these same molecules from

the analysis of control versus NSAID+indole (Figure 10b) and identified which of these molecules were altered (opposite fold-change either realized or predicted). This resulted in the identification of 11 genes that were altered between NSAID administration and NSAID+indole administration. We subsequently uploaded these genes into IPA in order to determine plausible pathways by which indole attenuated NSAID-induced GI injury (Figure 11).

To further derive biologically relevant information from the sparse CCA dataset (i.e., the list of genes that explain the greatest amount of correlation between exfoliated IEC transcriptome and tissue-level transcriptome), we uploaded fold-change and FDR P-values from the comparison of NSAID-treated animals to control animals into IPA as previously described [165]. The networks of canonical pathways represented by these genes are shown (Figure A-2.3). Interestingly, 5 of the 17 pathways to which these genes belong were associated with cytoskeletal signaling and the interaction of host cells with the extracellular matrix. As expected, the remainder of these pathways were primarily related to inflammatory responses (i.e., loss of barrier function and influx of lumenal contents).

A

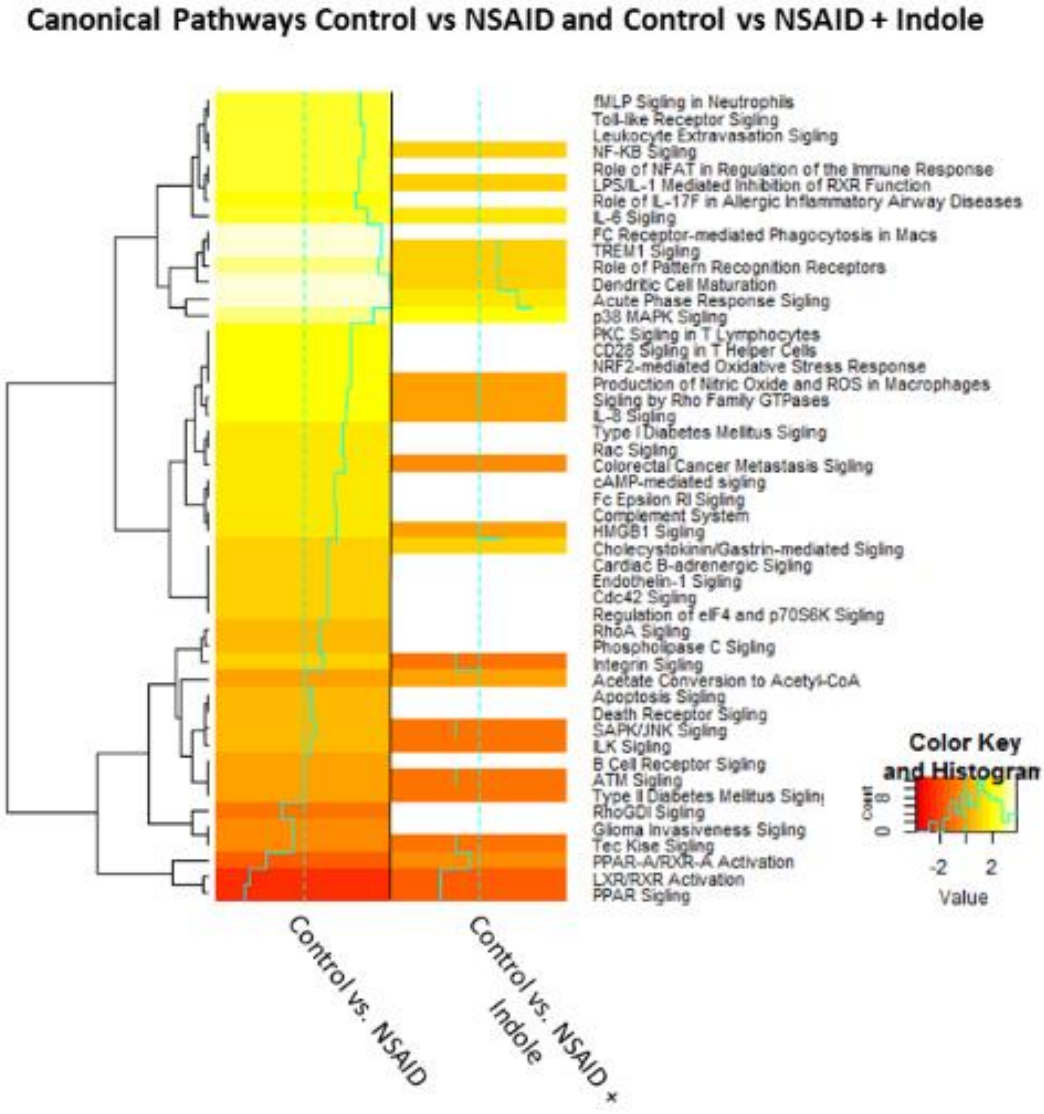

Figure 9 Co-administration of indole reduces inflammatory pathways in NSAID enteropathy. A)Heat map of the Z-scores of the canonical pathways to which the differentially expressed genes between control vs. NSAID-treated animals (left column) and control vs. NSAID+indole (right column) were mapped. B) Heat map of the Z-scores of the upstream regulators to which the differentially expressed genes between control vs. NSAID-treated animals (left column) and control vs. NSAID +indole (right column) were mapped.

B

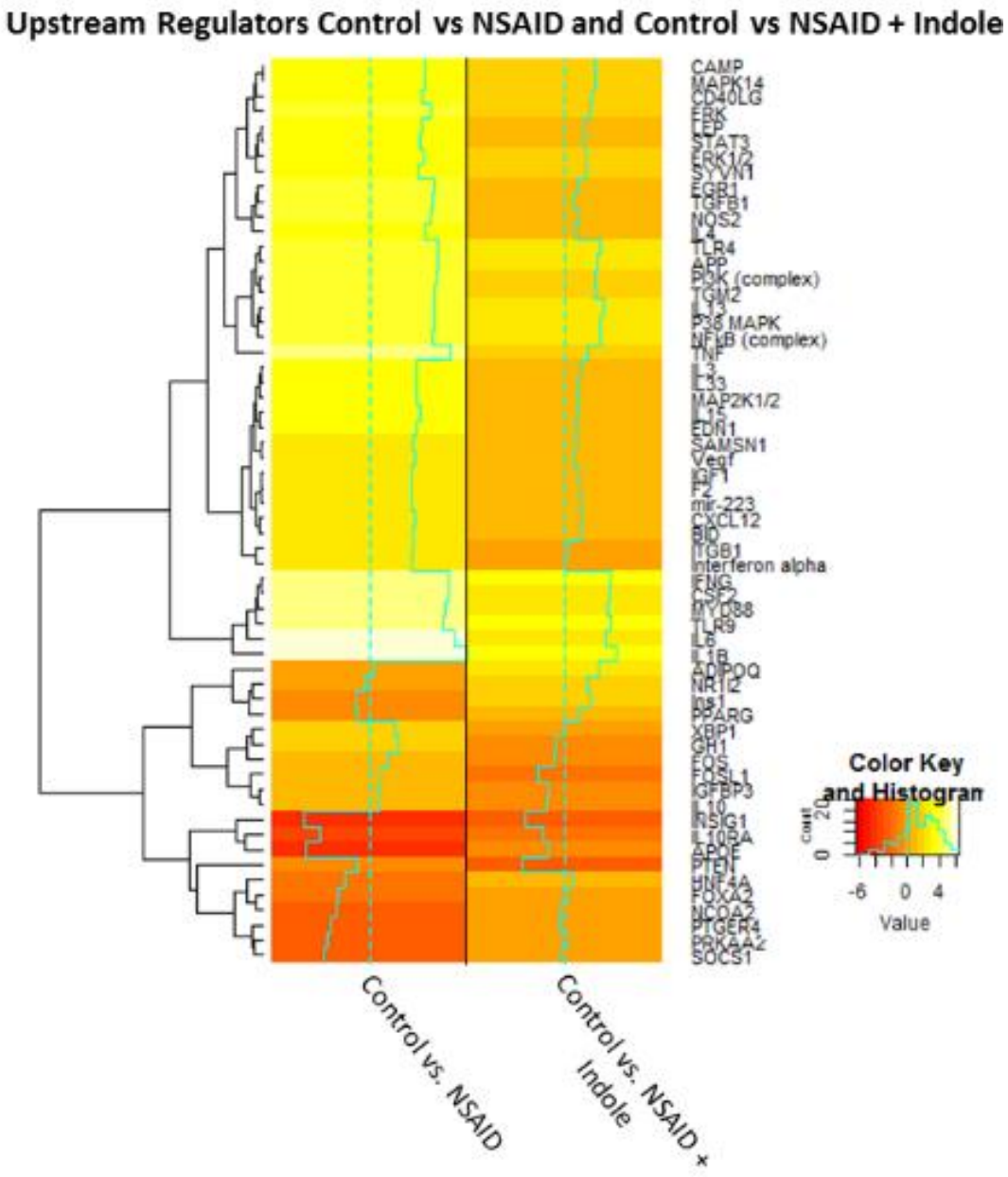

Figure 9 continued

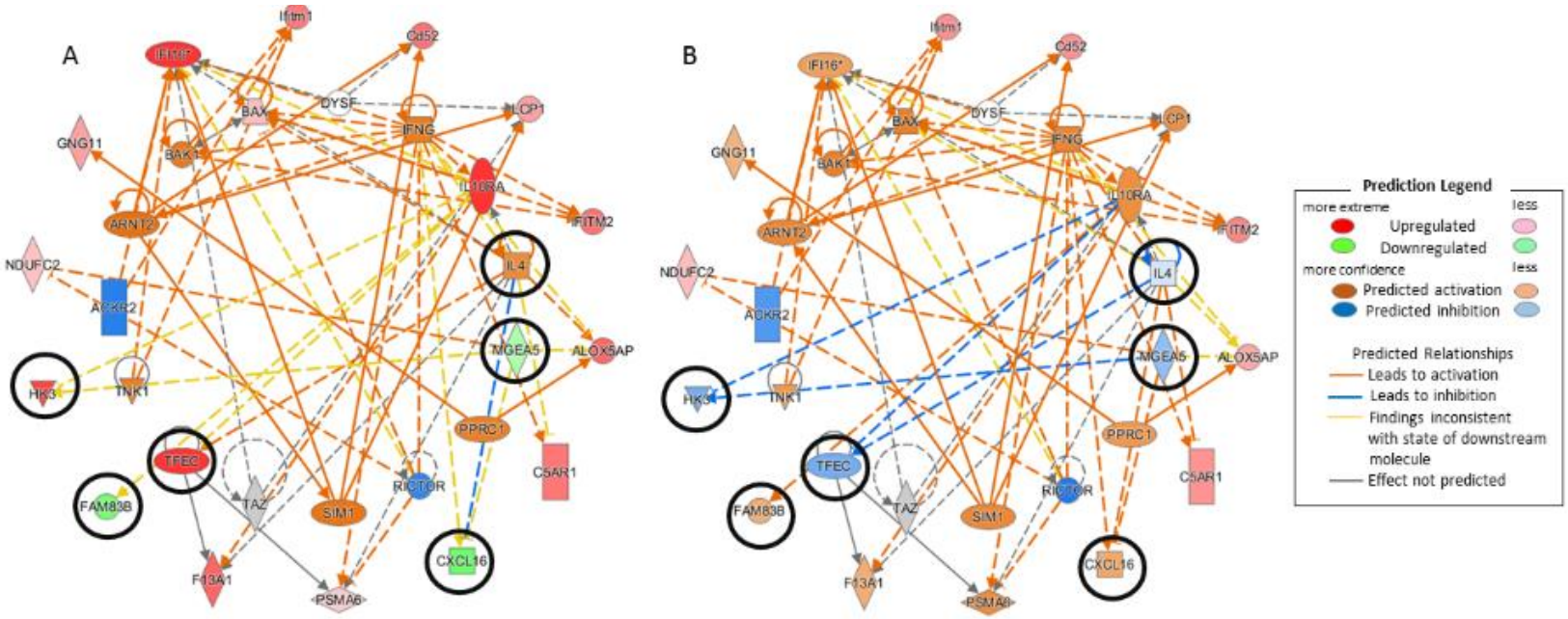

Figure 10 Noninvasive identification of 6 key genes altered between NSAID and NSAID + Indole treatments.
A) Network of the top 15 upstream regulator, identified by 2-feature LDA in the context of NSAID vs control animals with FDR P-values and fold changes overlaid. B) Same network with P-values and fold changes of NSAID+indole overlaid reveal 6 genes that were altered (opposite fold-change either realized or predicted) by the co-administration of indole.

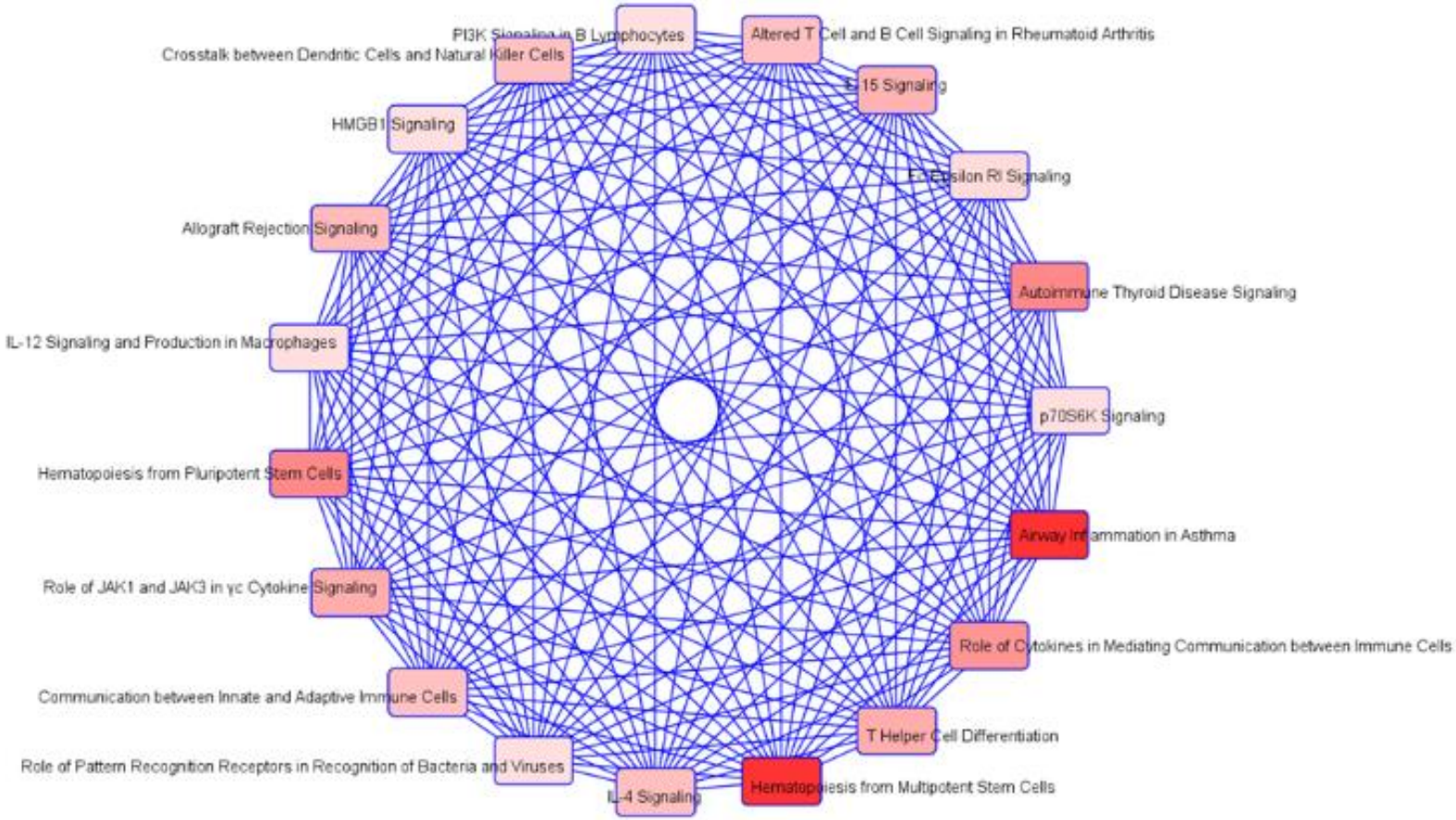

Figure 11 Pathways identified using the exfoliated IEC transcriptome and two-feature LDA.
The darker color correlates with lower P-value.

Discussion

Here we have shown that the transcriptome of exfoliated IECs closely resembles that at the tissue level in a murine model of NSAID enteropathy. Using RNA-Seq, we compared the exfoliated IEC transcriptome to the tissue transcriptome from samples obtained from mucosal scrapings of the mouse ileum, the region of the GI tract most severely affected in NSAID enteropathy in both mice and human subjects [29, 124, 166-168]. Although gene expression of exfoliated IECs has been used to examine GI development in neonates and for biomarkers of colorectal cancer, we show for the first time the application of this approach to examine a disease that primarily affects the small intestine [25, 32, 49, 99, 100]. The use of exfoliated IEC mRNA presents several important advantages relative to mRNA obtained from the standard approach of tissue biopsy. First, use of fecal samples is non-invasive and results in no physical pain to the patient. Second, greater requirement of time, effort, and cost is required for collection of biopsy specimens than for collection of feces. Third, although the primary area of injury with NSAID enteropathy is the distal small intestine, NSAIDs can affect both the large and small intestine of humans and other animals [169, 170]. Exfoliated IECs arise from both the colon and small intestine and thus provide an overview of the gene expression profiles of the entire gastrointestinal tract, whereas a tissue specimen only provides a site-specific gene expression profile [155]. Fourth, intestinal biopsies generally can be collected once (typically at a terminal stage of the study), whereas feces can be collected sequentially, thereby allowing the temporality of gene expression profiles from exfoliated IECs to be used to investigate and monitor disease progression.

In general, the exfoliated IEC transcriptome correlated well with the tissue transcriptome as evidenced by the intersection of genes present in both datasets, similarities of the pathways and processes of the genes and gene regulators, and results of sparse CCA analysis. These results are interesting because much of the RNA extracted from exfoliated IECs undoubtedly originates from the colon and we did not attempt to identify the precise source of these cells. Nonetheless, we have demonstrated that the exfoliated IEC data closely mirrors that of the ileal mucosa, indicating that studying IECs can yield informative results about the distal small intestine irrespective of knowledge of their precise source. Further investigation of the impact of concomitant colonic disease and other potential confounding factors on use of the IEC transcriptome is merited.

After demonstrating that the exfoliated IEC transcriptome reflects that of the mucosa of the distal small intestine, we used the IEC gene expression data to examine which pathways and processes were induced by NSAID enteropathy and the mechanism(s) by which the microbiota-derived metabolite indole ameliorated the severity of NSAID-induced GI injury [32]. Our results further substantiate the importance of innate immune responses in NSAID enteropathy [26, 171]. Specifically, and as reported previously, we identified several pro-inflammatory pathways and upstream regulators including IL-8 (mouse homologs), IL-17, NF-KB, IL-1, and MYD88 involved in NSAID enteropathy [25, 26, 124, 133, 171]. The consistency of our results based on using IECs with those of prior studies adds evidence to the validity of

using this novel approach for the study of NSAID enteropathy (and potentially numerous other small intestinal disorders).

Previously, we identified tryptophan metabolites, including indole, as an important class of GI microbiota-derived compounds [172]. We subsequently demonstrated that indole protected mice from indomethacin-induced enteropathy [32]. The specific molecular mechanism by which indole protects mice from NSAID enteropathy, however, remains to be clarified. Therefore, in addition to examining biological pathways and processes critical to NSAID enteropathy we also examined the exfoliated IEC transcriptome to assess alterations induced by the co-administration of indole. Although a number of pathways appear to be involved, our data highlight T-helper cell differentiation, IL-8 signaling (based on mouse homologs), cytoskeletal pathways, and inflammatory pathways as key contributors (Figure 7). Interestingly, dietary indoles including indole-3-carbinol and 3,3'-diindolylmethane have been shown to influence T-helper cell differentiation primarily by inducing anti-inflammatory T-regulatory cells [162, 173]. In addition, indole has been shown to inhibit NF-κB pathways, specifically LPS-induced IL-8 inflammation and TNF-α pathways in IECs [92]. Indole has also been shown to influence various cytoskeletal structures including tight-cell junctions and tubulin polymerization [101, 174]. Moreover, the anti-inflammatory effects of indole, indole-3-carninol, and indole-3-aldehyde have been repeatedly demonstrated, although the molecular mechanisms remain to be defined [32, 93, 101, 175]. One potential mechanism that might be involved is engagement of the aryl hydrocarbon receptor (AhR). Ligands of AhR have anti-inflammatory effects in various

models of colitis including the production of IL-22 [176-178]. Indeed, indole can serve as an AhR ligand in the context of IECs and this might, in part, explain indole's attenuation of inflammation in NSAID enteropathy [179-181]. Our unique finding that results of analysis of the exfoliated IEC transcriptome are consistent with our reports on the known in vitro and in vivo biological effects of indole further supports the concept that this novel approach will be an invaluable tool for studying NSAID enteropathy and other GI diseases in a non-invasive manner.

There were several limitations to this study. First, the evaluated sample size was small and consisted of a single time-point (day 7). Despite the small sample size, we clearly demonstrated that the exfoliated IEC transcriptome reflects that of the tissue at the level of the ileum. In addition, our approach revealed the importance of several pathways involved in both NSAID enteropathy and the effect of the co-administration of indole on this phenotype. Importantly, many of the highlighted pathways are known to mediate NSAID enteropathy and are consistent with the anti-inflammatory effects of indole. Therefore, even with a small sample size, we were able to recapitulate known biologically relevant findings with this technique. In the latter or more severe stages of NSAID enteropathy, the major pathways involved are the host response to increased mucosal permeability. Therefore, to better understand the temporal events contributing to NSAID enteropathy, a more appropriate approach may be to examine earlier time points.

In summary, we have demonstrated that the exfoliated IEC transcriptome closely mirrors the transcriptome of the tissue at the level of the ileum. Although this approach

has been described previously, this is the first time these findings have been correlated to the tissue-level transcriptome. In addition, this technique has not been utilized to examine a disease that primarily affects the small intestine. We have shown that the exfoliated IEC transcriptome can be a useful tool to examine NSAID enteropathy and potentially extend to a number of other GI diseases, including those that affect the small intestine. Additionally, the application of noninvasive exfoliated cell based techniques might be useful for the early identification and monitoring of therapeutic interventions targeting NSAID enteropathy and other small intestinal disorders.

CHAPTER IV

CONCLUSIONS AND FUTURE DIRECTIONS

Conclusions

As mentioned throughout this dissertation non-steroidal anti-inflammatory drugs (NSAIDs) are among the most frequently used pharmaceuticals in the world and yet cause enteropathy in an alarmingly high percentage of individuals using this class of medications. Importantly, the underlying mechanisms by which NSAIDs induce enteropathy are ill-defined and the diagnosis is difficult and typically not made until latter stages of progression. The microbiota-host interaction appears to play an important role in the pathophysiology of NSAID enteropathy. Although much work remains our work here has identified several important aspects of this disease. Namely, we have generated the first *in vivo* work documenting the NSAID induced alterations of the mucosal transcriptome. In addition, our work joins the growing body of evidence implication host-microbiota interactions in NSAID enteropathy. Specifically, we demonstrate the NSAIDs alter the fecal microbiota in a murine model of NSAID enteropathy AND show that co-administration of a microbiota-derived metabolite attenuates disease severity. These findings suggest that one possible mechanism by which the microbiota influences disease severity is alteration of the microbiota-derived metabolites (*i.e.*, the metabolome). Indeed, we demonstrate that co-administration of a specific microbiota-derived metabolite, indole, not only attenuated disease severity but

simultaneously prevented NSAID-induced dysbiosis and alterations of the fecal metabolome.

We then extended this work by examining the exfoliated cell transcriptome in this model in order to determine if the transcriptome of exfoliated intestinal epithelial cells (IECs) found in the stool could be reflective of NSAID enteropathy, thereby allowing longitudinal comparisons of fecal microbiota diversity and host intestinal mucosal transcriptome. A second objective was to determine how the microbiota-derived metabolite indole, which has been shown to protect against NSAID-enteropathy, altered the exfoliated IEC transcriptome. We compared exfoliated cell datasets and tissue-level datasets using well-described and novel computational approaches including linear discriminant analysis (LDA) and sparse canonical correlation analysis (CCA) to assess their inter-relatedness. This allowed us to demonstrate, for the first time, that the (noninvasive) fecal exfoliated cell and (invasive) small intestine-scraped mucosa global transcriptomes are highly correlated. These novel findings highlight important pathways involved in NSAID enteropathy and the mechanisms by which microbiota-derived metabolites protect the host from injury. Approximately 96% of all genes that were mapped from the IEC RNA were also present in the tissue-level RNA. Moreover, the pathways represented by these genes and their directional changes were similar in both the small intestinal mucosa and exfoliated IEC transcriptome. Specifically, innate immune response and pro-inflammatory pathways appeared to be critical in the pathophysiology of NSAID-induced enteropathy and indole attenuated severity of injury in this model via these pathways. These novel findings highlight important pathways

involved in NSAID enteropathy and the mechanisms by which microbiota-derived metabolites protect the host from injury.

Future Directions

Future directions for continuation of this work include specifically testing hypotheses regarding the novel pathways and biological processes identified as being critically important in NSAID enteropathy. In addition, confirming the exact mechanism by which indole exerted its beneficial effects in these phenotype remains an important step and a goal of future work. Finally, the notion of utilizing non-invasive data collected from exfoliated cells in freely voided feces is an exciting prospect for studying not ony NSAID enteropathy but a host of other gastrointestinal mucosal diseases. This technique could allow us to gain temporal data over time while also collecting data about the microbiota. This simultaneous collection of both host data and microbe data could begin to allow us to work out the exact mechanisms by which the microbiota influences the host response and vice versa. From a clinical stand point this technique is also promising as there is clearly potential for determine a set of genes that could be used as a screening tool or even diagnostic test for NSAID enteropathy and many other mucosal gastrointestinal diseases. While we demonstrated that this technique could successfully discriminate between healthy and diseased phenotypes, much work remains in order to utilize this technique and a screening or diagnostic tool and that remains an area of future work.

REFERENCES

1. Fujimori S, Gudis K, Takahashi Y, Seo T, Yamada Y, Ehara A, et al. Distribution of small intestinal mucosal injuries as a result of NSAID administration. European journal of clinical investigation. 2010;40(6):504-10. Epub 2010/04/24. doi: 10.1111/j.1365-2362.2010.02290.x. PubMed PMID: 20412292.

2. Maiden L. Capsule endoscopic diagnosis of nonsteroidal antiinflammatory drug-induced enteropathy. Journal of gastroenterology. 2009;44 Suppl 19:64-71. Epub 2009/02/20. doi: 10.1007/s00535-008-2248-8. PubMed PMID: 19148796.

3. Boelsterli U, Redinbo M, Saitta K. Multiple NSAID-induced hits injure the small intestine: underlying mechanisms and novel strategies. Toxicological sciences: an official journal of the Society of Toxicology. 2013;131(2):654-67. Epub 2012/10/24. doi: 10.1093/toxsci/kfs310. PubMed PMID: 23091168; PubMed Central PMCID: PMCPMC3551426.

4. Somasundaram S, Rafi S, Hayllar J, Sigthorsson G, Jacob M, Price A, et al. Mitochondrial damage: a possible mechanism of the "topical" phase of NSAID induced injury to the rat intestine. Gut. 1997;41(3):344-53. Epub 1998/02/12. PubMed PMID: 9378390; PubMed Central PMCID: PMCPMC1891477.

5. Seitz S, Boelsterli U. Diclofenac acyl glucuronide, a major biliary metabolite, is directly involved in small intestinal injury in rats. Gastroenterology. 1998;115(6):1476-82. Epub 1998/12/03. PubMed PMID: 9834275.

6. LoGuidice A, Wallace B, Bendel L, Redinbo M, Boelsterli U. Pharmacologic targeting of bacterial beta-glucuronidase alleviates nonsteroidal anti-inflammatory drug-induced enteropathy in mice. The Journal of pharmacology and experimental therapeutics. 2012;341(2):447-54. Epub 2012/02/14. doi: 10.1124/jpet.111.191122. PubMed PMID: 22328575; PubMed Central PMCID: PMCPMC3336811.

7. Lichtenberger LM, Zhou Y, Jayaraman V, Doyen JR, O'Neil RG, Dial EJ, et al. Insight into NSAID-induced membrane alterations, pathogenesis and therapeutics: characterization of interaction of NSAIDs with phosphatidylcholine. Biochimica et biophysica acta. 2012;1821(7):994-1002. Epub 2012/04/24. doi: 10.1016/j.bbalip.2012.04.002. PubMed PMID: 22521764; PubMed Central PMCID: PMCPMC3362734.

8. Matsui H, Shimokawa O, Kaneko T, Nagano Y, Rai K, Hyodo I. The pathophysiology of non-steroidal anti-inflammatory drug (NSAID)-induced mucosal injuries in stomach and small intestine. Journal of clinical biochemistry and nutrition. 2011;48(2):107-11. Epub 2011/03/05. doi: 10.3164/jcbn.10-79. PubMed PMID: 21373261; PubMed Central PMCID: PMCPMC3045681.

9. Tsutsumi S, Gotoh T, Tomisato W, Mima S, Hoshino T, Hwang H, et al. Endoplasmic reticulum stress response is involved in nonsteroidal anti-inflammatory drug-induced apoptosis. Cell death and differentiation. 2004;11(9):1009-16. Epub 2004/05/08. doi: 10.1038/sj.cdd.4401436. PubMed PMID: 15131590.

10. Handa O, Majima A, Onozawa Y, Horie H, Uehara Y, Fukui A, et al. The role of mitochondria-derived reactive oxygen species in the pathogenesis of non-steroidal anti-inflammatory drug-induced small intestinal injury. Free radical research. 2014;48(9):1095-9. Epub 2014/05/30. doi: 10.3109/10715762.2014.928411. PubMed PMID: 24870068.

11. Omatsu T, Naito Y, Handa O, Mizushima K, Hayashi N, Qin Y, et al. Reactive oxygen species-quenching and anti-apoptotic effect of polaprezinc on indomethacin-induced small intestinal epithelial cell injury. Journal of gastroenterology. 2010;45(7):692-702. Epub 2010/02/23. doi: 10.1007/s00535-010-0213-9. PubMed PMID: 20174833.

12. Ramirez-Alcantara V, LoGuidice A, Boelsterli U. Protection from diclofenac-induced small intestinal injury by the JNK inhibitor SP600125 in a mouse model of NSAID-associated enteropathy. American journal of physiology gastrointestinal and liver physiology. 2009;297(5):G990-8. Epub 2010/05/27. PubMed PMID: 20501447.

13. Fukui A, Naito Y, Handa O, Kugai M, Tsuji T, Yoriki H, et al. Acetyl salicylic acid induces damage to intestinal epithelial cells by oxidation-related modifications of ZO-1. American journal of physiology gastrointestinal and liver physiology. 2012;303(8):G927-36. Epub 2012/08/25. doi: 10.1152/ajpgi.00236.2012. PubMed PMID: 22917627.

14. Montrose D, Kadaveru K, Ilsley J, Root S, Rajan T, Ramesh M, et al. cPLA2 is protective against COX inhibitor-induced intestinal damage. Toxicological

sciences : an official journal of the Society of Toxicology. 2010;117(1):122-32. Epub 2010/06/22. doi: 10.1093/toxsci/kfq184. PubMed PMID: 20562220; PubMed Central PMCID: PMCPMC2923287.

15. Kaminsky L, Zhang Q. The small intestine as a xenobiotic-metabolizing organ. Drug metabolism and disposition: the biological fate of chemicals. 2003;31(12):1520-5. Epub 2003/11/20. doi: 10.1124/dmd.31.12.1520. PubMed PMID: 14625348.

16. Knights K, Mangoni A, Miners J. Defining the COX inhibitor selectivity of NSAIDs: implications for understanding toxicity. Expert review of clinical pharmacology. 2010;3(6):769-76. Epub 2011/11/25. doi: 10.1586/ecp.10.120. PubMed PMID: 22111779.

17. Vane J, Mitchell J, Appleton I, Tomlinson A, Bishop-Bailey D, Croxtall J, et al. Inducible isoforms of cyclooxygenase and nitric-oxide synthase in inflammation. Proceedings of the National Academy of Sciences of the United States of America. 1994;91(6):2046-50. Epub 1994/03/15. PubMed PMID: 7510883; PubMed Central PMCID: PMCPMC43306.

18. Langenbach R, Loftin C, Lee C, Tiano H. Cyclooxygenase knockout mice: models for elucidating isoform-specific functions. Biochemical pharmacology. 1999;58(8):1237-46. Epub 1999/09/16. PubMed PMID: 10487525.

19. Langenbach R, Loftin CD, Lee C, Tiano H. Cyclooxygenase-deficient mice. A summary of their characteristics and susceptibilities to inflammation and

carcinogenesis. Annals of the New York academy of sciences. 1999;889:52-61. Epub 2000/02/11. PubMed PMID: 10668482.

20. Takeuchi K, Tanaka A, Kato S, Amagase K, Satoh H. Roles of COX inhibition in pathogenesis of NSAID-induced small intestinal damage. Clinica chimica acta; international journal of clinical chemistry. 2010;411(7-8):459-66. Epub 2010/01/16. doi: 10.1016/j.cca.2009.12.026. PubMed PMID: 20074562.

21. Hotz-Behofsits C, Simpson R, Walley M, Bjarnason I. Role of COX-2 in nonsteroidal anti-inflammatory drug enteropathy in rodents. Scandinavian journal of gastroenterology. 2010;45(7-8):822-7. Epub 2010/05/06. doi: 10.3109/00365521003797205. PubMed PMID: 20441531.

22. Lanas A, Garcia-Rodriguez L, Polo-Tomas M, Ponce M, Alonso-Abreu I, Perez-Aisa M, et al. Time trends and impact of upper and lower gastrointestinal bleeding and perforation in clinical practice. The American journal of gastroenterology. 2009;104(7):1633-41. Epub 2009/07/04. doi: 10.1038/ajg.2009.164. PubMed PMID: 19574968.

23. Koga H, Aoyagi K, Matsumoto T, Iida M, Fujishima M. Experimental enteropathy in athymic and euthymic rats: synergistic role of lipopolysaccharide and indomethacin. The American journal of physiology. 1999;276(3 Pt 1):G576-82. Epub 1999/03/10. PubMed PMID: 10070032.

24. Beck P, Xavier R, Lu N, Nanda N, Dinauer M, Podolsky D, et al. Mechanisms of NSAID-induced gastrointestinal injury defined using mutant mice. Gastroenterology. 2000;119(3):699-705. Epub 2000/09/13. PubMed PMID: 10982764.

25. Watanabe T, Higuchi K, Kobata A, Nishio H, Tanigawa T, Shiba M, et al. Non-steroidal anti-inflammatory drug-induced small intestinal damage is Toll-like receptor 4 dependent. Gut. 2008;57(2):181-7. Epub 2007/07/20. doi: 10.1136/gut.2007.125963. PubMed PMID: 17639086.

26. Higashimori A, Watanabe T, Nadatani Y, Takeda S, Otani K, Tanigawa T, et al. Mechanisms of NLRP3 inflammasome activation and its role in NSAID-induced enteropathy. Mucosal immunology. 2016;9(3):659-68. Epub 2015/09/10. doi: 10.1038/mi.2015.89. PubMed PMID: 26349656.

27. Otte J, Cario E, Podolsky D. Mechanisms of cross hyporesponsiveness to Toll-like receptor bacterial ligands in intestinal epithelial cells. Gastroenterology. 2004;126(4):1054-70. Epub 2004/04/02. PubMed PMID: 15057745.

28. Kawai T, Akira S. TLR signaling. Cell death and differentiation. 2006;13(5):816-25.

29. Fukumoto K, Naito Y, Takagi T, Yamada S, Horie R, Inoue K, et al. Role of tumor necrosis factor-alpha in the pathogenesis of indomethacin-induced small intestinal injury in mice. International journal of molecular medicine. 2011;27(3):353-9. Epub 2011/01/21. doi: 10.3892/ijmm.2011.602. PubMed PMID: 21249312.

30. Bertrand V, Guimbaud R, Tulliez M, Mauprivez C, Sogni P, Couturier D, et al. Increase in tumor necrosis factor-alpha production linked to the toxicity of indomethacin for the rat small intestine. British journal of pharmacology. 1998;124(7):1385-94. Epub 1998/09/02. doi: 10.1038/sj.bjp.0701968. PubMed PMID: 9723949; PubMed Central PMCID: PMCPMC1565527.

31. Stadnyk AW, Dollard C, Issekutz TB, Issekutz AC. Neutrophil migration into indomethacin induced rat small intestinal injury is CD11a/CD18 and CD11b/CD18 co-dependent. Gut. 2002;50(5):629-35. Epub 2002/04/16. PubMed PMID: 11950807; PubMed Central PMCID: PMCPMC1773205.

32. Whitfield-Cargile C, Cohen N, Chapkin R, Weeks B, Davidson L, Goldsby J, et al. The microbiota-derived metabolite indole decreases mucosal inflammation and injury in a murine model of NSAID enteropathy. Gut microbes. 2016;7(3):246-61. Epub 2016/03/24. doi: 10.1080/19490976.2016.1156827. PubMed PMID: 27007819.

33. Wallace J, Keenan C, Granger D. Gastric ulceration induced by nonsteroidal anti-inflammatory drugs is a neutrophil-dependent process. The American journal of physiology. 1990;259(3 Pt 1):G462-7. Epub 1990/09/01. PubMed PMID: 2169206.

34. Watanabe T, Tanigawa T, Shiba M, Nadatani Y, Nagami Y, Sugimori S, et al. Anti-tumor necrosis factor agents reduce non-steroidal anti-inflammatory drug-induced small bowel injury in rheumatoid arthritis patients. Gut. 2014;63(3):409-14. Epub 2013/05/24. doi: 10.1136/gutjnl-2013-304713. PubMed PMID: 23697473.

35. Ju C, Uetrecht J. Oxidation of a metabolite of indomethacin (Desmethyldeschlorobenzoylindomethacin) to reactive intermediates by activated neutrophils, hypochlorous acid, and the myeloperoxidase system. Drug metabolism and disposition: the biological fate of chemicals. 1998;26(7):676-80. Epub 1998/07/14. PubMed PMID: 9660850.

36. Liang X, Bittinger K, Li X, Abernethy D, Bushman F, FitzGerald G. Bidirectional interactions between indomethacin and the murine intestinal microbiota. eLife. 2015;4:e08973. Epub 2015/12/25. doi: 10.7554/eLife.08973. PubMed PMID: 26701907; PubMed Central PMCID: PMCPMC4755745.

37. Mayo S, Song Y, Cruz M, Phan T, Singh K, Garsin D, et al. Indomethacin injury to the rat small intestine is dependent upon biliary secretion and is associated with overgrowth of enterococci. Physiological Reports. 2016;4(6). doi: 10.14814/phy2.12725. PubMed PMID: 27033447; PubMed Central PMCID: PMCPMC4814884.

38. Dalby A, Frank D, St Amand A, Bendele A, Pace N. Culture-independent analysis of indomethacin-induced alterations in the rat gastrointestinal microbiota. Applied and environmental microbiology. 2006;72(10):6707-15. Epub 2006/10/06. doi: 10.1128/aem.00378-06. PubMed PMID: 17021222; PubMed Central PMCID: PMCPMC1610281.

39. Uejima M, Kinouchi T, Kataoka K, Hiraoka I, Ohnishi Y. Role of intestinal bacteria in ileal ulcer formation in rats treated with a nonsteroidal antiinflammatory drug. Microbiology and immunology. 1996;40(8):553-60. Epub 1996/01/01. PubMed PMID: 8887349.

40. Teran-Ventura E, Aguilera M, Vergara P, Martinez V. Specific changes of gut commensal microbiota and TLRs during indomethacin-induced acute intestinal inflammation in rats. Journal of Crohn's & colitis. 2014;8(9):1043-54. Epub 2014/02/26. doi: 10.1016/j.crohns.2014.02.001. PubMed PMID: 24566169.

41. Blackler R, De Palma G, Manko A, Da Silva G, Flannigan K, Bercik P, et al. Deciphering the pathogenesis of NSAID enteropathy using proton pump inhibitors and a hydrogen sulfide-releasing NSAID. American journal of physiology Gastrointestinal and liver physiology. 2015;308(12):G994-1003. Epub 2015/04/18. doi: 10.1152/ajpgi.00066.2015. PubMed PMID: 25882612.

42. Makivuokko H, Tiihonen K, Tynkkynen S, Paulin L, Rautonen N. The effect of age and non-steroidal anti-inflammatory drugs on human intestinal microbiota composition. The British journal of nutrition. 2010;103(2):227-34. Epub 2009/08/26. doi: 10.1017/s0007114509991553. PubMed PMID: 19703328.

43. Reuter B, Davies N, Wallace J. Nonsteroidal anti-inflammatory drug enteropathy in rats: role of permeability, bacteria, and enterohepatic circulation. Gastroenterology. 1997;112(1):109-17. Epub 1997/01/01. PubMed PMID: 8978349.

44. Syer S, Blackler R, Martin R, de Palma G, Rossi L, Verdu E, et al. NSAID enteropathy and bacteria: a complicated relationship. Journal of gastroenterology. 2015;50(4):387-93. Epub 2015/01/13. doi: 10.1007/s00535-014-1032-1. PubMed PMID: 25572030.

45. Watanabe T, Nishio H, Tanigawa T, Yamagami H, Okazaki H, Watanabe K, et al. Probiotic Lactobacillus casei strain Shirota prevents indomethacin-induced small intestinal injury: involvement of lactic acid. American journal of physiology Gastrointestinal and liver physiology. 2009;297(3):G506-13. Epub 2009/07/11. doi: 10.1152/ajpgi.90553.2008. PubMed PMID: 19589943.

46. Endo H, Higurashi T, Hosono K, Sakai E, Sekino Y, Iida H, et al. Efficacy of Lactobacillus casei treatment on small bowel injury in chronic low-dose aspirin users: a pilot randomized controlled study. Journal of gastroenterology. 2011;46(7):894-905. Epub 2011/05/11. doi: 10.1007/s00535-011-0410-1. PubMed PMID: 21556830.

47. Montalto M, Gallo A, Curigliano V, D'Onofrio F, Santoro L, Covino M, et al. Clinical trial: the effects of a probiotic mixture on non-steroidal anti-inflammatory drug enteropathy - a randomized, double-blind, cross-over, placebo-controlled study. Alimentary pharmacology & therapeutics. 2010;32(2):209-14. Epub 2010/04/14. doi: 10.1111/j.1365-2036.2010.04324.x. PubMed PMID: 20384610.

48. Kinouchi T, Kataoka K, Bing S, Nakayama H, Uejima M, Shimono K, et al. Culture supernatants of Lactobacillus acidophilus and Bifidobacterium adolescentis repress ileal ulcer formation in rats treated with a nonsteroidal anti-inflammatory drug by suppressing unbalanced growth of aerobic bacteria and lipid peroxidation. Microbiology and immunology. 1998;42(5):347-55. Epub 1998/07/08. PubMed PMID: 9654366.

49. Wallace J, Syer S, Denou E, de Palma G, Vong L, McKnight W, et al. Proton pump inhibitors exacerbate NSAID-induced small intestinal injury by inducing dysbiosis. Gastroenterology. 2011;141(4):1314-22, 22.e1-5. Epub 2011/07/13. doi: 10.1053/j.gastro.2011.06.075. PubMed PMID: 21745447.

50. Rigottier-Gois L. Dysbiosis in inflammatory bowel diseases: the oxygen hypothesis. ISME J. 2013;7(7):1256-61. doi: 10.1038/ismej.2013.80.

51. Winter S, Thiennimitr P, Winter M, Butler B, Huseby D, Crawford R, et al. Gut inflammation provides a respiratory electron acceptor for Salmonella. Nature. 2010;467(7314):426-9. Epub 2010/09/25. doi: 10.1038/nature09415. PubMed PMID: 20864996; PubMed Central PMCID: PMCPMC2946174.

52. Tomita T, Sadakata H, Tamura M, Matsui H. Indomethacin-induced generation of reactive oxygen species leads to epithelial cell injury before the formation of intestinal lesions in mice. Journal of physiology and pharmacology : an official journal of the Polish Physiological Society. 2014;65(3):435-40. Epub 2014/06/17. PubMed PMID: 24930516.

53. Mohsen A, Gomaa A, Mohamed F, Ragab R, Eid M, Ahmed A, et al. Antibacterial, anti-biofilm activity of some non-steroidal anti-inflammatory drugs and N-acetyl cysteine against some biofilm producing uropathogens. American journal of epidemiology and infectious disease. 2015;3(1):1-9. PubMed PMID: doi:10.12691/ajeid-3-1-1.

54. Dastidar S, Ganguly K, Chaudhuri K, Chakrabarty A. The anti-bacterial action of diclofenac shown by inhibition of DNA synthesis. International journal of antimicrobial agents. 2000;14(3):249-51. Epub 2000/04/25. PubMed PMID: 10773497.

55. Yin Z, Wang Y, Whittell L, Jergic S, Liu M, Harry E, et al. DNA replication is the target for the antibacterial effects of nonsteroidal anti-inflammatory drugs. Chemistry & biology. 2014;21(4):481-7. Epub 2014/03/19. doi: 10.1016/j.chembiol.2014.02.009. PubMed PMID: 24631121.

56. Kent T, Cardelli R, Stamler F. Small intestinal ulcers and intestinal flora in rats given indomethacin. The American journal of pathology. 1969;54(2):237-49. Epub 1969/02/01. PubMed PMID: 5765565; PubMed Central PMCID: PMCPMC2013470.

57. Robert A, Asano T. Resistance of germfree rats to indomethacin-induced intestinal lesions. Prostaglandins. 1977;14(2):333-41. Epub 1977/08/01. PubMed PMID: 331401.

58. Mohri K, Okada K, Benet L. Stereoselective metabolism of benoxaprofen in rats. Biliary excretion of benoxaprofen taurine conjugate and glucuronide. Drug metabolism and disposition: the biological fate of chemicals. 1998;26(4):332-7. Epub 1998/05/16. PubMed PMID: 9531520.

59. King C, Tang W, Ngui J, Tephly T, Braun M. Characterization of rat and human UDP-glucuronosyltransferases responsible for the in vitro glucuronidation of diclofenac. Toxicological sciences : an official journal of the Society of Toxicology. 2001;61(1):49-53. Epub 2001/04/11. PubMed PMID: 11294973.

60. Kuehl G, Lampe J, Potter J, Bigler J. Glucuronidation of nonsteroidal anti-inflammatory drugs: identifying the enzymes responsible in human liver microsomes. Drug metabolism and disposition: the biological fate of chemicals. 2005;33(7):1027-35. Epub 2005/04/22. doi: 10.1124/dmd.104.002527. PubMed PMID: 15843492.

61. Saitta K, Zhang C, Lee K, Fujimoto K, Redinbo M, Boelsterli U. Bacterial beta-glucuronidase inhibition protects mice against enteropathy induced by

indomethacin, ketoprofen or diclofenac: mode of action and pharmacokinetics. Xenobiotica; the fate of foreign compounds in biological systems. 2014;44(1):28-35. Epub 2013/07/09. doi: 10.3109/00498254.2013.811314. PubMed PMID: 23829165; PubMed Central PMCID: PMCPMC3972617.

62. Hawksworth G, Drasar B, Hill M. Intestinal bacteria and the hydrolysis of glycosidic bonds. Journal of medical microbiology. 1971;4(4):451-9. Epub 1971/11/01. doi: 10.1099/00222615-4-4-451. PubMed PMID: 5002686.

63. Hofmann A, Hagey L, Krasowski M. Bile salts of vertebrates: structural variation and possible evolutionary significance. Journal of lipid research. 2010;51(2):226-46. Epub 2009/07/30. doi: 10.1194/jlr.R000042. PubMed PMID: 19638645; PubMed Central PMCID: PMCPMC2803226.

64. Ajouz H, Mukherji D, Shamseddine A. Secondary bile acids: an underrecognized cause of colon cancer. World journal of surgical oncology. 2014;12:164. doi: 10.1186/1477-7819-12-164. PubMed PMID: 24884764; PubMed Central PMCID: PMCPMC4041630.

65. Stenman LK, Holma R, Korpela R. High-fat-induced intestinal permeability dysfunction associated with altered fecal bile acids. World journal of gastroenterology. 2012;18(9):923-9. doi: 10.3748/wjg.v18.i9.923. PubMed PMID: 22408351; PubMed Central PMCID: PMCPMC3297051.

66. Payne C, Bernstein C, Dvorak K, Bernstein H. Hydrophobic bile acids, genomic instability, Darwinian selection, and colon carcinogenesis. Clinical and

experimental gastroenterology. 2008;1:19-47. PubMed PMID: 21677822; PubMed Central PMCID: PMCPMC3108627.

67. Ogilvie L, Jones B. Dysbiosis modulates capacity for bile acid modification in the gut microbiomes of patients with inflammatory bowel disease: a mechanism and marker of disease? Gut. 2012. doi: 10.1136/gutjnl-2012-302137.

68. Sagar N, Cree I, Covington J, Arasaradnam R. The interplay of the gut microbiome, bile acids, and volatile organic compounds. Gastroenterology research and practice. 2015;2015:398585. Epub 2015/03/31. doi: 10.1155/2015/398585. PubMed PMID: 25821460; PubMed Central PMCID: PMCPMC4363917.

69. Begley M, Gahan C, Hill C. The interaction between bacteria and bile. FEMS microbiology reviews. 2005;29(4):625-51. Epub 2005/08/17. doi: 10.1016/j.femsre.2004.09.003. PubMed PMID: 16102595.

70. Petruzzelli M, Moschetta A, Renooij W, de Smet M, Palasciano G, Portincasa P, et al. Indomethacin enhances bile salt detergent activity: relevance for NSAIDs-induced gastrointestinal mucosal injury. Digestive diseases and sciences. 2006;51(4):766-74. Epub 2006/04/15. doi: 10.1007/s10620-006-3204-1. PubMed PMID: 16615001.

71. Zhou Y, Dial E, Doyen R, Lichtenberger L. Effect of indomethacin on bile acid-phospholipid interactions: implication for small intestinal injury induced by nonsteroidal anti-inflammatory drugs. American journal of physiology gastrointestinal and liver physiology. 2010;298(5):G722-31. Epub 2010/03/06. doi:

10.1152/ajpgi.00387.2009. PubMed PMID: 20203063; PubMed Central PMCID: PMCPMC2867422.

72. Jacob M, Foster R, Sigthorsson G, Simpson R, Bjarnason I. Role of bile in pathogenesis of indomethacin-induced enteropathy. Archives of toxicology. 2007;81(4):291-8. Epub 2006/12/08. doi: 10.1007/s00204-006-0149-2. PubMed PMID: 17151867.

73. Kumar S, Ingle H, Prasad DV, Kumar H. Recognition of bacterial infection by innate immune sensors. Critical reviews in microbiology. 2013;39(3):229-46. Epub 2012/08/08. doi: 10.3109/1040841x.2012.706249. PubMed PMID: 22866947.

74. Abreu M. Toll-like receptor signaling in the intestinal epithelium: how bacterial recognition shapes intestinal function. Nature reviews immunology. 2010;10(2):131-44. Epub 2010/01/26. doi: 10.1038/nri2707. PubMed PMID: 20098461.

75. Fernandes P, MacSharry J, Darby T, Fanning A, Shanahan F, Houston A, et al. Differential expression of key regulators of Toll-like receptors in ulcerative colitis and Crohn's disease: a role for Tollip and peroxisome proliferator-activated receptor gamma? Clinical and experimental immunology. 2016;183(3):358-68. Epub 2015/10/16. doi: 10.1111/cei.12732. PubMed PMID: 26462859; PubMed Central PMCID: PMCPMC4750602.

76. Carvalho F, Aitken J, Vijay-Kumar M, Gewirtz A. Toll-like receptor–gut microbiota interactions: perturb at your own risk! Annual Review of Physiology. 2012;74(1):177-98. doi: doi:10.1146/annurev-physiol-020911-153330. PubMed PMID: 22035346.

77. Ignacio A, Morales C, Câmara N, Almeida R. Innate sensing of the gut microbiota: modulation of inflammatory and autoimmune diseases. Frontiers in immunology. 2016;7. doi: 10.3389/fimmu.2016.00054. PubMed PMID: 26925061; PubMed Central PMCID: PMCPMC4759259.

78. Hagiwara M, Kataoka K, Arimochi H, Kuwahara T, Ohnishi Y. Role of unbalanced growth of gram-negative bacteria in ileal ulcer formation in rats treated with a nonsteroidal anti-inflammatory drug. The journal of medical investigation: JMI. 2004;51(1-2):43-51. Epub 2004/03/06. PubMed PMID: 15000255.

79. Cario E, Podolsky D. Differential alteration in intestinal epithelial cell expression of toll-like receptor 3 (TLR3) and TLR4 in inflammatory bowel disease. Infection and immunity. 2000;68(12):7010-7. Epub 2000/11/18. PubMed PMID: 11083826; PubMed Central PMCID: PMCPMC97811.

80. Round J, Mazmanian S. The gut microbiome shapes intestinal immune responses during health and disease. Nature reviews immunology. 2009;9(5):313-23. doi: 10.1038/nri2515. PubMed PMID: 19343057; PubMed Central PMCID: PMCPMC4095778.

81. Ewaschuk J, Backer J, Churchill T, Obermeier F, Krause D, Madsen K. Surface expression of Toll-like receptor 9 is upregulated on intestinal epithelial cells in response to pathogenic bacterial DNA. Infection and immunity. 2007;75(5):2572-9. Epub 2007/02/28. doi: 10.1128/iai.01662-06. PubMed PMID: 17325049; PubMed Central PMCID: PMCPMC1865769.

82. Brandl K, Schnabl B. Is intestinal inflammation linking dysbiosis to gut barrier dysfunction during liver disease? Expert review of gastroenterology & hepatology. 2015;9(8):1069-76. doi: 10.1586/17474124.2015.1057122. PubMed PMID: 26088524; PubMed Central PMCID: PMCPMC4828034.

83. Willing B, Dicksved J, Halfvarson J, Andersson A, Lucio M, Zheng Z, et al. A pyrosequencing study in twins shows that gastrointestinal microbial profiles vary with inflammatory bowel disease phenotypes. Gastroenterology. 2010;139(6):1844-54.e1. Epub 2010/09/08. doi: 10.1053/j.gastro.2010.08.049. PubMed PMID: 20816835.

84. Khan M, Duncan S, Stams A, van Dijl J, Flint H, Harmsen H. The gut anaerobe Faecalibacterium prausnitzii uses an extracellular electron shuttle to grow at oxic-anoxic interphases. ISME J. 2012;6(8):1578-85. doi: http://www.nature.com/ismej/journal/v6/n8/suppinfo/ismej20125s1.html.

85. Machiels K, Joossens M, Sabino J, De Preter V, Arijs I, Eeckhaut V, et al. A decrease of the butyrate-producing species Roseburia hominis and Faecalibacterium prausnitzii defines dysbiosis in patients with ulcerative colitis. Gut. 2014;63(8):1275-83. Epub 2013/09/12. doi: 10.1136/gutjnl-2013-304833. PubMed PMID: 24021287.

86. Bing S, Kinouchi T, Kataoka K, Kuwahara T, Ohnishi Y. Protective effects of a culture supernatant of Lactobacillus acidophilus and antioxidants on ileal ulcer formation in rats treated with a nonsteroidal antiinflammatory drug. Microbiology and immunology. 1998;42(11):745-53. Epub 1999/01/14. PubMed PMID: 9886147.

87. Sivaprakasam S, Prasad P, Singh N. Benefits of short-chain fatty acids and their receptors in inflammation and carcinogenesis. Pharmacology & therapeutics.

2016;164:144-51. Epub 2016/04/27. doi: 10.1016/j.pharmthera.2016.04.007. PubMed PMID: 27113407; PubMed Central PMCID: PMCPMC4942363.

88. Nicholson J, Holmes E, Kinross J, Burcelin R, Gibson G, Jia W, et al. Host-gut microbiota metabolic interactions. Science (New York, NY). 2012;336(6086):1262-7. Epub 2012/06/08. doi: 10.1126/science.1223813. PubMed PMID: 22674330.

89. Marcobal A, Kashyap P, Nelson T, Aronov P, Donia M, Spormann A, et al. A metabolomic view of how the human gut microbiota impacts the host metabolome using humanized and gnotobiotic mice. Isme j. 2013;7(10):1933-43. Epub 2013/06/07. doi: 10.1038/ismej.2013.89. PubMed PMID: 23739052; PubMed Central PMCID: PMCPMC3965317.

90. Larsen P, Dai Y. Metabolome of human gut microbiome is predictive of host dysbiosis. GigaScience. 2015;4(1):1-16. doi: 10.1186/s13742-015-0084-3.

91. Sridharan G, Choi K, Klemashevich C, Wu C, Prabakaran D, Pan L, et al. Prediction and quantification of bioactive microbiota metabolites in the mouse gut. Nat commun. 2014;5. doi: 10.1038/ncomms6492.

92. Bansal T, Alaniz R, Wood T, Jayaraman A. The bacterial signal indole increases epithelial-cell tight-junction resistance and attenuates indicators of inflammation. Proceedings of the National Academy of Sciences of the United States of America. 2010;107(1):228-33. Epub 2009/12/08. doi: 10.1073/pnas.0906112107. PubMed PMID: 19966295; PubMed Central PMCID: PMCPMC2806735.

93. Zelante T, Iannitti R, Cunha C, De Luca A, Giovannini G, Pieraccini G, et al. Tryptophan catabolites from microbiota engage aryl hydrocarbon receptor and balance mucosal reactivity via interleukin-22. Immunity. 2013;39(2):372-85. Epub 2013/08/27. doi: 10.1016/j.immuni.2013.08.003. PubMed PMID: 23973224.

94. Thun M, Henley S, Patrono C. Nonsteroidal anti-inflammatory drugs as anticancer agents: mechanistic, pharmacologic, and clinical issues. Journal of the National Cancer Institute. 2002;94(4):252-66. Epub 2002/02/21. PubMed PMID: 11854387.

95. Garcia Rodriguez L, Huerta-Alvarez C. Reduced incidence of colorectal adenoma among long-term users of nonsteroidal anti-inflammatory drugs: a pooled analysis of published studies and a new population-based study. Epidemiology (Cambridge, Mass). 2000;11(4):376-81. Epub 2000/06/30. PubMed PMID: 10874542.

96. Becker J, Domschke W, Pohle T. Current approaches to prevent NSAID-induced gastropathy--COX selectivity and beyond. British journal of clinical pharmacology. 2004;58(6):587-600. Epub 2004/11/26. doi: 10.1111/j.1365-2125.2004.02198.x. PubMed PMID: 15563357; PubMed Central PMCID: PMCPMC1884640.

97. Wallace J. Mechanisms, prevention and clinical implications of nonsteroidal anti-inflammatory drug-enteropathy. World journal of gastroenterology. 2013;19(12):1861-76. Epub 2013/04/10. doi: 10.3748/wjg.v19.i12.1861. PubMed PMID: 23569332; PubMed Central PMCID: PMCPMC3613102.

98. Wolfe M, Lichtenstein D, Singh G. Gastrointestinal toxicity of nonsteroidal antiinflammatory drugs. The New England journal of medicine. 1999;340(24):1888-99. Epub 1999/06/17. doi: 10.1056/nejm199906173402407. PubMed PMID: 10369853.

99. Graham D, Opekun A, Willingham F, Qureshi W. Visible small-intestinal mucosal injury in chronic NSAID users. Clinical gastroenterology and hepatology: the official clinical practice journal of the American Gastroenterological Association. 2005;3(1):55-9. Epub 2005/01/13. PubMed PMID: 15645405.

100. Wallace J. NSAID gastropathy and enteropathy: distinct pathogenesis likely necessitates distinct prevention strategies. British journal of pharmacology. 2012;165(1):67-74. Epub 2011/06/02. doi: 10.1111/j.1476-5381.2011.01509.x. PubMed PMID: 21627632; PubMed Central PMCID: PMCPMC3252967.

101. Shimada Y, Kinoshita M, Harada K, Mizutani M, Masahata K, Kayama H, et al. Commensal bacteria-dependent indole production enhances epithelial barrier function in the colon. PloS one. 2013;8(11):e80604. Epub 2013/11/28. doi: 10.1371/journal.pone.0080604. PubMed PMID: 24278294; PubMed Central PMCID: PMCPMC3835565.

102. Lee J, Jayaraman A, Wood T. Indole is an inter-species biofilm signal mediated by SdiA. BMC microbiology. 2007;7:42. Epub 2007/05/22. doi: 10.1186/1471-2180-7-42. PubMed PMID: 17511876; PubMed Central PMCID: PMCPMC1899176.

103. Lee J, Lee J. Indole as an intercellular signal in microbial communities. FEMS microbiology reviews. 2010;34(4):426-44. Epub 2010/01/15. doi: 10.1111/j.1574-6976.2009.00204.x. PubMed PMID: 20070374.

104. Venkatesh M, Mukherjee S, Wang H, Li H, Sun K, Benechet A, et al. Symbiotic bacterial metabolites regulate gastrointestinal barrier function via the xenobiotic sensor PXR and Toll-like receptor 4. Immunity. 2014;41(2):296-310. Epub 2014/07/30. doi: 10.1016/j.immuni.2014.06.014. PubMed PMID: 25065623; PubMed Central PMCID: PMCPMC4142105.

105. Wang N, Strugnell R, Wijburg O, Brodnicki T. Measuring bacterial load and immune responses in mice infected with Listeria monocytogenes. Journal of visualized experiments: JoVE. 2011;(54). Epub 2011/08/24. doi: 10.3791/3076. PubMed PMID: 21860372; PubMed Central PMCID: PMCPMC3211132.

106. Dobin A, Davis C, Schlesinger F, Drenkow J, Zaleski C, Jha S, et al. STAR: ultrafast universal RNA-seq aligner. Bioinformatics (Oxford, England). 2013;29(1):15-21. Epub 2012/10/30. doi: 10.1093/bioinformatics/bts635. PubMed PMID: 23104886; PubMed Central PMCID: PMCPMC3530905.

107. Robinson M, McCarthy D, Smyth G. edgeR: a Bioconductor package for differential expression analysis of digital gene expression data. Bioinformatics (Oxford, England). 2010;26(1):139-40. Epub 2009/11/17. doi: 10.1093/bioinformatics/btp616. PubMed PMID: 19910308; PubMed Central PMCID: PMCPMC2796818.

108. A framework for human microbiome research. Nature. 2012;486(7402):215-21. Epub 2012/06/16. doi: 10.1038/nature11209. PubMed PMID: 22699610; PubMed Central PMCID: PMCPMC3377744.

109. Structure, function and diversity of the healthy human microbiome. Nature. 2012;486(7402):207-14. Epub 2012/06/16. doi: 10.1038/nature11234. PubMed PMID: 22699609; PubMed Central PMCID: PMCPMC3564958.

110. Caporaso J, Lauber C, Walters W, Berg-Lyons D, Huntley J, Fierer N, et al. Ultra-high-throughput microbial community analysis on the Illumina HiSeq and MiSeq platforms. Isme j. 2012;6(8):1621-4. Epub 2012/03/10. doi: 10.1038/ismej.2012.8. PubMed PMID: 22402401; PubMed Central PMCID: PMCPMC3400413.

111. Caporaso J, Kuczynski J, Stombaugh J, Bittinger K, Bushman F, Costello E, et al. QIIME allows analysis of high-throughput community sequencing data. Nature methods. 2010;7(5):335-6. Epub 2010/04/13. doi: 10.1038/nmeth.f.303. PubMed PMID: 20383131; PubMed Central PMCID: PMCPMC3156573.

112. Edgar R, Haas B, Clemente J, Quince C, Knight R. UCHIME improves sensitivity and speed of chimera detection. Bioinformatics (Oxford, England). 2011;27(16):2194-200. Epub 2011/06/28. doi: 10.1093/bioinformatics/btr381. PubMed PMID: 21700674; PubMed Central PMCID: PMCPMC3150044.

113. Edgar R. Search and clustering orders of magnitude faster than BLAST. Bioinformatics (Oxford, England). 2010;26(19):2460-1. Epub 2010/08/17. doi: 10.1093/bioinformatics/btq461. PubMed PMID: 20709691.

114. DeSantis T, Hugenholtz P, Larsen N, Rojas M, Brodie E, Keller K, et al. Greengenes, a chimera-checked 16S rRNA gene database and workbench compatible with ARB. Applied and environmental microbiology. 2006;72(7):5069-72. Epub 2006/07/06. doi: 10.1128/aem.03006-05. PubMed PMID: 16820507; PubMed Central PMCID: PMCPMC1489311.

115. McDonald D, Price M, Goodrich J, Nawrocki E, DeSantis T, Probst A, et al. An improved Greengenes taxonomy with explicit ranks for ecological and evolutionary analyses of bacteria and archaea. Isme j. 2012;6(3):610-8. Epub 2011/12/03. doi: 10.1038/ismej.2011.139. PubMed PMID: 22134646; PubMed Central PMCID: PMCPMC3280142.

116. Clarke K. Non-parametric multivariate analyses of changes in community structure. Australian journal of ecology. 1993;18(1):117-43. doi: 10.1111/j.1442-9993.1993.tb00438.x.

117. Lozupone C, Knight R. UniFrac: a new phylogenetic method for comparing microbial communities. Applied and environmental microbiology. 2005;71(12):8228-35. doi: 10.1128/aem.71.12.8228-8235.2005. PubMed PMID: 16332807; PubMed Central PMCID: PMCPMC1317376.

118. Bray J, Curtis J. An ordination of the upland forest communities of southern Wisconsin. Ecological monographs. 1957;27(4):325-49. doi: 10.2307/1942268.

119. Hammer O, Harper D. PAST: paleon statictics software package for education and data analysis. Palaeontologica electronica 2001;4(1):9.

120. Langille M, Zaneveld J, Caporaso J, McDonald D, Knights D, Reyes J, et al. Predictive functional profiling of microbial communities using 16S rRNA marker gene sequences. Nature biotechnology. 2013;31(9):814-21. Epub 2013/08/27. doi: 10.1038/nbt.2676. PubMed PMID: 23975157; PubMed Central PMCID: PMCPMC3819121.

121. Charles N, Hardwick D, Daugas E, Illei G, Rivera J. Basophils and the T helper 2 environment can promote the development of lupus nephritis. Nature medicine. 2010;16(6):701-7. Epub 2010/06/01. doi: 10.1038/nm.2159. PubMed PMID: 20512127; PubMed Central PMCID: PMCPMC2909583.

122. Jia Q, Lupton J, Smith R, Weeks B, Callaway E, Davidson L, et al. Reduced colitis-associated colon cancer in Fat-1 (n-3 fatty acid desaturase) transgenic mice. Cancer research. 2008;68(10):3985-91. Epub 2008/05/17. doi: 10.1158/0008-5472.can-07-6251. PubMed PMID: 18483285; PubMed Central PMCID: PMCPMC2648804.

123. Sidak Z. Rectangular Confidence Regions for the Means of Multivariate Normal Distributions. Journal of the American Statistical Association. 1967;62(318):626-33. doi: 10.2307/2283989.

124. Narimatsu K, Higashiyama M, Kurihara C, Takajo T, Maruta K, Yasutake Y, et al. Toll-like receptor (TLR) 2 agonists ameliorate indomethacin-induced murine ileitis by suppressing the TLR4 signaling. Journal of gastroenterology and hepatology. 2015;30(11):1610-7. Epub 2015/04/14. doi: 10.1111/jgh.12980. PubMed PMID: 25867219.

125. Adebayo D, Bjarnason I. Is non-steroidal anti-inflammaory drug (NSAID) enteropathy clinically more important than NSAID gastropathy? Postgraduate medical journal. 2006;82(965):186-91. Epub 2006/03/07. doi: 10.1136/pgmj.2005.039586. PubMed PMID: 16517800; PubMed Central PMCID: PMCPMC2563708.

126. Caunedo-Alvarez A, Gomez-Rodriguez B, Romero-Vazquez J, Arguelles-Arias F, Romero-Castro R, Garcia-Montes J, et al. Macroscopic small bowel mucosal injury caused by chronic nonsteroidal anti-inflammatory drugs (NSAID) use as assessed by capsule endoscopy. Revista espanola de enfermedades digestivas : organo oficial de la Sociedad Espanola de Patologia Digestiva. 2010;102(2):80-5. Epub 2010/04/07. PubMed PMID: 20361843.

127. Tacheci I, Bradna P, Douda T, Bastecka D, Kopacova M, Rejchrt S, et al. NSAID-Induced Enteropathy in Rheumatoid Arthritis Patients with Chronic Occult Gastrointestinal Bleeding: A Prospective Capsule Endoscopy Study. Gastroenterology research and practice. 2013;2013:268382. Epub 2014/01/03. doi: 10.1155/2013/268382. PubMed PMID: 24382953; PubMed Central PMCID: PMCPMC3870618.

128. Kim H, Alonzo E, Dorothee G, Pollard J, Sant'Angelo D. Selective depletion of eosinophils or neutrophils in mice impacts the efficiency of apoptotic cell clearance in the thymus. PloS one. 2010;5(7):e11439. Epub 2010/07/14. doi: 10.1371/journal.pone.0011439. PubMed PMID: 20625428; PubMed Central PMCID: PMCPMC2897847.

129. Jones-Hall Y, Kozik A, Nakatsu C. Ablation of tumor necrosis factor is associated with decreased inflammation and alterations of the microbiota in a mouse model of inflammatory bowel disease. PloS one. 2015;10(3):e0119441. Epub 2015/03/17. doi: 10.1371/journal.pone.0119441. PubMed PMID: 25775453; PubMed Central PMCID: PMCPMC4361568.

130. Sands S, Tsau S, Yankee T, Parker B, Ericsson A, LeVine S. The effect of omeprazole on the development of experimental autoimmune encephalomyelitis in C57BL/6J and SJL/J mice. BMC research notes. 2014;7:605. Epub 2014/09/06. doi: 10.1186/1756-0500-7-605. PubMed PMID: 25190469; PubMed Central PMCID: PMCPMC4167283.

131. Tibble J, Sigthorsson G, Foster R, Scott D, Fagerhol M, Roseth A, et al. High prevalence of NSAID enteropathy as shown by a simple faecal test. Gut. 1999;45(3):362-6. Epub 1999/08/14. PubMed PMID: 10446103; PubMed Central PMCID: PMCPMC1727647.

132. Lopetuso L, Scaldaferri F, Petito V, Gasbarrini A. Commensal Clostridia: leading players in the maintenance of gut homeostasis. Gut pathogens. 2013;5(1):23. Epub 2013/08/15. doi: 10.1186/1757-4749-5-23. PubMed PMID: 23941657; PubMed Central PMCID: PMCPMC3751348.

133. Zeino Z, Sisson G, Bjarnason I. Adverse effects of drugs on small intestine and colon. Best practice & research Clinical gastroenterology. 2010;24(2):133-41. Epub 2010/03/17. doi: 10.1016/j.bpg.2010.02.008. PubMed PMID: 20227027.

134. Konaka A, Kato S, Tanaka A, Kunikata T, Korolkiewicz R, Takeuchi K. Roles of enterobacteria, nitric oxide and neutrophil in pathogenesis of indomethacin-induced small intestinal lesions in rats. Pharmacological research. 1999;40(6):517-24. Epub 2000/02/08. doi: 10.1006/phrs.1999.0550. PubMed PMID: 10660951.

135. Saud B, Nandi J, Ong G, Finocchiaro S, Levine R. Inhibition of TNF-alpha improves indomethacin-induced enteropathy in rats by modulating iNOS expression. Digestive diseases and sciences. 2005;50(9):1677-83. Epub 2005/09/01. doi: 10.1007/s10620-005-2914-0. PubMed PMID: 16133968.

136. Al-Sadi R, Ma T. IL-1beta causes an increase in intestinal epithelial tight junction permeability. Journal of immunology (Baltimore, Md : 1950). 2007;178(7):4641-9. Epub 2007/03/21. PubMed PMID: 17372023; PubMed Central PMCID: PMCPMC3724221.

137. Handa O, Naito Y, Fukui A, Omatsu T, Yoshikawa T. The impact of non-steroidal anti-inflammatory drugs on the small intestinal epithelium. Journal of clinical biochemistry and nutrition. 2014;54(1):2-6. Epub 2014/01/16. doi: 10.3164/jcbn.13-84. PubMed PMID: 24426183; PubMed Central PMCID: PMCPMC3882490.

138. Teran-Ventura E, Roca M, Martin M, Abarca M, Martinez V, Vergara P. Characterization of housing-related spontaneous variations of gut microbiota and expression of toll-like receptors 2 and 4 in rats. Microbial ecology. 2010;60(3):691-702. Epub 2010/08/19. doi: 10.1007/s00248-010-9737-z. PubMed PMID: 20717659.

139. Karlin D, Mastromarino A, Jones R, Stroehlein J, Lorentz O. Fecal skatole and indole and breath methane and hydrogen in patients with large bowel polyps

or cancer. Journal of cancer research and clinical oncology. 1985;109(2):135-41. Epub 1985/01/01. PubMed PMID: 3980562.

140. Zuccato E, Venturi M, Di Leo G, Colombo L, Bertolo C, Doldi S, et al. Role of bile acids and metabolic activity of colonic bacteria in increased risk of colon cancer after cholecystectomy. Digestive diseases and sciences. 1993;38(3):514-9. Epub 1993/03/01. PubMed PMID: 8444084.

141. Sartor R. Gut microbiota: Optimal sampling of the intestinal microbiota for research. Nature reviews Gastroenterology & hepatology. 2015;12(5):253-4. Epub 2015/03/25. doi: 10.1038/nrgastro.2015.46. PubMed PMID: 25802025.

142. Lavelle A, Lennon G, O'Sullivan O, Docherty N, Balfe A, Maguire A, et al. Spatial variation of the colonic microbiota in patients with ulcerative colitis and control volunteers. Gut. 2015;64(10):1553-61. Epub 2015/01/18. doi: 10.1136/gutjnl-2014-307873. PubMed PMID: 25596182; PubMed Central PMCID: PMCPMC4602252.

143. Takeuchi K, Miyazawa T, Tanaka A, Kato S, Kunikata T. Pathogenic importance of intestinal hypermotility in NSAID-induced small intestinal damage in rats. Digestion. 2002;66(1):30-41. Epub 2002/10/16. doi: 64419. PubMed PMID: 12379813.

144. Satoh H. Role of dietary fiber in formation and prevention of small intestinal ulcers induced by nonsteroidal anti-inflammatory drug. Current pharmaceutical design. 2010;16(10):1209-13. Epub 2010/02/20. PubMed PMID: 20166992.

145. Bjarnason I, Fehilly B, Smethurst P, Menzies I, Levi A. Importance of local versus systemic effects of non-steroidal anti-inflammatory drugs in increasing

small intestinal permeability in man. Gut. 1991;32(3):275-7. Epub 1991/03/01. PubMed PMID: 1901563; PubMed Central PMCID: PMCPMC1378833.

146. Bjarnason I, Hayllar J, MacPherson AJ, Russell AS. Side effects of nonsteroidal anti-inflammatory drugs on the small and large intestine in humans. Gastroenterology. 1993;104(6):1832-47. Epub 1993/06/01. PubMed PMID: 8500743.

147. Shaheen N, Straus W, Sandler R. Chemoprevention of gastrointestinal malignancies with nonsteroidal antiinflammatory drugs. Cancer. 2002;94(4):950-63. Epub 2002/03/29. PubMed PMID: 11920463.

148. Cohen N, Carter G, Mealey R, Taylor T. Medical management of right dorsal colitis in 5 horses: a retrospective study (1987-1993). Journal of veterinary internal medicine / American College of Veterinary Internal Medicine. 1995;9(4):272-6. Epub 1995/07/01. PubMed PMID: 8523325.

149. McConnico R, Morgan T, Williams C, Hubert J, Moore R. Pathophysiologic effects of phenylbutazone on the right dorsal colon in horses. American journal of veterinary research. 2008;69(11):1496-505. Epub 2008/11/05. doi: 10.2460/ajvr.69.11.1496. PubMed PMID: 18980433.

150. Marshall J, Blikslager A. The effect of nonsteroidal anti-inflammatory drugs on the equine intestine. Equine veterinary journal Supplement. 2011;(39):140-4. Epub 2011/08/04. doi: 10.1111/j.2042-3306.2011.00398.x. PubMed PMID: 21790769.

151. Santucci L, Fiorucci S, Giansanti M, Brunori P, Di Matteo F, Morelli A. Pentoxifylline prevents indomethacin induced acute gastric mucosal damage in rats: role

of tumour necrosis factor alpha. Gut. 1994;35(7):909-15. Epub 1994/07/01. PubMed PMID: 8063218; PubMed Central PMCID: PMCPmc1374837.

152. Appleyard C, McCafferty D, Tigley A, Swain M, Wallace J. Tumor necrosis factor mediation of NSAID-induced gastric damage: role of leukocyte adherence. The American journal of physiology. 1996;270(1 Pt 1):G42-8. Epub 1996/01/01. PubMed PMID: 8772499.

153. Potten C, Schofield R, Lajtha L. A comparison of cell replacement in bone marrow, testis and three regions of surface epithelium. Biochimica et biophysica acta. 1979;560(2):281-99. Epub 1979/08/10. PubMed PMID: 380653.

154. Chapkin R, Clark A, Davidson L, Schroeder F, Zoran D, Lupton J. Dietary fiber differentially alters cellular fatty acid-binding protein expression in exfoliated colonocytes during tumor development. Nutrition and cancer. 1998;32(2):107-12. Epub 1999/01/27. doi: 10.1080/01635589809514727. PubMed PMID: 9919620.

155. Chapkin R, Zhao C, Ivanov I, Davidson L, Goldsby J, Lupton J, et al. Noninvasive stool-based detection of infant gastrointestinal development using gene expression profiles from exfoliated epithelial cells. American journal of physiology gastrointestinal and liver physiology. 2010;298(5):G582-9. Epub 2010/03/06. doi: 10.1152/ajpgi.00004.2010. PubMed PMID: 20203060; PubMed Central PMCID: PMCPmc2867429.

156. Davidson L, Aymond C, Jiang Y, Turner N, Lupton J, Chapkin R. Non-invasive detection of fecal protein kinase C betaII and zeta messenger RNA: putative

biomarkers for colon cancer. Carcinogenesis. 1998;19(2):253-7. Epub 1998/03/14. PubMed PMID: 9498273.

157. Schwartz S, Friedberg I, Ivanov I, Davidson L, Goldsby J, Dahl D, et al. A metagenomic study of diet-dependent interaction between gut microbiota and host in infants reveals differences in immune response. Genome biology. 2012;13(4):r32. Epub 2012/05/02. doi: 10.1186/gb-2012-13-4-r32. PubMed PMID: 22546241; PubMed Central PMCID: PMCPMC3446306.

158. Knight J, Davidson L, Herman D, Martin C, Goldsby J, Ivanov I, et al. Non-invasive analysis of intestinal development in preterm and term infants using RNA-Sequencing. Scientific reports. 2014;4:5453. Epub 2014/06/27. doi: 10.1038/srep05453. PubMed PMID: 24965658; PubMed Central PMCID: PMCPMC4071321.

159. Davidson L, Lupton J, Miskovsky E, Fields A, Chapkin R. Quantification of human intestinal gene expression profiles using exfoliated colonocytes: a pilot study. Biomarkers : biochemical indicators of exposure, response, and susceptibility to chemicals. 2003;8(1):51-61. Epub 2003/01/10. doi: 10.1080/1354750021000042268. PubMed PMID: 12519636.

160. Witten D, Tibshirani R, Hastie T. A penalized matrix decomposition, with applications to sparse principal components and canonical correlation analysis. Biostatistics (Oxford, England). 2009;10(3):515-34. Epub 2009/04/21. doi: 10.1093/biostatistics/kxp008. PubMed PMID: 19377034; PubMed Central PMCID: PMCPMC2697346.

161. Witten D, Tibshirani R. Extensions of sparse canonical correlation analysis with applications to genomic data. Statistical applications in genetics and molecular biology. 2009;8:Article28. Epub 2009/07/04. doi: 10.2202/1544-6115.1470. PubMed PMID: 19572827; PubMed Central PMCID: PMCPMC2861323.

162. Rouse M, Singh N, Nagarkatti P, Nagarkatti M. Indoles mitigate the development of experimental autoimmune encephalomyelitis by induction of reciprocal differentiation of regulatory T cells and Th17 cells. British journal of pharmacology. 2013;169(6):1305-21. Epub 2013/04/17. doi: 10.1111/bph.12205. PubMed PMID: 23586923; PubMed Central PMCID: PMCPMC3831710.

163. Warde-Farley D, Donaldson SL, Comes O, Zuberi K, Badrawi R, Chao P, et al. The GeneMANIA prediction server: biological network integration for gene prioritization and predicting gene function. Nucleic acids research. 2010;38(Web Server issue):W214-20. Epub 2010/07/02. doi: 10.1093/nar/gkq537. PubMed PMID: 20576703; PubMed Central PMCID: PMCPMC2896186.

164. Braga-Neto U, Dougherty E. Bolstered error estimation. Pattern recognition. 2004;37(6):1267-81. doi: http://dx.doi.org/10.1016/j.patcog.2003.08.017.

165. Lin D, Zhang J, Li J, Calhoun V, Deng H, Wang Y. Group sparse canonical correlation analysis for genomic data integration. BMC bioinformatics. 2013;14:245. Epub 2013/08/14. doi: 10.1186/1471-2105-14-245. PubMed PMID: 23937249; PubMed Central PMCID: PMCPMC3751310.

166. DiLauro S, Crum-Cianflone N. Ileitis: When It Is Not Crohn's Disease. Current gastroenterology reports. 2010;12(4):249-58. doi: 10.1007/s11894-010-0112-5. PubMed PMID: 20532706; PubMed Central PMCID: PMCPMC2914216.

167. Kwo P, Tremaine W. Nonsteroidal anti-inflammatory drug-induced enteropathy: case discussion and review of the literature. Mayo clinic proceedings. 1995;70(1):55-61. Epub 1995/01/01. doi: 10.1016/s0025-6196(11)64666-1. PubMed PMID: 7808053.

168. Bjarnason I, Zanelli G, Smith T, Prouse P, Williams P, Smethurst P, et al. Nonsteroidal anti-inflammatory drug-induced intestinal inflammation in humans. Gastroenterology. 1987;93(3):480-9. Epub 1987/09/01. PubMed PMID: 3609658.

169. Ananthakrishnan A, Higuchi L, Huang E, Khalili H, Richter J, Fuchs C, et al. Aspirin, nonsteroidal anti-inflammatory drug use, and risk for Crohn disease and ulcerative colitis: a cohort study. Annals of internal medicine. 2012;156(5):350-9. Epub 2012/03/07. doi: 10.7326/0003-4819-156-5-201203060-00007. PubMed PMID: 22393130; PubMed Central PMCID: PMCPMC3369539.

170. Imaeda H, Fujimoto T, Takahashi K, Kasumi E, Fujiyama Y, Andoh A. Terminal-restriction fragment length polymorphism (T-RFLP) analysis for changes in the gut microbiota profiles of indomethacin- and rebamipide-treated mice. Digestion. 2012;86(3):250-7. Epub 2012/09/12. doi: 10.1159/000341508. PubMed PMID: 22964750.

171. Nadatani Y, Watanabe T, Tanigawa T, Machida H, Okazaki H, Yamagami H, et al. High mobility group box 1 promotes small intestinal damage

induced by nonsteroidal anti-inflammatory drugs through Toll-like receptor 4. The American journal of pathology. 2012;181(1):98-110. Epub 2012/05/29. doi: 10.1016/j.ajpath.2012.03.039. PubMed PMID: 22634181.

172. Sridharan G, Choi K, Klemashevich C, Wu C, Prabakaran D, Pan L, et al. Prediction and quantification of bioactive microbiota metabolites in the mouse gut. Nature communications. 2014;5:5492. Epub 2014/11/21. doi: 10.1038/ncomms6492. PubMed PMID: 25411059.

173. Singh N, Singh U, Rouse M, Zhang J, Chatterjee S, Nagarkatti P, et al. Dietary Indoles Suppress Delayed-Type Hypersensitivity by Inducing a Switch from Proinflammatory Th17 Cells to Anti-Inflammatory Regulatory T Cells through Regulation of MicroRNA. Journal of immunology (Baltimore, Md : 1950). 2016;196(3):1108-22. Epub 2015/12/30. doi: 10.4049/jimmunol.1501727. PubMed PMID: 26712945; PubMed Central PMCID: PMCPMC4724476.

174. Sang Y, Zhang W, Lv P, Zhu H. Indole-based, Antiproliferative Agents Targeting Tubulin Polymerization. Current topics in medicinal chemistry. 2016. Epub 2016/05/31. PubMed PMID: 27237326.

175. Julliard W, De Wolfe T, Fechner J, Safdar N, Agni R, Mezrich J. Amelioration of Clostridium difficile Infection in Mice by Dietary Supplementation With Indole-3-carbinol. Annals of surgery. 2016. Epub 2016/06/10. doi: 10.1097/sla.0000000000001830. PubMed PMID: 27280500.

176. Ji T, Xu C, Sun L, Yu M, Peng K, Qiu Y, et al. Aryl Hydrocarbon Receptor Activation Down-Regulates IL-7 and Reduces Inflammation in a Mouse Model

of DSS-Induced Colitis. Digestive diseases and sciences. 2015;60(7):1958-66. Epub 2015/03/25. doi: 10.1007/s10620-015-3632-x. PubMed PMID: 25799939.

177. Chng S, Kundu P, Dominguez-Brauer C, Teo W, Kawajiri K, Fujii-Kuriyama Y, et al. Ablating the aryl hydrocarbon receptor (AhR) in CD11c+ cells perturbs intestinal epithelium development and intestinal immunity. Scientific reports. 2016;6:23820. Epub 2016/04/14. doi: 10.1038/srep23820. PubMed PMID: 27068235; PubMed Central PMCID: PMCPMC4828637.

178. Monteleone I, Rizzo A, Sarra M, Sica G, Sileri P, Biancone L, et al. Aryl hydrocarbon receptor-induced signals up-regulate IL-22 production and inhibit inflammation in the gastrointestinal tract. Gastroenterology. 2011;141(1):237-48, 48.e1. Epub 2011/05/24. doi: 10.1053/j.gastro.2011.04.007. PubMed PMID: 21600206.

179. Rasmussen M, Balaguer P, Ekstrand B, Daujat-Chavanieu M, Gerbal-Chaloin S. Skatole (3-Methylindole) Is a Partial Aryl Hydrocarbon Receptor Agonist and Induces CYP1A1/2 and CYP1B1 Expression in Primary Human Hepatocytes. PloS one. 2016;11(5):e0154629. Epub 2016/05/04. doi: 10.1371/journal.pone.0154629. PubMed PMID: 27138278; PubMed Central PMCID: PMCPMC4854444.

180. Cheng Y, Jin UH, Allred C, Jayaraman A, Chapkin R, Safe S. Aryl Hydrocarbon Receptor Activity of Tryptophan Metabolites in Young Adult Mouse Colonocytes. Drug metabolism and disposition: the biological fate of chemicals. 2015;43(10):1536-43. Epub 2015/04/16. doi: 10.1124/dmd.115.063677. PubMed PMID: 25873348; PubMed Central PMCID: PMCPMC4576676.

181. Jin U, Lee S, Sridharan G, Lee K, Davidson LA, Jayaraman A, et al. Microbiome-derived tryptophan metabolites and their aryl hydrocarbon receptor-dependent agonist and antagonist activities. Molecular pharmacology. 2014;85(5):777-88. Epub 2014/02/25. doi: 10.1124/mol.113.091165. PubMed PMID: 24563545; PubMed Central PMCID: PMCPMC3990014.

APPENDIX I

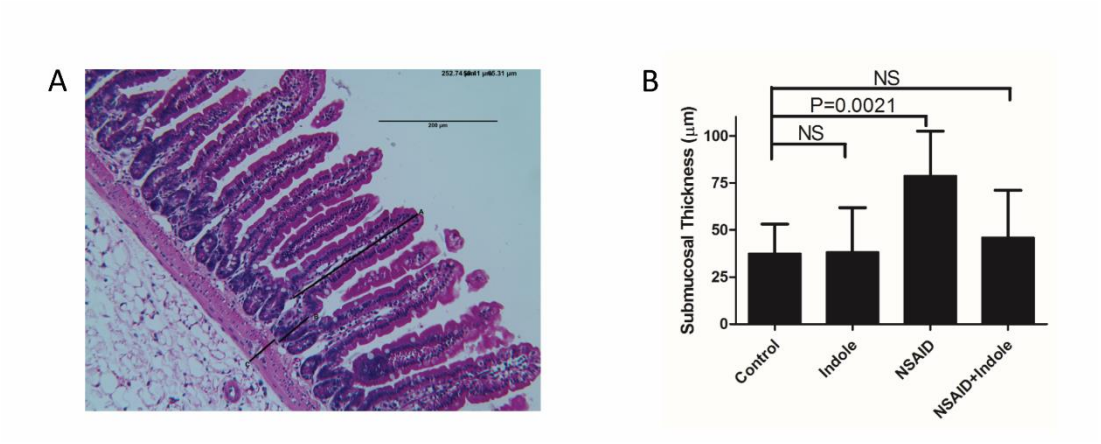

Figure A-1.1: Indole attenuates small intestinal mural thickening associated with NSAID enteropathy. A) Diagram of location of representative measures for calculating villus height [A], crypt depth [B], and mural thickness [C]. Three sets of measurements from 3 separate sections were recorded for each animal by an observer blinded to treatment group. B) Graphical representation of mural thickness among all groups.

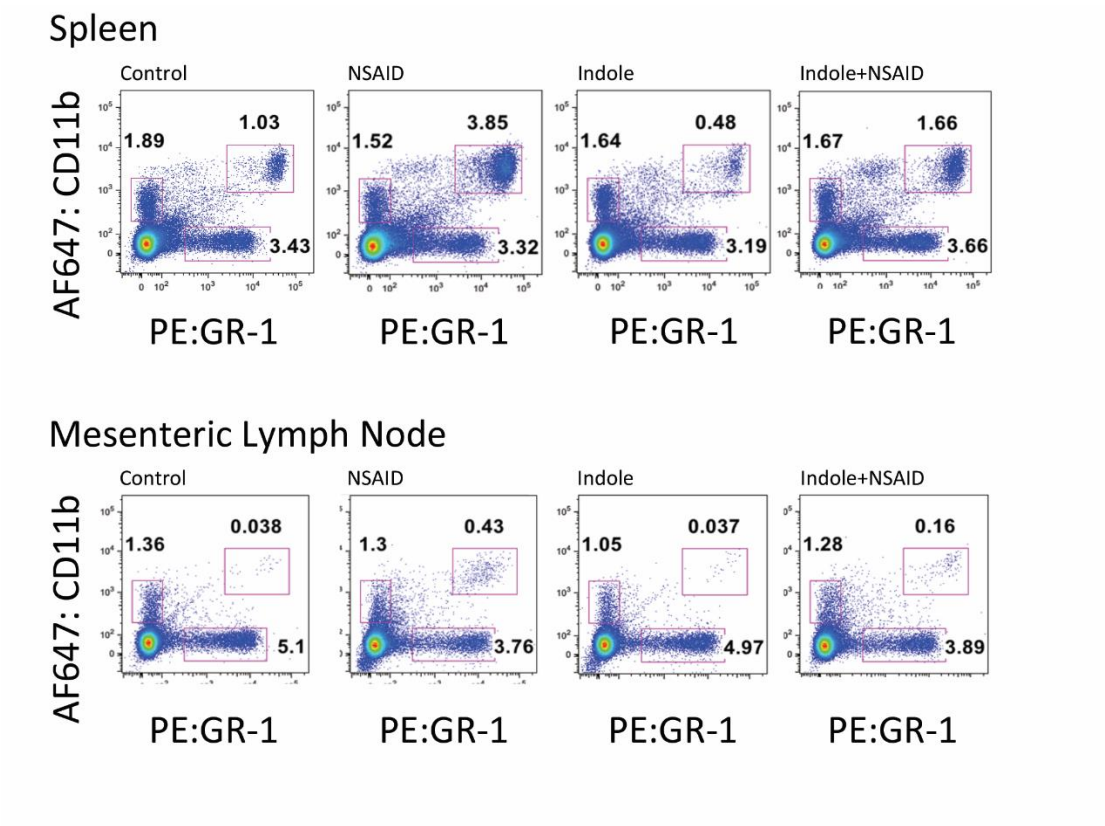

Figure A-1.2: Co-administration of indole reduces NSAID-induced neutrophilic infiltration. A) Representative dot-plots of double-positive CD11b/GR-1 cells (neutrophils) from spleen and B) mesenteric lymph nodes.

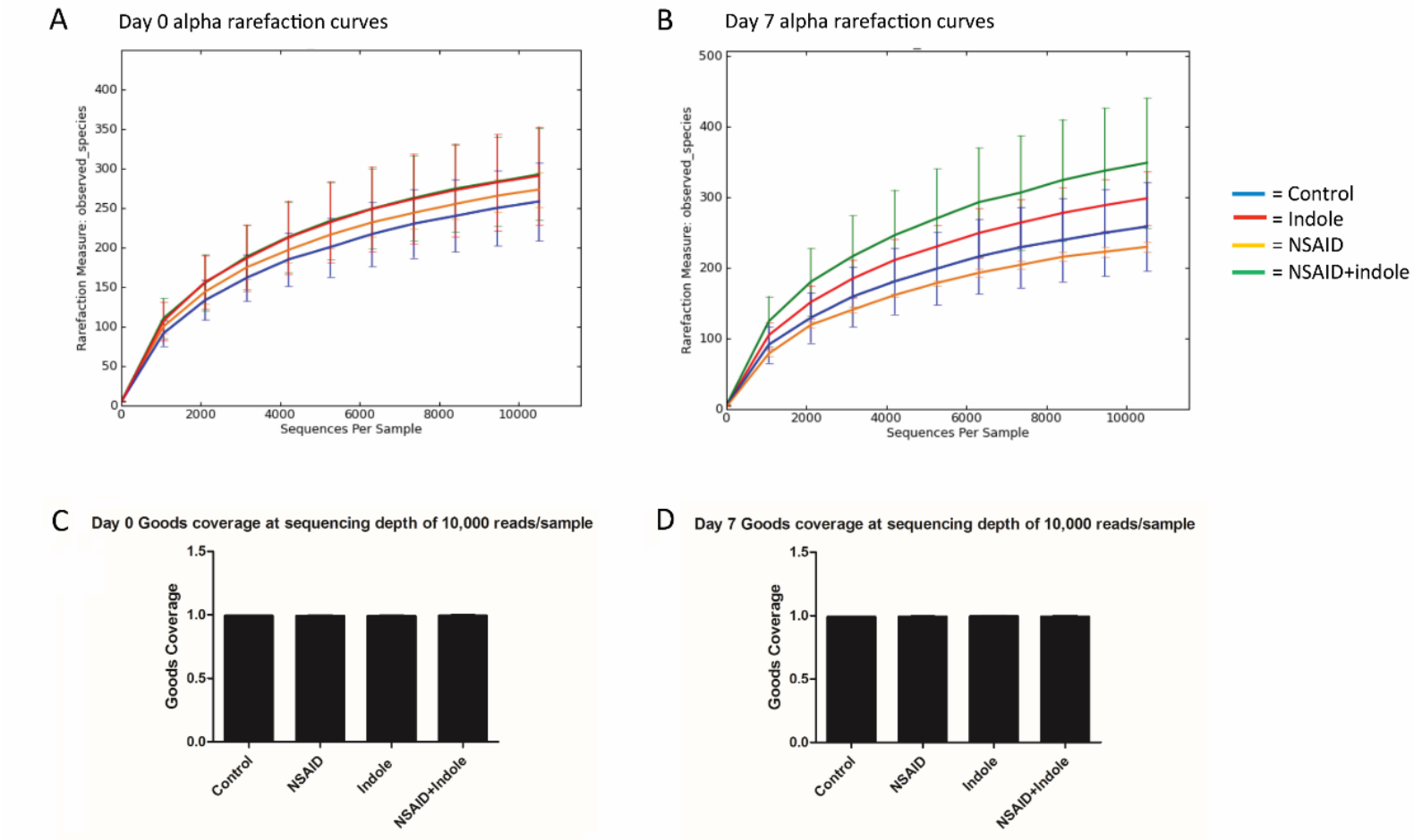

Figure A-1.3: There are no differences in alpha rarefaction among the groups but coverage is adequate. A) Alpha rarefaction curves for each treatment group showing numbers of observed species (richness) at each sampling depth on the y-axis and sequences/sample on the x-axis up to a sampling depth of 10,800 sequences/sample at Day 0 and B) Day 7. C) Bar charts of estimated Good's coverage at an even sampling depth of 10,800 reads/sample at Day 0 and D) Day 7.

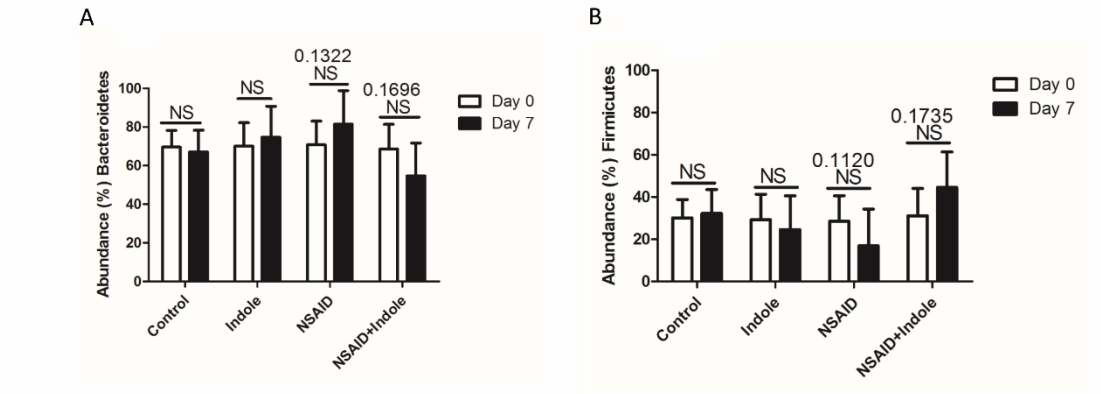

Figure A-1.4: Abundance of critical phyla among the groups at 2 time points: A) Abundance of members of the phylum *Bacteroidetes* in fecal 16S rRNA sequences on Day 0 (white bar) and Day 7 (black bar). B) Abundance of members of the phylum *Firmicutes* in fecal 16S rRNA sequences on Day 0 (white bar) and Day 7 (black bar).

Phylum	% Contribution to dissimalarity	% Cumulative dissimalarity	Control mean % abundance	NSAID mean % abundance
k__Bacteria;p__Firmicutes	49.22	49.22	32.2	17.1
k__Bacteria;p__Bacteroidetes	47.32	96.54	67.1	81.2
k__Bacteria;p__Tenericutes	3.215	99.75	0.611	1.66
k__Bacteria;p__Actinobacteria	0.1128	99.87	0.0552	0.0476
k__Bacteria;p__Proteobacteria	0.05056	99.92	0.0171	0.00317
Unassigned;Other	0.04668	99.96	0.0171	0.00317
k__Bacteria;p__Cyanobacteria	0.01555	99.98	0.0038	0.00634
k__Bacteria;p__Verrucomicrobia	0.01167	99.99	0.0038	0
k__Bacteria;p__Acidobacteria	0.009721	100	0	0.00317
k__Bacteria;Other	0	100	0	0

Phylum	% Contribution to dissimilarity	% Cumulative dissimilarity	Control mean % abundance	NSAID+Indole mean % abundance
k__Bacteria;p__Firmicutes	49.41	49.41	32.2	44.5
k__Bacteria;p__Bacteroidetes	49.19	98.6	67.1	54.7
k__Bacteria;p__Tenericutes	1.174	99.77	0.611	0.671
k__Bacteria;p__Actinobacteria	0.09981	99.87	0.0552	0.0452
k__Bacteria;p__Proteobacteria	0.06521	99.94	0.0171	0.0262
Unassigned;Other	0.03194	99.97	0.0171	0.0143
k__Bacteria;p__Cyanobacteria	0.01197	99.98	0.0038	0.00238
k__Bacteria;p__Verrucomicrobia	0.01197	99.99	0.0038	0.00238
k__Bacteria;Other	0.006652	100	0	0.00238
k__Bacteria;p__Acidobacteria	0	100	0	0

Phylum	% Contribution to dissimilarity	% Cumulative dissimilarity	Control mean % abundance	Indole mean % abundance
k__Bacteria;p__Bacteroidetes	49.21	49.21	67.1	74.7
k__Bacteria;p__Firmicutes	49.01	98.22	32.2	24.6
k__Bacteria;p__Tenericutes	1.37	99.59	0.611	0.656
k__Bacteria;p__Actinobacteria	0.1894	99.78	0.0552	0.0381
k__Bacteria;p__Proteobacteria	0.09238	99.87	0.0171	0.0285
Unassigned;Other	0.06467	99.94	0.0171	1.90E-03
k__Bacteria;p__Cyanobacteria	0.02925	99.97	3.80E-03	9.51E-03
k__Bacteria;p__Verrucomicrobia	0.01693	99.98	3.80E-03	1.90E-03
k__Bacteria;Other	0.0154	100	0	3.81E-03
k__Bacteria;p__Acidobacteria	0	100	0	0

Table A-1.1: Pair-wise SIMPER analysis based on the bray Curtis dissimilarity measure of fecal 16S rRNA data at the phylum level of each treatment group compared to the control group based on day 7 feces. Top panel) The first column identifies the bacterial phylum explained by that row, the second column shows % contribution of that phylum to the Bray Curtis dissimilarity measure between the 2 groups, the third column tallies the cumulative Bray Curtis dissimilarity measure thus far represented in the table, and the last 2 columns show mean abundance in control mice and mean abundance for NSAID-treated mice, Middle panel) control mice and NSAID + indole-treated mice, and Bottom panel) control mice and indole-treated mice.

Metabolite	Score <2 Median (Range)	Score >2 Median (Range)	P value
Hydroxytryptophan	11.9 (3.5-24.5)	27.3 (6.0-28.4)	0.3097
Hydroxyindole	23.7 (15.7-58.1)	38.3 (18.0-78.6)	0.3301
Arginine	11.2 (1.9-241.6)	8.9 (4.9-24.6)	1
Glutamic Acid	404 (56-4,857)	345 (77-1,814)	0.953
Indole-3-acetamide	0.001 (<0.001-0.004)	0.001 (<0.001-0.002)	0.5941
Indole-3-actetate	0.021 (0.0.080)	0 (0-0.238)	0.3879
Indole-3-carboxaldehyde	0.324 (0.162-0.867)	0.441 (0.179-0.582)	0.5135
Indole	21.5 (0-157.2)	97.1 (53.3-131.3)	0.0922
Kyneurine	0 (0-0.184)	0 (0 to 0.061)	0.6287
Ornithine	6.2 (2.0-9.6)	13.3 (6.3-32.8)	0.3277
Phenylalanine	2053 (1109-6247)	3,108 (1,192-3,957)	0.8591
Serotonin	1.28 (0.62-1.73)	2.60 (0.60-3.32)	0.0992
Tryptamine	0.076 (0.050-0.314)	0.094 (0.053-0.166)	0.2065
Tryptophan	3.38 (1.33-19.22)	4.66 (1.64-7.95)	0.5135
Tyramine	**2.32 (1.44-11.66)**	**22.77 (2.68-208.17)**	**0.008**
Tyrosine	48.0 (20.9-231.0)	24.88 (10.52-134.37)	0.206

Table A-1.2: Correlation of fecal tryptophan metabolites with histopathology scores ≤ 2 or > 2. Only the tryptophan metabolite tyramine correlated with microscopic pathology score.

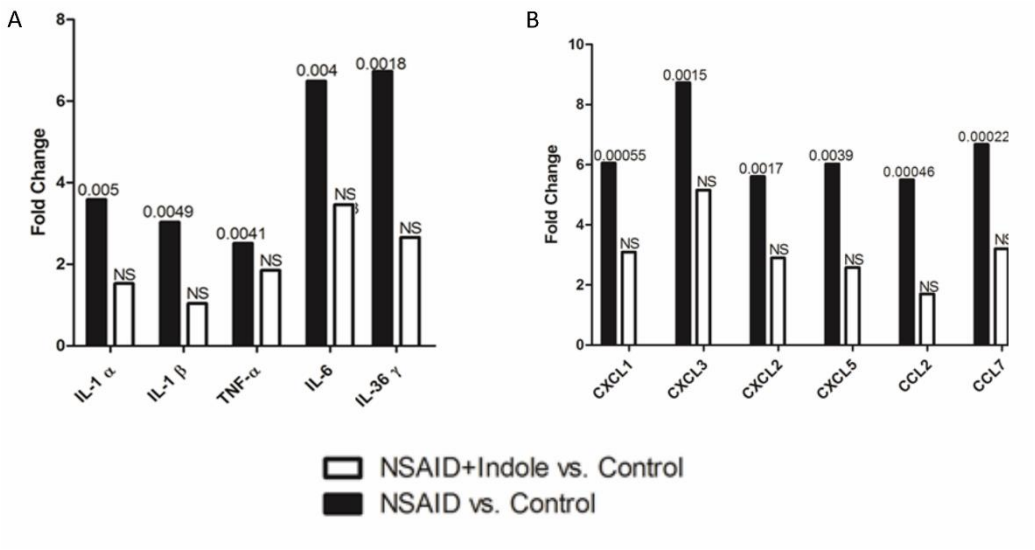

Figure A-1.5: Co-administration of indole decreased expression of several pro-inflammatory cytokines and chemokines. A) Log fold-change, and FDR P-value of several pro-inflammatory cytokines and chemokines that differed between NSAID vs. control (black) and NSAID+Indole vs. control (white).

APPENDIX II

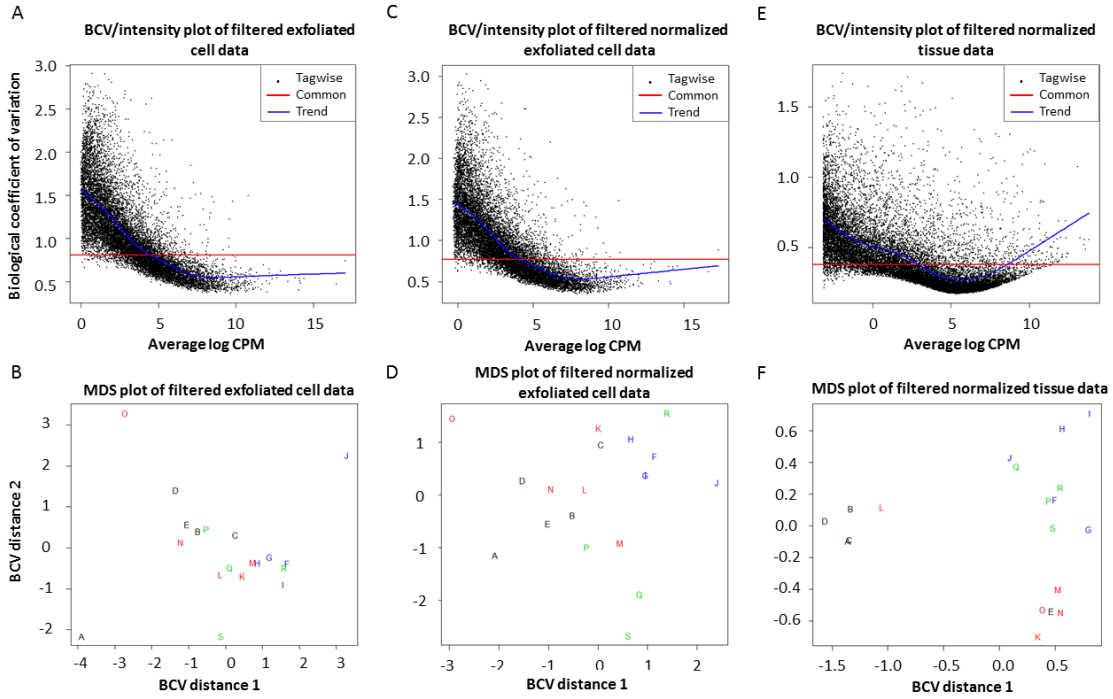

Figure A-2.1: Biological variability in the exfoliated IEC data is higher than the tissue data but is improved by normalization and is not based on treatment group. A) Biological coefficient of variation (BCV) versus the mean log counts per million (CPM) of exfoliated IECs after filtering. B) Treatment-based multi-dimensional scaling (MDS) plots of exfoliated IEC data after filtering. C) BCV versus CPM of exfoliated IECs after filtering and normalization. D) Treatment-based MDS plots of exfoliated IEC data after filtering and normalization. E) BCV versus CPM of tissue data after filtering and normalization. F) Treatment-based MDS plots of tissue data after filtering and normalization.

Gene Symbol	Error
MMP13	0
APAF1	0.0001
CLUH	0.0001
HP	0.0006
NDUFB2	0.0022
LZTFL1	0.0039
NLN	0.0054
SLC47A1	0.0076
GPX3	0.0087
SLC35F5	0.01
MELK	0.01
MTCH1	0.0119
SMYD5	0.0119
SCL11A1	0.0127
CFL2	0.0127
GSDMC	0.014
ARFGEF3	0.0189
HLA-DQA1	0.0195
BPTF	0.0209
G0S2	0.0239

Table A-2.1: Gene symbol and bolstered re-substituted error rate of the top 20 genes identified by one-feature linear discriminate analysis (LDA) that classify NSAID treated animals from control animals with less than 5% error.

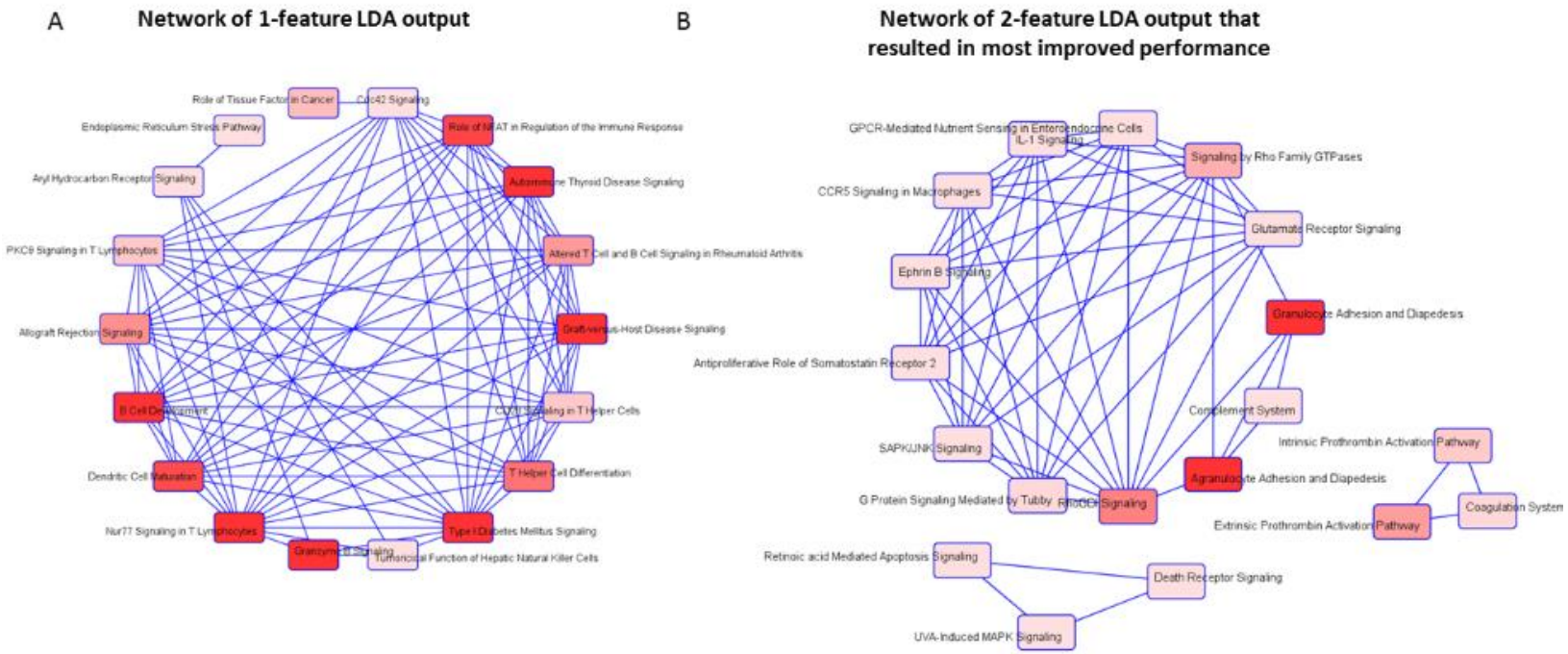

Figure A-2.2: LDA identifies several pathways important in the development of NSAID enteropathy. A) Network of canonical pathways, identified by 1-feature LDA. B) Network of canonical pathways to the sets of genes that showed the greatest improvement in the estimated error rates when moving from 1-feature to 2-feature LDA.

Upstream Regulator	P-value of Overlap	Target Genes in Dataset
ARNT2	5.52E-05	CD86, CFL2, FCGR2A, GPX3, OAZ1
SIM1	6.33E-05	CD86, CFL2, FCGR2A, GPX3, OAZ1
S100A12	2.12E-04	APAF1, MMP13
ACTB	5.20E-04	Cald1, SLC11A1
LTF	7.98E-04	CD86, MMP13
IL13	9.00E-04	CD86, FCGR2A, G0S2, GPX3, MMP13
APOE	9.95E-04	CD86, GPX3, MGEA5, MTCH1
ADAMTS12	1.23E-03	IRG1, MMP13
MYD88	1.37E-03	CD86, HP, IRG1, LZTFL1
SOCS1	1.82E-03	CD86, IRG1, MMP13

Table A-2.2: Upstream regulators identified by 1-feature LDA. Top upstream regulators of the genes identified by 1-feature LDA imply importance in the pathophysiology of NSAID enteropathy. Respective P-values of overlap (*i.e.*, overlap of target genes with genes in the upstream regulator pathway) and target genes are also shown.

Gene 1	Gene 2	2-Feature Error
RASGEF1B	KIAA1217	0
Dst	MSN	0
TNFRSF21	MSN	0
RIN2	MAPKAPK2	0
RIN2	ANXA6	0
RIN2	ITGB8	0
RIN2	C1QC	0
RIN2	SELPLG	0
RIN2	HLA-A	0
RIN2	IFI16	0
RIN2	Gm5150	0
RIN2	BCL2A1	0
RIN2	MOB3A	0
IL15	SMYD5	0
IL15	CBL	0
IL15	TTLL7	0
IL15	HOXB4	0
IL15	S100PBP	0
IL15	FOXF1	0
IL15	C5AR1	0

Table A-2.3: Top 20 gene pairs that accurately classify NSAID from control animals Top 20 gene sets and resubstituted error rate of the genes identified by 2-feature LDA that classify NSAID treated animals from control animals with less than 5% error.

Gene 1	Gene 2	2-Feature Error	1-Feature Error
QTRT1	HK3	0	>5%
IFITM1	GNG11	0	>5%
LCP1	IFITM2	0.0001	>5%
ASRGL1	GM26698	0.0002	>5%
GM2848	GM26698	0.0003	>5%
QTRT1	IFI16	0.0005	>5%
PARP11	F13A1	0.0005	>5%
CXCL16	C5AR1	0.0007	>5%
IFITM1	TBC1D8B	0.0007	>5%
ST5	MSN	0.0012	>5%
MSN	ANK3	0.0012	>5%
PTMA	MSN	0.0013	>5%
CXCL16	MSN	0.0014	>5%
ADH6A	IFI16	0.0017	>5%
Cd52	FAM83B	0.0018	>5%
PSMA6	MSN	0.0018	>5%
IFITM1	ALOX5AP	0.0019	>5%
GM12848	GM1586	0.0019	>5%
NDUFC2	MSN	0.0021	>5%
CXCL16	UTP14	0.0022	>5%
CD52	Klf9	0.0026	>5%

Table A-2.4: 2-Feature LDA reduces error rate and identifies important genes involved in NSAID enteropathy. Top 20 gene sets that performed better in combination, in terms of reduced error rate, than either gene set alone.

Upstream Regulator	P-Value of Overlap
DYSF	5.47E-05
IL4	6.37E-05
TNK1	1.14E-04
TFEC	1.28E-04
IL10RA	1.80E-04
BAK1	3.38E-04
MGEA5	3.51E-04
ACKR2	5.51E-04
PPRC1	8.16E-04
IFNG	8.84E-04
ARNT2	9.18E-04
SIM1	9.98E-04
BAX	1.09E-03
TAZ	1.45E-03
RICTOR	1.85E-03

Table A-2.5: Upstream regulators identified by improved error rate between 1-feature and 2-feature LDA. Upstream regulators were identified using genes that performed better in combination, in terms of reduced error rate, as compared to either gene set alone.

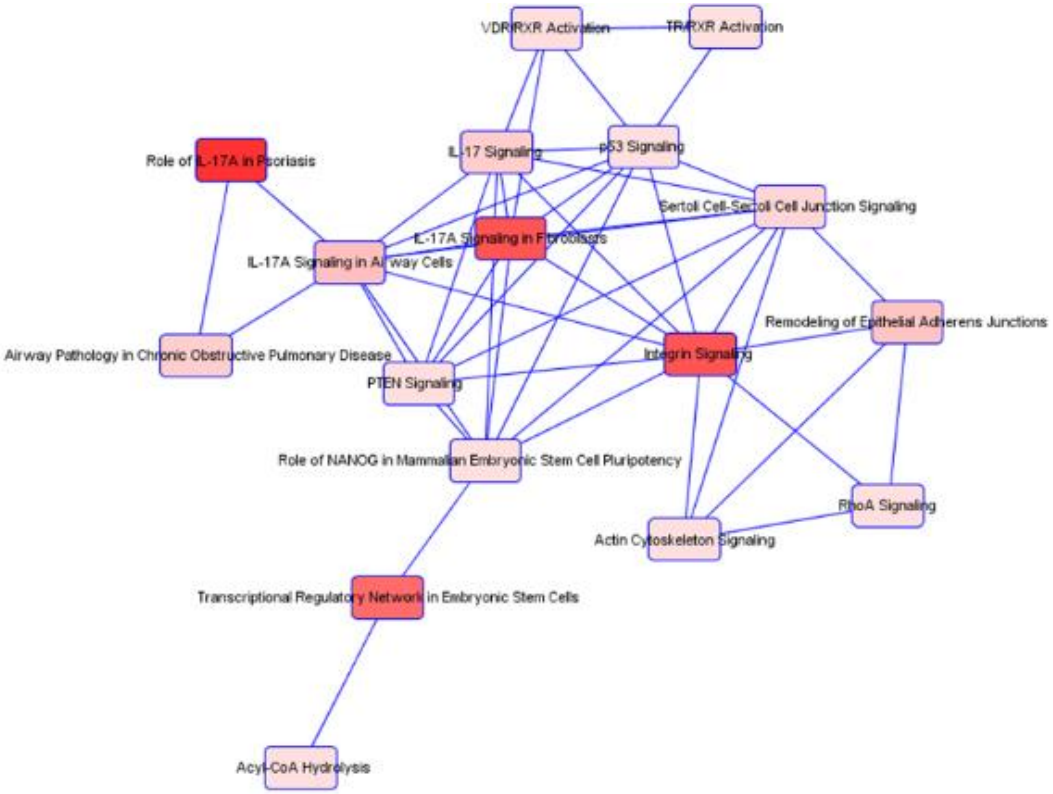

Figure A-2.3: Sparse CCA of the exfoliated IEC transcriptome identifies cytoskeletal signaling and inflammatory pathways reflecting NSAID enteropathy. The network of pathways to which the genes identified by sparse CCA map are shown. The darker color correlates with lower P-value.